

Contract No:

This document was prepared in conjunction with work accomplished under Contract No. DE-AC09-08SR22470 with the U.S. Department of Energy (DOE) Office of Environmental Management (EM).

Disclaimer:

This work was prepared under an agreement with and funded by the U.S. Government. Neither the U. S. Government or its employees, nor any of its contractors, subcontractors or their employees, makes any express or implied:

- 1) warranty or assumes any legal liability for the accuracy, completeness, or for the use or results of such use of any information, product, or process disclosed; or
- 2) representation that such use or results of such use would not infringe privately owned rights; or
- 3) endorsement or recommendation of any specifically identified commercial product, process, or service.

Any views and opinions of authors expressed in this work do not necessarily state or reflect those of the United States Government, or its contractors, or subcontractors.

Key Words:
Metal Hydride
Hydrogen Storage
Engineering Analysis
Hydrogen Vehicles

Retention:
Permanent

**HYDROGEN STORAGE ENGINEERING CENTER OF EXCELLENCE
METAL HYDRIDE FINAL REPORT**



T. Motyka

MAY 2014

**SAVANNAH RIVER NATIONAL LABORATORY
SAVANNAH RIVER SITE
AIKEN, SC 29808**

**PREPARED FOR THE U.S. DEPARTMENT OF ENERGY UNDER
CONTRACT NUMBER DEAC09-08-SR22470**



DISCLAIMER

THIS WORK WAS PREPARED UNDER AN AGREEMENT WITH AND FUNDED BY THE U.S. GOVERNMENT. NEITHER THE U. S. GOVERNMENT OR ITS EMPLOYEES, NOR ANY OF ITS CONTRACTORS, SUBCONTRACTORS OR THEIR EMPLOYEES, MAKES ANY EXPRESS OR IMPLIED:

- 1. WARRANTY OR ASSUMES ANY LEGAL LIABILITY FOR THE ACCURACY, COMPLETENESS, OR FOR THE USE OR RESULTS OF SUCH USE OF ANY INFORMATION, PRODUCT, OR PROCESS DISCLOSED; OR**
- 2. REPRESENTATION THAT SUCH USE OR RESULTS OF SUCH USE WOULD NOT INFRINGE PRIVATELY OWNED RIGHTS; OR**
- 3. ENDORSEMENT OR RECOMMENDATION OF ANY SPECIFICALLY IDENTIFIED COMMERCIAL PRODUCT, PROCESS, OR SERVICE.**

ANY VIEWS AND OPINIONS OF AUTHORS EXPRESSED IN THIS WORK DO NOT NECESSARILY STATE OR REFLECT THOSE OF THE UNITED STATES GOVERNMENT, OR ITS CONTRACTORS, OR SUBCONTRACTORS.

PRINTED IN THE UNITED STATES OF AMERICA

**PREPARED FOR
U.S. DEPARTMENT OF ENERGY**

Key Words:
Metal Hydride
Hydrogen Storage
Engineering Analysis
Hydrogen Vehicles

Retention:
Permanent

**HYDROGEN STORAGE ENGINEERING CENTER OF EXCELLENCE
METAL HYDRIDE FINAL REPORT**

T. Motyka

Major Contributors:

**B.J. Hardy, C. Corgnale, J.M. Pasini, B.A. van Hassel, S. Kumar,
M. Thornton, M. Veenstra, K.L. Simmons, M.R. Weimar, M.K. Drost**

MAY 2014

**SAVANNAH RIVER NATIONAL LABORATORY
SAVANNAH RIVER SITE
AIKEN, SC 29808**

**PREPARED FOR THE U.S. DEPARTMENT OF ENERGY UNDER
CONTRACT NUMBER DEAC09-08-SR22470**



This page intentionally left blank.

TABLE OF CONTENTS

LIST OF FIGURES	iv
LIST OF TABLES	v
LIST OF ACRONYMS	vii
EXECUTIVE SUMMARY	1
1.0 INTRODUCTION.....	4
2.0 METAL HYDRIDE HISTORY.....	10
2.1 Metal Hydride Materials	10
2.2 Metal Hydride Systems	14
3.0 HSECOE METAL HYDRIDE RESULTS	1Error! Bookmark not defined.
3.1 Material Operating Requirements	Error! Bookmark not defined.
3.2 Modeling and Analysis	25
3.3 System Elements, BOP Components and Cost Estimation.....	47
4.0 DISUSSION AND SUMMARY	57
4.1 Phase 1 to Phase 2 Transition Analysis.....	57
4.2 "Ideal" Metal Hydride Study	60
5.0 CONCLUSTION AND PATH FORWARD.....	63
6.0 REFERENCES.....	65
APPENDICES	I
A-1 Guideline for up- and down-selection of HSECoE materials	II
A-2 Sodium Alanate Hydride Mateiral Property Database	IV
A-3 Metal Hydride HSECoE Publications	XI

LIST OF FIGURES

Figure 1: Overall HSECoE project schedule and timeline.....	9
Figure 2: Intermetallic hydrides versus hydrogen capacity in wt%.....	11
Figure 3: Conversion of DOE hydrogen storage system parameters and targets.....	13
Figure 4: Measured values of material goals for onboard regenerated metal hydride systems.....	14
Figure 5: Large-scale NaAlH ₄ prototype vessels used for automotive-based testing and evaluation.....	17
Figure 6: Compaction results for NaAlH ₄	21
Figure 7: Relative change in NaAlH ₄ pellets as a function of hydrogen absorption and desorption cycles.....	22
Figure 8: Comparison of NaAlH ₄ compact Expansion versus absorption and desorption cycles for unreinforced and reinforced aluminum mesh material samples	23
Figure 9: Thermal Conductivity of pelletized Ti-doped NaH + Al and Ti-doped NaAlH ₄ compared with density.....	23
Figure 10: Thermal conductivity of Ti-doped NaAlH ₄ with and without 5 mol% ENG ...	24
Figure 11: Illustration of confinement of NaAlH ₄ pellets in aluminum tubing	25
Figure 12: Schematic of integrated models employed by the HSECoE	25
Figure 13: Acceptability Envelope Analysis equation.....	27
Figure 14: Linear relationship between vessel and media parameters an charging/discharging rate	28
Figure 15: NaAlH ₄ bed profiles vs charging times and thermal conductivity for rectangular coordinates with and without added graphite to the material	29
Figure 16: Results from applying Acceptability Envelope screening analyses to various candidate metal hydride materials with and without added graphite	30
Figure 17: Cross section illustration and geometry slice of a NaAlH ₄ vessel used for computation of 3-D model	31
Figure 18: Multi-tubular reactor configuration	32
Figure 19: An example of a honeycomb core - cell size: 0.952 cm	33
Figure 20: Schematic of NaAlH ₄ hydrogen storage bed showing profile and cross-sectional views	34
Figure 21: Effect of different geometric parameters on the system level targets for a shell and tube heat exchanger configuration with NaAlH ₄ in the shell	36
Figure 22: Helical coil heat exchanger design	36
Figure 23: GM shell and tube heat exchanger schematic with NaAlH ₄ in tubes	37
Figure 24: HSECoE framework system model showing main blocks, inputs, outputs and a sample of storage systems	38
Figure 25: Test cases for exercising the storage systems using various EPA fuel efficiency drive cycles	40
Figure 26: System flow chart of high-pressure metal hydride system	41
Figure 27: System flow chart for a NaAlH ₄ storage system	41
Figure 28: Example of tradeoff study on hydrogen stored versus glider mass on vehicle range for a NaAlH ₄ system	45

Figure 29: Schematic of the acoustical experimental setup for hydrogen fuel gauge testing	48
Figure 30: Preliminary results showing charged and discharged state of metal hydride containers	49
Figure 31: Proof of concept for acoustical hydrogen fuel gauge for a metal hydride system	49
Figure 32: Baseline metal hydride system schematic	50
Figure 33: Baseline metal hydride system and BOP mass and vol. projections	51
Figure 34: Reduced mass and volume scenario analysis for a metal hydride system	52
Figure 35: Integrated microchannel combustor sketch and unit test cell	53
Figure 36: Cost breakdown major system components	56
Figure 37: Comparison of Phase I system cost estimates	56
Figure 38: Baseline metal hydride design results compared with the DOE 2010 system Targets	58
Figure 39: Weight and volume distribution for a 11 wt% H ₂ material and a $\Delta H = -27$ kJ/mol	62
Figure 40: Weight and volume distribution for a 17 wt% H ₂ material and a $\Delta H = -40$ kJ/mol	62

LIST OF TABLES

Table 1: Original DOE Onboard Hydrogen Storage System Targets	6
Table 2: Current DOE Onboard Hydrogen Storage System Targets	7
Table 3: Properties of Complex Metal Hydride Materials	11
Table 4: Vehicle Demonstration Using Metal Hydride Tanks	15
Table 5: Onboard Hydrogen Storage Comparison	16
Table 6: Large-scale NaAlH ₄ Prototypes Storage System Comparison	21
Table 7: Minimum Screening Criteria for Metal Hydrides	22
Table 8: HSCoE Metal Hydride Material Categories	23
Table 9: Comparison of Material Properties and System Parameters for TiCrMn and NaAlH ₄ Systems	42
Table 10: Comparison of hydrogen gravimetric and volumetric system capacities for various materials and system configurations	43
Table 11: Vehicle Performance results for NaAlH ₄ and TiCrMn compared to Compressed Gas	46
Table 12: Vehicle WTW results for NaAlH ₄ compared to Compressed Gas	46
Table 13: HSECoE Base Assumptions for HDSAM	47
Table 14: Storage System Information Required for HDSAM Analysis	47
Table 15: Metal hydride system cost across all production levels for baseline NaAlH ₄ system case	54
Table 16: Cost estimates for metal hydride system balance of plant components...	55
Table 17: DOE 2010 System Targets Compared to SAH Base Case Model results.....	58

LIST OF ACRONYMS

2-D	Two-Dimensional
3-D	Three-Dimensional
AE	Acceptability Envelope
BC	Base Case
BOP	Balance of Plant
CC	Cylindrical Coordinates
DAQ	Data Acquisition
DME	Dimethyl Ether
DOE	Department of Energy
ECD	Energy Conversion Devices
ENG	Expanded Natural Graphite
EPA	Environmental Protection Agency
FC	Fuel Cell
FTP	Federal Test Procedure
FY	Fiscal Year
GfE	Gesellschaft für Elektrometallurgie
GHG	Greenhouse Gas
GKSS	GKSS Research Center
GM	General Motors
HDSAM	Hydrogen Delivery Scenario Model
HSECoE	Hydrogen Storage Engineering Center of Excellence
HSSIM	Hydrogen Storage SIMulator
HVAC	Heating, Ventilation and Air Conditioning
HWFET	Highway Fuel Economy Test (Cycle)
ICE	Internal Combustion Engine
IPPSSM	Integrated Power Plant Storage System Modeling
JMC	Japan Metals Corporation
LANL	Los Alamos National Laboratory
MBI	Microproducts Breakthrough Institute
MHCoE	Metal Hydride Center of Excellence
MOF	Metal Organic Framework
NREL	National Renewable Energy Laboratory
OSU	Oregon State University
PNNL	Pacific Northwest National Laboratory
RC	Rectangular Coordinates
SNL	Sandia National Laboratory
SRNL	Savannah River National Laboratory
UDDS	Urban Dynamometer Driving Schedule
UQTR	University of Quebec Trois Rivieres
UTRC	United Technology Research Center
WTPP	Well-to-power-plant

This page intentionally left blank.

EXECUTIVE SUMMARY

The Hydrogen Storage Engineering Center of Excellence (HSECoE) was established in 2009 by the U.S. Department of Energy (DOE) to advance the development of materials-based hydrogen storage systems for hydrogen-fueled light-duty vehicles. The overall objective of the HSECoE is to develop complete, integrated system concepts that utilize reversible metal hydrides, adsorbents, and chemical hydrogen storage materials through the use of advanced engineering concepts and designs that can simultaneously meet or exceed all the DOE targets. This report describes the activities and accomplishments during Phase 1 of the reversible metal hydride portion of the HSECoE, which lasted 30 months from February 2009 to August 2011. A complete list of all the HSECoE partners can be found later in this report but for the reversible metal hydride portion of the HSECoE work the major contributing organizations to this effort were the United Technology Research Center (UTRC), General Motors (GM), Pacific Northwest National Laboratory (PNNL), the National Renewable Energy Laboratory (NREL) and the Savannah River National Laboratory (SRNL). Specific individuals from these and other institutions that supported this effort and the writing of this report are included in the list of contributors and in the acknowledgement sections of this report.

The efforts of the HSECoE are organized into three phases each approximately 2 years in duration. In Phase I, comprehensive system engineering analyses and assessments were made of the three classes of storage media that included development of system level transport and thermal models of alternative conceptual storage configurations to permit detailed comparisons against the DOE performance targets for light-duty vehicles. Phase 1 tasks also included identification and technical justifications for candidate storage media and configurations that should be capable of reaching or exceeding the DOE targets. Phase 2 involved bench-level testing and evaluation of system configurations, including material packaging and balance-of-plant components, and conceptual design validation. Phase 3 includes fabrication and testing of the selected prototype storage system(s) for model validation and performance evaluation against the DOE targets. A DOE decision was needed for the HSECoE to advance to each phase and work on some classes of storage materials were recommended not to continue.

On August 31, 2011, upon DOE review of the information provided by the HSECoE on completion of Phase 1 activities, which included comparisons of all targets required for light-duty vehicles, work on reversible metal hydrides was recommended not to continue into Phase 2. It was determined that the analyses performed and presented to the DOE by the HSECoE for reversible onboard hydrogen storage required to meet the DOE performance targets imposed requirements substantially exceeding the properties and behavior of any single, currently existing candidate metal hydride. In particular, the necessary combination of gravimetric and volumetric capacities, reaction kinetics, thermodynamic properties and reversibility have not been found simultaneously in any metal hydride investigated to date. Furthermore, the HSECoE had not identified any engineering solutions that will allow any currently known metal hydride, when incorporated into a complete system, to simultaneously

meet all DOE performance targets. Therefore the decision was made to not continue work on metal hydride systems during Phase 2 and 3 of the HSECoE project.

Despite the only 30 months duration of the metal hydride portion of the HSECoE, a considerable amount was accomplished. These accomplishments are summarized below by several of the HSECoE Technologies Areas.

Material Operating Requirements

The metal hydride system team was able to expand on the existing material properties data by supplying additional engineering property data on some of the best candidate metal hydride materials provided to the HSECoE from the Metal Hydride Material Center of Excellence. This engineering property data was collected and organized into a new material property database. Preliminary material screening criteria was developed and used to select the most promising candidate metal hydride materials for further more extensive system evaluations.

Engineering material studies were conducted to increase the volumetric density of several low density metal hydride materials by performing various compacting and pelletizing experiments. Several of these studies showed significant improvement to the overall volumetric capacity of the system can be made by material compaction. Other engineering studies examined methods to improve the heat transfer properties and thermal conductivity of hydride materials. The use of Expanded Natural Graphite in powder and “worms-shaped” forms showed more than a 10X improvement in thermal conductivity was possible.

Transport Phenomena and Screening Analysis

Two and three dimensional, heat and mass transfer, finite element models were developed to evaluate metal hydride tank and associated internal heat exchanger designs. These models were used to evaluate and optimize various heat exchange and tank design concepts and to develop overall heat and mass transport correlations for use in system level models.

A novel hierarchical modeling approach was adopted that used a combination of screening and one dimensional models in combination with more detailed finite element models to accelerate the analyses and to make the best use of available resources. One of these screening tools that was used and developed as part of this effort was the Acceptability Envelope (AE). The AE made use of a simplified energy balance to identify the range of parameters for the coupled media and storage vessel system that allow it to meet performance targets. The AE was used to rapidly screen various metal hydride materials against DOE system targets and to select the best candidate materials for more detailed modeling and analysis. Both the detailed finite element bed models and the AE screening models are available to the public on the HSECoE website (<http://hsecoe.org/models.php>).

Integrated Power Plant Storage System Modeling (IPPSSM) Analysis

The HSECoE developed an integrated framework system model to evaluate the performance of all three classes of hydrogen storage material systems coupled to a standard fuel cell model developed by the Ford Motor Company. The metal hydride system was the first system to be evaluated in the integrated framework model. The metal hydride framework

model was used to develop the baseline system design, evaluate various operational and system improvements and to investigate the properties of an “ideal” metal hydride material that could meet all of the DOE system targets. The IPPSSM team of Matthew Thornton (NREL), Michael Veenstra (Ford) and José Miguel Pasini (UTRC) won the 2012 DOE Hydrogen and Fuel Cell Annual Merit Review Award for outstanding technical contribution in Hydrogen Storage Technology.

Performance Analysis

The integrated power plant and storage system models developed by the HSECoE were coupled with a vehicle performance model developed by NREL for comparisons of vehicles with different hydrogen storage systems to evaluate typical vehicle performance criteria such as: range, efficiency, Greenhouse Gas (GHG) emission, fuel economy and cost of ownership. The metal hydride system was the first material storage system to be evaluated, which aided in the development and integration of the performance analysis model for use by the HSECoE. An example of the IPPSSM and Vehicle models with a metal hydride storage system is also available on the HSECoE website (<http://hsecoe.org/models.php>).

Enabling Technologies

Two novel technologies were developed as part of the metal hydride system studies. One developed by LANL was a method to determine the state-of-charge of a metal hydride container using a simple acoustical method. Determining the state-of-charge in a metal hydride is not easily determined and the acoustical method showed high potential during preliminary tests. The other novel technology was the development of a compact and highly efficient hydrogen combustor/heat exchanger by Oregon State University (OSU) using an innovative microchannel design. Both of these technologies have been submitted for patent consideration.

Overall

In addition to the above mentioned accomplishment, the metal hydride system team published over 15 peer reviewed papers and made over 30 presentations at national and international meeting and conferences. A list of these can be found in Appendix A-3 of this report.

1.0 HSECOE OVERVIEW

Background

In the fall of 2008, the U.S. Department of Energy (DOE) selected a team led by DOE's Savannah River National Laboratory (SRNL) for its new Hydrogen Storage Engineering Center of Excellence (HSECoE). The HSECoE is a virtual center comprised of 14 partners at various locations around the country and from universities, industry and other federal laboratories. The partners bring to the Center extensive experience in metal, chemical, and sorbent hydrogen storage materials, and supporting systems engineering expertise. The team members include:

- Savannah River National Laboratory (Aiken, South Carolina)
- Pacific Northwest National Laboratory (Richland, Washington)
- Los Alamos National Laboratory (Los Alamos, New Mexico)
- National Renewable Energy Laboratory (Golden, Colorado)
- Jet Propulsion Laboratory (Pasadena, California)
- United Technologies Research Center (East Hartford, Connecticut)
- General Motors Corporation (Warren, Michigan)
- Ford Motor Company (Dearborn, Michigan)
- Hexagon Lincoln (Lincoln, Nebraska)
- BASF (Ludwigshafen, Germany)
- Oregon State University (Corvallis, Oregon)
- University of Quebec Trois Rivieres (Quebec, Canada)
- University of Michigan (Ann Arbor, Michigan)
- California Institute of Technology (Pasadena, California)

Funding for the 6-year HSECoE was approximately \$6 million per year of DOE funding with an additional 20% cost-share funding coming from university and industrial participants.

Mission

The mission of the HSECoE was to address the significant engineering challenges associated with developing lower-pressure, materials-based, hydrogen storage systems for hydrogen fuel cell light-duty vehicles, with the goal of meeting customer expectations for driving range, passenger and cargo space, performance and cost. The HSECoE was created to complement the work of the previous materials-focused Centers of Excellence and independent projects by addressing these onboard system concerns, providing both assessments of realistic onboard system performance and important feedback to the material developers.

Hydrogen storage systems, particularly materials-based systems, are complex and have a multitude of design parameters, subsystems, and input/output variables that impact overall system performance. System issues include, but are not limited to, thermal management, material handling, refueling, cost, start-up/shut-down, transient control, manufacturability, geometric constraints/packaging, safety and interface with the power plant and the fueling infrastructure.

Objectives

The focus of the HSECoE is on systems engineering and design for materials-based onboard vehicular systems using adsorbents, metal hydrides and chemical hydrogen storage materials. Storage systems utilizing all three media types have been addressed in the HSECoE. The boundary of the HSECoE is the interface of the onboard vehicle storage system with the vehicle power plant. The scope also addresses the interface between the onboard storage system and the vehicle forecourt (e.g. fueling station) for fuel dispensing, spent material recovery into/from the vehicle and heat rejection requirements. For the chemical hydrogen storage material approaches, the engineering of the off-board regeneration of the recovered spent material was not included in the scope of work. The HSECoE effort includes the development of engineering, design, and system models that address onboard subsystems. The HSECoE would also design, construct, test and evaluate sub-scale prototypes based on various hydrogen storage materials, subject to progress and go/no-go decisions.

The specific objectives identified by DOE [1] for the HSECoE included:

- a. Develop and utilize an understanding of storage system requirements for light-duty vehicles to design innovative components and systems with the potential to meet DOE performance and cost targets;
- b. Develop innovative onboard system concepts for materials-based storage technologies;
- c. Develop and test innovative concepts for storage subsystems and component designs;
- d. Develop engineering, design and system models which address both onboard subsystems and the fuel cycle, including refueling, transfer and separation of fresh and spent fuel for chemical approaches, hydrogen discharge profiles, thermal management and the storage-delivery interface; and
- e. Design, fabricate and test subscale prototype components and systems for each material-based technology (adsorbents, metal hydrides and chemical hydrogen storage materials).

Targets

The HSECoE was chartered to develop onboard vehicular hydrogen storage systems and components that will allow for a driving range of greater than 300 miles while meeting safety, cost and performance requirements. To guide and focus materials development efforts, the DOE developed detailed system performance targets for the specific applications of interest, and has supported system engineering analyses to determine the system-level performance delivered when the materials are incorporated into a complete system. Table 1 shows a list of Onboard Hydrogen Storage System Targets that were originally adopted by DOE at the start of the HSECoE project. Starting in 2009 the HSECoE focused primarily on 2010 and 2015 targets. Later in the program DOE updated their Onboard Hydrogen Storage System Targets to those shown in Table 2. The new targets were updated to reflect elapsed time and were aimed at where DOE ultimately wants to see the performance and cost of tomorrow's onboard hydrogen storage systems. Comparing the original 2010 and 2015 targets to the current 2020 and Ultimate targets the values for most of the parameters are similar. The one parameter that increased substantially from the old to the new table was system cost. In this report, 2010 and 2015 will be used to refer to the DOE Onboard

Hydrogen Storage Performance Targets that were in place at the start of the HSECoE and shown in Table 1.

Table 1: Original DOE Onboard Hydrogen Storage System Targets [1]

Technical Targets: On-Board Hydrogen Storage Systems				
Storage Parameter	Units	2007	2010	2015
System Gravimetric Capacity: Usable, specific-energy from H ₂ (net useful energy/max system mass) ^a	kWh/kg (kg H ₂ /kg system)	1.5 (0.045)	2 (0.06)	3 (0.09)
System Volumetric Capacity: Usable energy density from H ₂ (net useful energy/max system volume)	kWh/L (kg H ₂ /L system)	1.2 (0.036)	1.5 (0.045)	2.7 (0.081)
Storage system cost ^b (& fuel cost) ^c	\$/kWh net (\$/kg H ₂) \$/gge at pump	6 (200) ---	4 (133) 2-3	2 (67) 2-3
Durability/Operability <ul style="list-style-type: none"> Operating ambient temperature^d Min/max delivery temperature Cycle life (1/4 tank to full)^e Cycle life variation^f Min delivery pressure from tank; FC= fuel cell, I=ICE Max delivery pressure^g 	°C °C Cycles % of mean (min) at % confidence Atm (abs) Atm (abs)	-20/50 (sun) -30/85 500 N/A 8FC / 10ICE 100	-30/50 (sun) -40/85 1000 90/90 4FC / 35ICE 100	-40/60 (sun) -40/85 1500 99/90 3FC / 35ICE 100
Charging/discharging Rates <ul style="list-style-type: none"> System fill time (for 5 kg) Minimum full flow rate Start time to full flow (20 °C)^h Start time to full flow (-20 °C)^h Transient response 10%-90% and 90% -0%ⁱ 	min (g/s)/kW s s s	10 0.02 15 30 1.75	3 0.02 5 15 0.75	2.5 0.02 5 15 0.75
Fuel Purity (H ₂ from storage) ^j	% H ₂	99.99 (dry basis) See Appendix C		
Environmental Health & Safety <ul style="list-style-type: none"> Permeation & leakage^k Toxicity Safety Loss of useable H₂^l 	Scch - - (g/h)/kg H ₂ stored	Meets or exceeds applicable standards		
		1	0.1	0.05

Table 2: Current DOE Onboard Hydrogen Storage System Targets [2]

Technical System Targets: Onboard Hydrogen Storage for Light-Duty Fuel Cell Vehicles			
Storage Parameter	Units	2020	Ultimate
System Gravimetric Capacity:	kWh/kg	1.8	2.5
Usable, specific-energy from H ₂ (net useful energy/max system mass)	(kg H ₂ /kg system)	(0.055)	(0.075)
System Volumetric Capacity:	kWh/L	1.3	2.3
Usable energy density from H ₂ (net useful energy/max system volume)	(kg H ₂ /L system)	(0.040)	(0.070)
Storage System Cost:	\$/kWh net	12	8
	(\$/kg H ₂ stored)	400	266
• Fuel cost	\$/gge at pump	2-4	2-4
Durability/Operability:			
• Operating ambient temperature	°C	-40/60 (sun)	-40/60 (sun)
• Min/max delivery temperature	°C	-40/85	-40/85
• Operational cycle life (1/4 tank to full)	Cycles	1500	1500
• Min delivery pressure from storage system	bar (abs)	5	3
• Max delivery pressure from storage system	bar (abs)	12	12
• Onboard Efficiency	%	90	90
• “Well” to Power plant Efficiency	%	60	60
Charging / Discharging Rates:			
• System fill time (5 kg)	min	3.3	2.5
	(kg H ₂ /min)	(1.5)	(2.0)
• Minimum full flow rate	(g/s)/kW	0.02	0.02
• Start time to full flow (20 °C)	s	5	5
• Start time to full flow (-20 °C)	s	15	15
• Transient response at operating temperature 10%-90% and 90%-0%	s	0.75	0.75
Fuel Quality (H₂ from storage):	% H ₂	SAE J2719 and ISO/PDTS 14687-2 (99.97% dry basis)	
Environmental Health & Safety:			
• Permeation & leakage	-	Meets or exceeds applicable	
• Toxicity	-	standards, for example SAE J2579	
• Safety	-		
• Loss of usable H ₂	(g/h)/kg H ₂ stored	0.05	0.05

Approach

The approach taken by the HSECoE was to bring together a team of leading national laboratories, universities, and industrial laboratories, each with a high degree of hydrogen storage engineering expertise cultivated through prior DOE, international, and privately sponsored programs. The project tasks spanned the design space of vehicle requirements, power plant and balance of plant requirements, storage system components, and materials engineering efforts. The data and models obtained from this effort were used to design components and sub-scale prototypes of hydrogen storage systems which were evaluated and tested to determine the status of potential system against the DOE technical targets for hydrogen storage systems for light-duty vehicles.

The technical activities of the HSECoE were organized into three System Architectures: adsorbent, chemical hydrogen storage and metal hydride which were matrixed with six Technologies Areas: Performance Analysis, Integrated Power Plant/Storage System Analysis, Materials Operating Requirements, Transport Phenomena, Enabling Technologies and Subscale Prototype Construction, Testing and Evaluation. The program was divided into three phases; Phase 1: System Requirements and Novel Concepts, Phase 2: Novel Concept Modeling Design and Evaluation and Phase 3: Subscale System Design, Testing and Evaluation.

The objectives of Phases 1 and 2 were to utilize an understanding of storage system requirements for light-duty vehicles and to design innovative system concepts and components (including fuel delivery/recovery, as appropriate) with the potential to meet DOE performance targets. Novel system and component concepts based on adsorbents, metal hydrides and/or chemical hydrogen storage/hydride materials were to be considered. The emphasis is on fuel cell power plants consistent with the goals of the DOE Hydrogen Program. Phase 3 involves the construction, testing, evaluation and decommissioning of the subscale prototypes.

The end-product of both Phase 1 and Phase 2 are comprehensive reports to DOE on the updated system performance projections (e.g. weight, volume, transient performance, well-to-wheels cost and efficiency, and manufacturability) and assumptions with a recommended, prioritized list of next research steps. In addition, the reports are to document the novel concepts developed, such as thermal management concepts/designs or hydrogen discharge reactors and how they may be applicable to selected materials-based storage technologies. The end-product of Phase 2 also is to include a prioritized research, development and test plan for recommended Phase 3 subscale prototype(s) construction, testing, evaluation and decommissioning activities.

DOE worked with input and recommendations from the Center to make Go/No-Go decisions at the end of Phase 1 and Phase 2 on whether a particular material or a material class should undergo further investigation by the HSECoE program. DOE also determined whether any of the materials and material systems that have been identified by the HSECoE would move to subscale prototype construction and testing activities in Phase 3.

Schedule

The HSECoE project was identified as a 5-6 year program. Funding delays early in the project resulted in the program to include seven funding years from FY09-FY15. Phase 1 officially began on February 1, 2009, Phase 2 began on July 1, 2011 and Phase 3 on July 1, 2013 with the Center ending in June of 2015. An abbreviated project schedule showing the key project timelines is shown below in Figure 1.

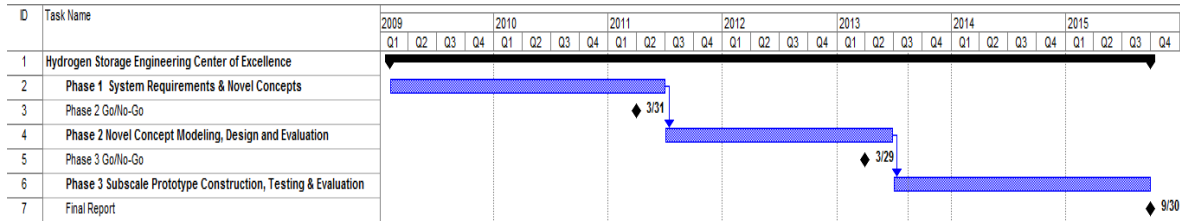


Figure 1: Overall HSECoE project schedule and timeline

At the end of Phase 1 (June 30, 2011), DOE reviewed the current progress for each of the material systems: metal hydride, adsorbents and chemical hydrogen storage and made several material and system related recommendations. One of those recommendations was to move certain adsorbent and chemical hydrogen storage materials and systems into Phase 2 but to only provide metal hydride materials and system a conditional “go” into Phase 2 based on a follow up study by the HSECoE. The purpose of the study [3] was to estimate the properties that a metal hydride material would need in a highly optimized system design to meet the DOE 2015 targets. The study and its results will be described in more detail in Section IV of this report. However, based on this study DOE determined that no current or near-term metal hydride material or systems had a reasonable expectation of meeting the DOE targets in a reasonable timeframe and therefore the decision was made to not continue the work on metal hydride materials and systems into Phase 2 and 3 of the HSECoE. This decision was made on August 31, 2011. Therefore, the HSECoE metal hydride activities reported here spans activities from February 1, 2009 until August 31, 2011 and only involved work predominantly carried out during Phase 1.

2.0 METAL HYDRIDE HISTORY

2.1 METAL HYDRIDE MATERIALS

Of the three material-based systems under investigation by the HSECoE, metal hydrides have the longest history and track record with respect to materials discovery as well as application development. There are numerous articles on metal hydrides in the literature and the intent of this report is not to review this historic record but to highlight and emphasize some of the past research to better understand how the HSECoE selected the metal hydride materials it did during its Phase 1 investigation.

The general definition for a metal hydride is broad and can involve many different inorganic and organic materials that bond with hydrogen. A brief summary of metal hydrides can be found in reference [4], Chapter 4, which discusses hydrides as: 1) covalent, 2) metallic, and 3) ionic or saline. This classification of hydrides is based on how the atoms or molecules in the material bonds with hydrogen. Covalent hydrides are typically liquids and gases at room temperature and many covalent hydrides that are solid at room temperature are unstable. Some examples of these are hydrogen sulfide, silane, methane and other hydrocarbons. Most of these are not good candidates for hydrogen storage applications [4].

Elemental metallic hydrides like palladium and titanium hydride have been known for more than a hundred years. However, it was not until the late 1960s when the properties of a new class of metallic hydrides, intermetallic hydrides (e.g., TiFe and LaNi₅) were discovered at Brookhaven National Laboratory and Phillips Laboratories, respectively [5]. These discoveries led to the characterization of hundreds of other intermetallic hydrides over the next 30 years. Many of these intermetallic hydrides, because of their fast reversible hydrogen charging and discharging rates as well as their ability to do so at or around ambient conditions, found their way into a variety of new hydrogen storage and other novel applications. The various applications of intermetallic hydrides will be described in more detail in the subsequent section of this report. Despite the many years spent on developing new intermetallic materials and applications, virtually all of the intermetallic materials suffer from having low hydrogen gravimetric densities (typically 1-2wt% hydrogen). This is mainly due to the fact that the elements in these materials are comprised of metals which have a fairly high density, especially compared with that of hydrogen. For some applications like stationary storage, the weight of the hydrogen storage system may not be so important, but for many other applications like transportation, a high overall storage system weight can be a problem. Over the past decade, interest in developing clean alternatives to gasoline as a transportation fuel and improvements in fuel cell technologies have put hydrogen and hydrogen storage in the spotlight. One of the key objectives of metal hydrides for onboard hydrogen storage was to make the materials lighter to improve their hydrogen gravimetric density. Alloying metallic hydrides with lighter weight materials like magnesium, calcium and vanadium became common but only achieving modest hydrogen capacity improvements of an additional 1% or so at the expense of higher discharge temperatures and rates. Figure 2 is a plot of several intermetallic metal hydride materials showing their gravimetric hydrogen density from the DOE Hydrogen Storage Materials Database [6]. From Figure 2 it can be

seen that most of the intermetallic hydrides of primary interest have hydrogen capacities less than or equal to about 2 wt%.

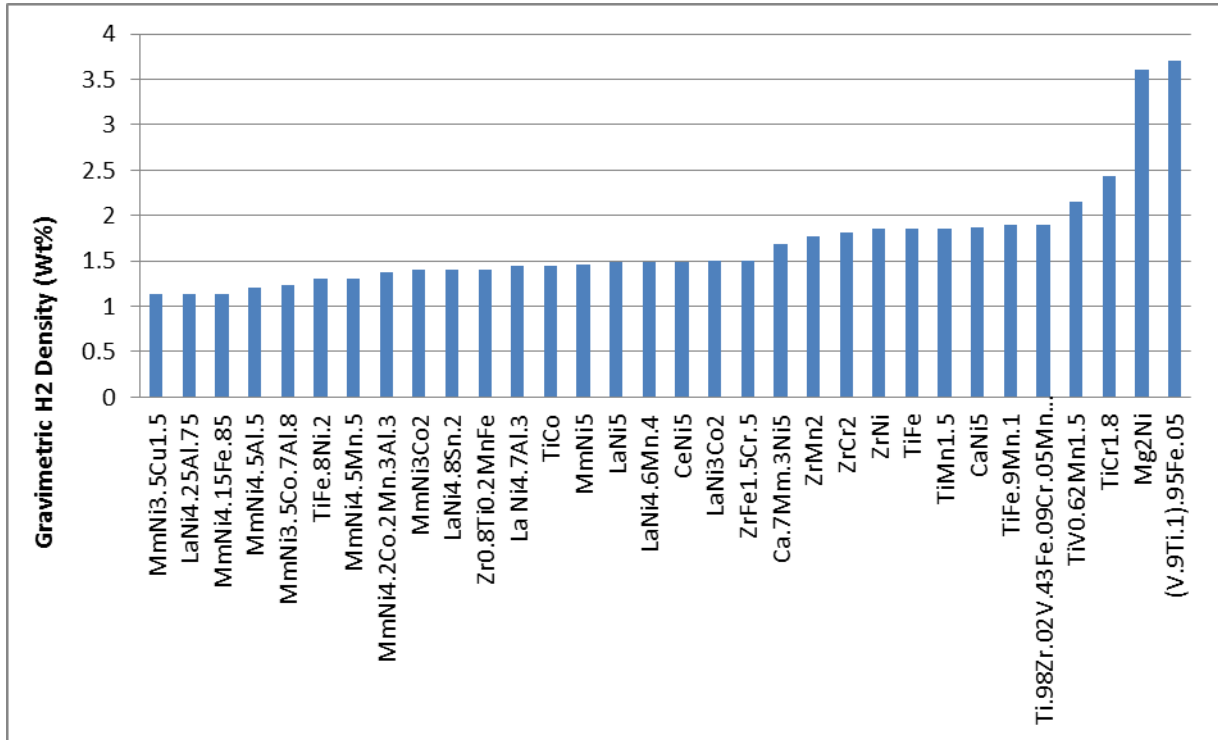


Figure 2: Intermetallic hydrides versus hydrogen capacity in wt%

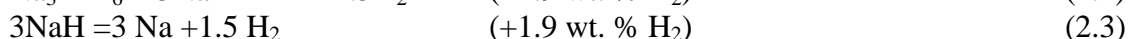
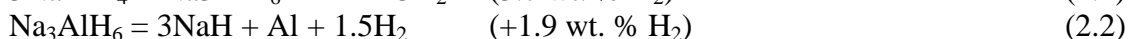
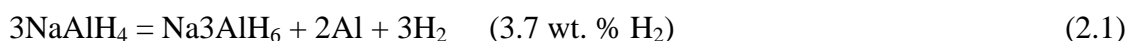
Another type of hydride, ionic hydrides, typically involve alkali metals and alkaline earth metals such as calcium and sodium. While most ionic hydrides have not been regarded previously as good candidates for hydrogen storage, some binary materials like magnesium hydride (which is not truly ionic), calcium hydride and sodium hydride have and are being considered for a variety of high temperature storage applications that include stationary and thermal energy storage systems [7, 8]. Other ionic hydrides termed “complex hydrides,” such as LiAlH₄, NaAlH₄, NaBH₄ and others, where the hydrogen is covalently bonded to another element form a “complex” anion have gained considerable interest in the past 10 to 15 years [4]. While many of these materials were well known and widely used as reducing agents in chemical processes, the situation changed in 1997 when Bodganovic and Schwickardi showed that with the addition of Ti catalysts to NaAlH₄ it could be rehydrogenated at moderate conditions and rates [9]. This discovery opened the door to a world-wide investigation of a new previously unconsidered class of high capacity reversible metal hydride materials. The hydrogen properties of some of the more common complex metal hydrides that were investigated are shown in Table 3.

Table 3: Properties of Complex Metal Hydride Materials [3]

Material	Decomposition Starting T (°C)	Hydrogen Content (wt. %)
NaAlH ₄	230	7.5
LiAlH ₄	170	10.6

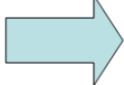
Mg(AlH ₄) ₂	110-130	9.3
LiBH ₄	320	18.4
NaBH ₄	450	10.6
Mg(BH ₄) ₂	320	14.8

From Table 3 it can be seen that while many of the complex hydrides do have very high hydrogen capacities, some even approaching 20 wt%, most also exhibit high decomposition temperatures and slow discharge kinetics. In addition, for most of the materials the full hydrogen reversible hydrogen capacity shown in Table 3 is not achievable. For example, in the case of NaAlH₄ the material decomposes in three stages.



For the decomposition of sodium hydride, the third stage of the reaction shown above, requires temperatures in excess of 500 °C making it impractical for transportation and many other applications. Therefore the maximum reversible capacity for NaAlH₄ is limited to 5.6 wt% from the first two reaction stages. Even for the first 2 reaction steps, despite the addition of catalysts and other material improvements and enhancements to NaAlH₄, it is often found that the usable reversible hydrogen capacity of NaAlH₄ is about 4 wt%.

In 2005 DOE initiated three hydrogen storage material-based Centers of Excellence focusing mainly on new materials discovery and characterization. One of these Centers was the Metal Hydride Center of Excellence (MHCoe). The MHCoe which was led by Sandia National Laboratory and involved researchers from 20 institutions, combined both materials development with mechanism and modeling studies to develop new reversible hydrogen storage materials that could meet or exceed the DOE 2010 and 2015 system targets (see Table 1). During its 5-year duration the MHCoe explored 94 new materials leading to 279 journal publications [10]. One of the final tasks of the MHCoe was to select the most promising reversible materials for additional engineering and system analysis by the HSECoE. The MHCoe focused on 5 of the DOE 2010 targets which included: *system gravimetric density, material reversibility, thermodynamic requirements, material stability and volatilization* and *material kinetics*. While none of the materials selected were deemed to meet all of the DOE targets, several materials were identified as priority materials for the HSECoE and materials worthy of further study. These materials included Mg(BH₄)₂, LiMgN, 2LiNH₂/MgH₂, AlH₃ regenerated by organometallic approaches and electrochemical means, and LiAlH₄ regenerated with hydrogen in dimethyl ether (DME). Of the materials selected by the MHCoe, the last two materials AlH₃ and LiAlH₄, are not considered onboard reversible materials. While these latter materials were evaluated by the HSECoE, they were include in the Chemical Hydrogen Storage efforts and will not be reported on here in the Metal Hydride report, which only examined onboard reversible candidate materials. Figure 3 shows a chart from the MHCoe that converts the DOE hydrogen storage system targets to material parameters to aide in the comparison of the selected materials for the HSECoE and future studies. More detail on the assumptions and rationale used for the conversion can be found in reference [10].

(A)			(B)	
Storage System Parameter	2010 DOE Target (New)	Convert to inferred materials properties for making Spider Charts 	Storage Material Parameter	"Goal"
System Grav.: kgH ₂ /kg-system	4.5%		Material Grav.: kgH ₂ /kg-material	9.0%*
System Vol.: gH ₂ /L system	28		System Vol.: gH ₂ /L material	56**
System Fill Time (5kg H ₂): mins	4.2		1/(Fill Time) Min ⁻¹	0.238
Operational Cycle Life: cycles	1000		Operational Cycle Life: cycles	1000
Hydrogen Purity	99.97% (dry)		1/(Fuel Impurities) ppm ⁻¹	0.01

* Assumes 50% system gravimetric penalty
** Assumes 50% system volumetric penalty (including packing density penalty)

Figure 3: Conversion of DOE hydrogen storage system parameters and targets (A) to hydrogen storage material parameters, and "goals" (B), assuming 50% system gravimetric and volumetric penalties [10].

Figure 4 shows a chart from the MHCoe study [10] that compares some of the selected onboard reversible metal hydride materials values against the converted DOE 2010 material targets from Figure 3B. Material A was a material that was developed prior to the start of the MHCoe and was included in the chart but not recommended to the HSECoE because of its very slow kinetics and its decomposition to diborane on cycling. Material B is a new material that was included because of its lower decomposition temperature but it was also not recommended for the HSECoE because of its low gravimetric density and its diborane decomposition product similar to Material A. Materials C, D and E were recommended for further investigation by the HSECoE and these will be discussed in more detail later in this report. Material F was also not evaluated by the MHCoe but was included here for comparison because it is one of the better gravimetric density intermetallic materials with excellent kinetics and cycling abilities at low temperatures. The investigation of TiCrMn, one of the materials in this class of materials, was investigated by the HSECoE and will be reported on later in this report. Finally Material G, NaAlH₄, was included in the chart because as mentioned earlier - it is still the best complex metal hydride candidate material today and despite only having a reversible hydrogen capacity of 4 wt%, it makes a good surrogate material for future studies and material comparisons. More detail information on NaAlH₄ from HSECoE studies will be provided later in this report.

2010 Materials "Goals"		A	B	C	D	E	F	G
		LiBH ₄ / MgH ₂	LiBH ₄ / Mg ₂ NiH ₄	2LiNH ₂ / MgH ₂	Mg(BH ₄) ₂	LiNH ₂ / MgH ₂	AB ₂ H ₃ A = Ti, Zr B = V, Cr, Mn	NaAlH ₄
Gravimetric Density (wt. %)	9%	10%	1.7%	5%	11%	6.5%	2.1%	4%
Volumetric Density (gH ₂ /L)	56	95	48	70	147	107	110	80
Min. Delivery Pressure @ 85 °C (PEMFC) (bar)	5	0.022	10	1.2	0.035	0.2	70	0
Cycle Life	1000	10	10	235	2	10	1000	100
Minimum Flow Rate (gH ₂ /sec) @ 85 °C	1	~0	~0	~0	~0	~0	1.5	~0
1/(Recharge Time = 4.2 min), min ⁻¹	0.238	0.0333	0.0083	0.1667	0.0028	0.0110	0.0660	0.1
1/(Fuel Impurities = 100 ppm), ppm ⁻¹	0.010	unknown	unknown	0.0056	0.0005	0.0088	∞	∞

Figure 4: Measured values of "material goals" for "onboard regenerated" metal hydride systems LiBH₄/MgH₂, LiBH₄/Mg₂NiH₄, 2LiNH₂/MgH₂, Mg(BH₄)₂, LiNH₂/MgH₂, NaAlH₄ and AB₂H₃ (A = Ti, Zr; B = V, Cr, Mn) [10].

2.2 METAL HYDRIDE SYSTEMS

Since the early 1970s, the ability to store hydrogen in metal hydride materials has found its way into a variety of applications from hydrogen vehicles, to compressors and to batteries. In addition to numerous published articles, several review articles [11-15] on this subject have been published by authors from the U.S., China, Russia, Germany and other countries. A recent publication by Bowman and Klebanoff [16] describes more than 10 energy conversion and storage applications for metal hydrides. These include portable power, stationary storage, compressors, heat pumps, thermal switches, gas purification, isotope separation, getters for vacuum systems and metal hydride batteries. Some of these applications have made their way to commercial systems with the most successful of these being metal hydride batteries. One of the metal hydride applications that have received the most interest and research funding in the past decade has been transportation. While a variety of specialty vehicle applications (scooters, buses, boats, submarines and fork lifts) have been demonstrated in the past [16-20], only a few applications like fork lifts have begun to be seriously considered for commercialization. Light-duty vehicles have always been the "holy grail" of applications for metal hydrides and other hydrogen storage materials. Table 4 from Sandrock and Bowman [15] shows a list of light duty and specialty vehicles that used metal hydride technology. From Table 4 one can see that most of the interest in metal

hydride automotive systems came from Europe and Asia, while the U.S. seems to have been in specialty vehicles.

Table 4: Vehicle Demonstration Using Metal Hydride Tanks

Maker	Designation	Power	Size (kW)	Hydride	Year
GM Opel	Precept FCEV	FC	75	?	2000
Honda	FCX-V1	FC	60	JMC	1999
Mazda	Cappela	ICE	?	JMC	1994
Mazda	Demio	FC	50	?	1997
Toyota	RAV4 FCEV	FC	20	?	1996
Toyota	FCHV-3	FC	90	JMC	2001
John Deere	Gator 1	FC hybrid	8.5	Mm(Ni,Al)	1998
John Deere	Gator 2	FC hybrid	8.5	Ti(Fe,Mn)	1998
SRTC Bus	Augusta	ICE hybrid	75	Lm(Ni,Al) ₅	1996
FCPI /SNL	Mine Locomotive	FC	12	(Ti,Zr)(Mn,V,Cr,Fe)	2001
ECD	Motor Scooter	ICE	?	ECD	2002
Germany	U212 Submarine	FC hybrid	300	GfEh	2004

As discussed previously in Section II, the low hydrogen gravimetric density of many popular intermetallic hydrides (similar to those identified in Table 4), has caused many automotive manufacturers to shy away from using these metal hydrides despite their good volumetric density and fast uptake and release kinetics. Many manufacturers feel that most intermetallic hydrides are just too heavy and expensive. This has led to several alternative approaches. One of these championed by Toyota [21] examined combining metal hydrides with high pressure carbon fiber-composite tanks. This approach, which is sometimes referred to as a “hybrid tank”, can increase the volumetric density compared to that of a compressed gas tank but at the expense of a lower gravimetric density (but higher than the gravimetric density of a straight metal hydride tank). Table 5 adapted from Toyota results [21] compares the hybrid tank to metal hydride, compressed gas and DOE targets.

Table 5: Onboard Hydrogen Storage Comparison[¥]

	Low P MH Tank (<10 bar)	High P Gas Tank (350 bar)	Hybrid Tank (350 bar)	DOE 2015 Target
H₂ Storage Capacity (kg/l)	0.029	0.017	0.040	0.040
H₂ Storage Capacity (kg/kg)	0.011	>0.030	0.017	0.055
H₂ filling time (min)	30-60	5-10	5*	3.3

[¥] taken from reference [21]

* 80% of full charge without cooling

Table 5 shows the benefits of a hybrid tank in being able to achieve good volumetric densities compared to 350 bar compressed tanks. Basically, one can store twice the amount of hydrogen in the same space as a 350 bar compressed tank. However, while the filling time is also good, the gravimetric hydrogen densities for hybrid tanks are still too low for many light-duty vehicle applications. A Toyota study [21] on hybrid tank development determined that even after assuming a material gravimetric density of 0.03 kgH₂/kg that further increases in alloy capacity would be required to provide an acceptable hydrogen storage tank mass. Toyota believes that a storage tank mass over 200 kg is predicted to have an adverse effect on fuel economy and acceleration performance if adopted in a passenger vehicle.

A second approach to overcoming the low gravimetric density typically associated with most metal hydride materials was to investigate higher hydrogen capacity complex metal hydrides. Three large-scale, automotive-based studies using complex metal hydride materials as the hydrogen storage medium were performed by Sandia National Lab (partnering with General Motors) [22], United Technology Research Center (funded by DOE) [23] and the Hamburg University of Technology (working with the GKSS Research Center under the EU's STORHY program) [24]. All of the studies used the complex metal hydride, sodium aluminum hydride (NaAlH₄) as their storage medium. In the discussion of complex metal hydride materials in Section II of this report it was mentioned that NaAlH₄ was the best complex metal hydride candidate material today and despite only having a reversible hydrogen capacity of 4wt% it was a good surrogate material for future studies and material comparisons. Figures 5 a through c shows the NaAlH₄ vessel designs for each of the large-scale automotive-based studies.

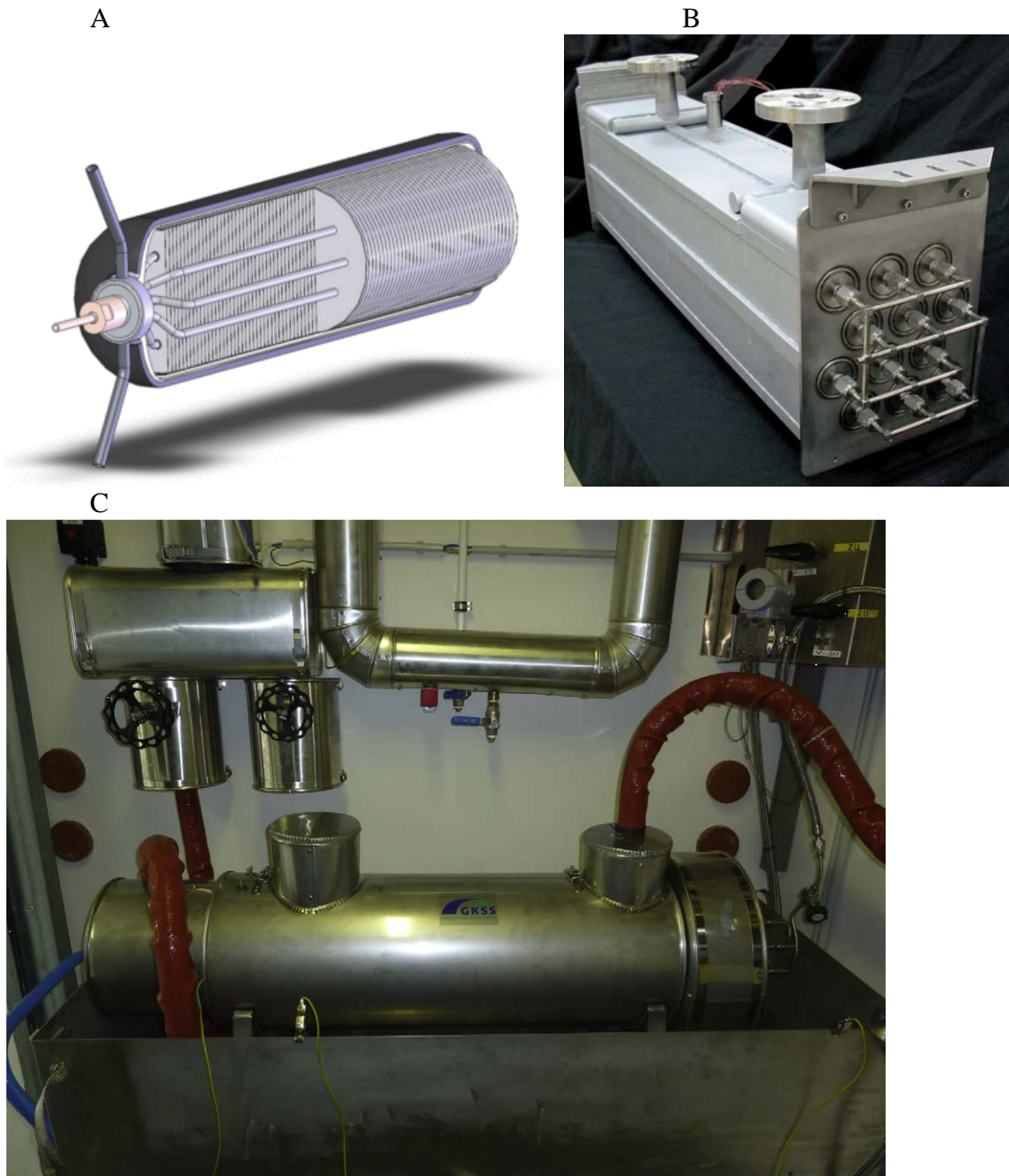


Figure 5: Large-scale NaAlH_4 prototype vessels used for automotive-based testing and evaluation: a) UTRC prototype 2 design comprised of a carbon fiber composite vessel and finned tube heat exchanger b) completed SNL/GM hydrogen storage module (4 modules comprised the demonstration system) and c) 8 kg GKSS hydrogen storage tank (Germany).

From 2001 to 2007 UTRC designed, fabricated and tested two NaAlH_4 prototype storage systems. Prototype I used 19kg of NaAlH_4 (about 1 kg H_2 scale) and a shell and tube heat exchanger with open-cell aluminum foam to increase the internal heat transfer within the

vessel. Prototype II was a 1/8th scale of Prototype I to allow for more complex fabrication methods at reduced cost. Prototype II employed a high efficiency finned tube heat exchange instead of aluminum foam. The UTRC design and testing was motivated by maximizing storage capacity. The larger 3 kg H₂, SNL/GM design also used a shell and tube design but reversed the arrangement by putting the metal hydride material in the tubes and the heat transfer fluid in the shell. The SNL/GM plan emphasized a lower cost design and more rapid cycling at the expense of storage capacity. The SNL/GM system went through extensive cycling tests including performance testing using standard automotive drive cycles. The GKSS storage system was an 8 kg of NaAlH₄ demonstration with a goal of achieving a 10 minute charging time at 80% capacity (similar to SNL/GM system). The system used seven 60mm diameter tubes approximately 1 m in length to make up the storage system. Table 6 shows the performance of each of the 3 large-scale prototype systems versus the DOE 2015 target. While it is difficult to get an exact comparison of each of the large-scale NaAlH₄ storage systems, Table 6 does show that even when a higher capacity complex metal hydride is used in a system that the system still cannot meet DOE Targets. The Table also shows that there is often a tradeoff between achieving faster refueling rates and capacity.

Table 6: Large-scale NaAlH₄ Prototypes Storage System Comparison

	UTRC (1/8 kg H ₂) Prototype II	SNL/GM (3 kg H ₂)	GKSS (~0.3 kg H ₂)	DOE 2015 Target
H ₂ Storage Capacity (kg/l)	0.021	0.0105	~0.01**	0.040
H ₂ Storage Capacity (kg/kg)	0.020	0.0085	~0.011**	0.055
H ₂ filling time (min)	30	30*	10	3.3

* 10 min filling times were achieved at about 13% lower capacities

** values estimated from figures and tables in references [22], [23] and [24]

3.0 HSECOE METAL HYDRIDE RESULTS

This section of the report will describe in more detail the metal hydride activities carried out under the HSECoE to further evaluate metal hydride systems as viable hydrogen storage solution for light-duty vehicles. As mentioned in Section I, this work covers predominantly Phase 1 activities that took place from February 2009 through August 31, 2011. The efforts of the metal hydride team will be summarized by work performed in three main Technology Areas: a) Material Operating Requirements, b) Modeling and Analyses and c) System and BOP Components.

3.1 MATERIAL OPERATING REQUIREMENTS

3.1.1 Material Property Data Collection and Selection Process

As part of Phase 1, the material operation requirements for candidate metal hydride materials needed to be determined. The objectives for the HSECoE did not include developing new storage materials but rather to evaluate existing materials that came from activities in the Metal Hydride Center of Excellence (MHCoe), from other DOE independent projects and the open literature. Figure 4 in Section 2.0 lists 7 metal hydride materials selected by the MHCoe for further investigation by the HSECoE. Some of the materials were developed by participants during the MHCoe's operation and some were identified in earlier studies and were suggested by the MHCoe as materials worthy of further consideration. During Phase 1, the HSECoE developed preliminary screening criteria for the hydrogen storage materials. The preliminary criteria for metal hydride materials are shown below in Table 7.

Table 7: Minimum Screening Criteria for Metal Hydrides

Capacity: > 9wt% materials capacity to be able to meet the DOE 2015 system target
 Absorption: RT to 250°C at 1-700 bar H₂ pressure, rate >20g/s (storing 5 kg usable H₂)
 Desorption: 80°C to 250°C at 1-3 bar H₂-pressure, rate >20g/s (storing 5 kg usable H₂)
 Enthalpy: <50kJ/mol
 Crystal density: > 1g/cm³
 Availability: (quantitative cost & time i.e. <\$10,000/kg in 30 day delivery)

Applying the preliminary screening criteria to existing metal hydride materials (those identified by the MHCoe in Figure 4 and other candidate materials) the available metal hydride candidate materials were grouped into three categories shown below in Table 8. Tier 1 materials were identified as developed materials, where sufficient material property data was already available from the MHCoe or other sources to begin further engineering and screening analyses. Note these materials did not meet all of the minimum screening criteria but they did have sufficient material property data to begin preliminary engineering analyses. Tier 2 materials were identified as developing materials of interest that still needed additional material property and engineering data. Non-selected (or rejected) materials were materials that were judged not to warrant any additional consideration at this time based on the minimum screening criteria. For the magnesium materials identified in Table 8 it was determined that these materials were too thermodynamically stable, which made them

impractical due to high desorption enthalpies. Appendix A-1 contains additional information on the guidelines for selection of HSECoE hydrogen storage materials along with documentation on the HSECoE's rationale for the categorization of the materials shown in Table 8. Note that during data collection and analyses in Phase 1, new materials were added or changed categories as warranted.

Table 8: HSECoE Metal Hydride Material Categories

	<i>Tier 1</i> Developed Materials	<i>Tier 2</i> Developing Materials	Down-selected Materials
Metal Hydrides	NaAlH ₄ 2LiNH ₂ +MgH ₂	Mg(NH ₂) ₂ +MgH ₂ +2LiH TiCr(Mn)H ₂	MgH ₂ Mg ₂ NiH ₄

Material property data for the metal hydride materials of interest (particularly Tier 1 and Tier 2 materials) were collected from a variety of sources, which included MHCoe reports and investigator data, previous studies and the open literature. To perform preliminary engineering analyses several key material properties were identified as a high priority requirement. These key material properties included:

1. Chemical kinetics parameters and types of reactions (as functions of temperature and species concentration). Not necessary for mass transfer limited systems (i.e. very rapid kinetics).
2. Hydrogen capacity (isotherms).
3. Bulk density.
4. Material density (sometimes called crystal density).
5. Total porosity.
6. Inter-particle porosity (same as total porosity for non-porous particles).
7. Intra-particle porosity (if the particles are porous).
8. Heats of reaction.
9. Bulk thermal conductivity.
10. Specific heat.

Material property databases containing the available key properties shown above for each of the metal hydride materials in Table 8 were created. Some of the databases were more complete than others but most included at least some information on kinetics, hydrogen capacity, material density and heat of reaction. The most complete database developed was for NaAlH₄ using data from prior work at UTRC [23], Sandia National Lab [25] and others [26]. An example of the database for NaAlH₄ is available in Appendix A-2.

3.1.2 Material Engineering Property Measurements

None of the metal hydride candidate materials shown in Table 8 are expected to meet all of the DOE storage targets, which are system targets. The HSECoE was created to modify and engineer the available materials and to engineer new storage system designs to better assess the available materials against the system level targets. As part of this effort, HSECoE partners, UTRC [27, 28] and GM [29, 30], undertook material engineering studies to

determine if the properties of some of the available materials could be enhanced and improved. Sodium Aluminum Hydride (NaAlH_4) was chosen as a surrogate material for the studies because of its material availability and the extent of available material property data. Another reason for choosing NaAlH_4 was that it is a complex metal hydride material which has similar material property characteristics to other complex hydrides like the lithium amide – magnesium hydride materials.

One advantage that many complex metal hydrides offer is higher gravimetric hydrogen capacities compared with intermetallic metal hydride materials. While higher gravimetric capacity has been a persistent issue for most traditional metal hydrides, most complex metal hydrides bring with them slower charging times, poorer cycling performance and lower volumetric hydrogen capacities. Both UTRC and GM led experimental efforts to address these issues. Both efforts were fairly similar and involved compacting NaAlH_4 , as the surrogate material and adding constituents to enhance the compacted material's mechanical strength, thermal conductivity and heat transfer properties.

The work at UTRC [27] involved NaAlH_4 with 4 mol % TiCl_3 as the model material. A uniaxial press was used to compact the material into pellets over the range of 14MPa – 282 MPa. It was reported that volume of the original material was reduced by 42% and the thermal conductivity was increased by a factor of seven over that of the unconsolidated material to 1.64 W/m/K at the higher applied pressures. Figures 6a and 6b show the relationship between compaction pressure on the density and thermal conductivity of NaAlH_4 , respectively. These results show that the higher the applied pressure the higher the density and the higher the resulting thermal conductivity is achieved.

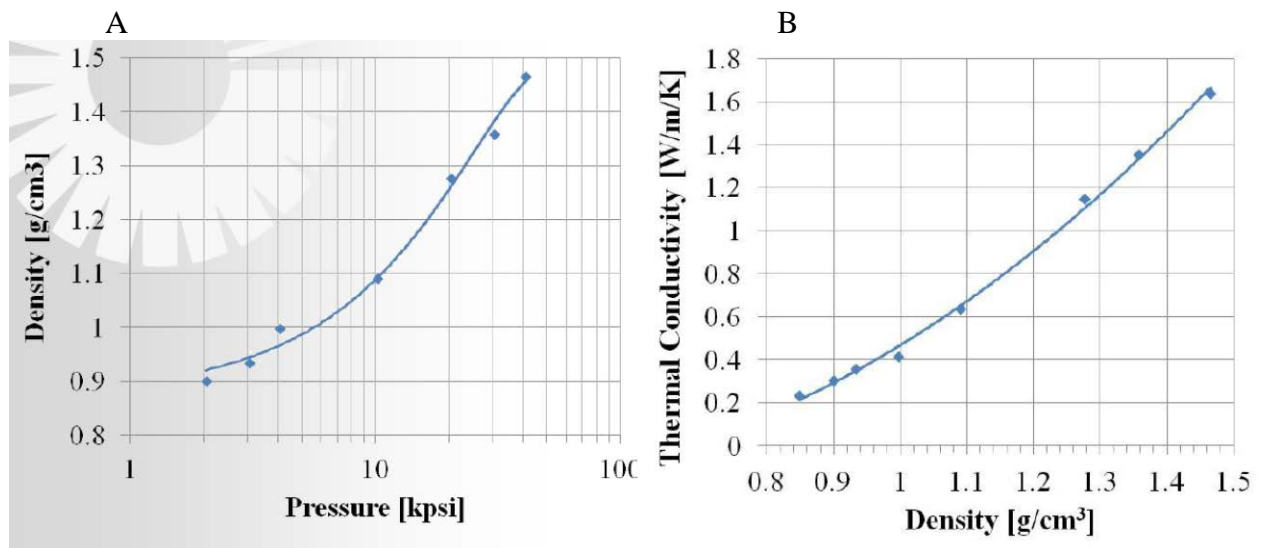


Figure 6: Compaction results for NaAlH_4 : a) impact of compaction pressure on density b) thermal conductivity versus density.

UTRC also experimented with the addition of aluminum powder and Expanded Natural Graphite (ENG) by low energy milling with the NaAlH_4 to further increase the thermal conductivity. The addition of ENG powder was found to lead to higher thermal

conductivities (on the order of 5 W/m/K) with the addition of lower amounts of materials than in the case of aluminum powder. This leads to a smaller penalty on weight and volume for the hydrogen storage tank. UTRC also measured the thermal conductivity of the compact in both the axial and radial direction but did not find an appreciable difference. In another part of the study UTRC [28] switched from ENG powder to ENG “worms”, which as the name implies are longer thread-like graphite materials. The thermal conductivity in the radial direction for the case of 5% ENG work was measured as 10.8 W/m/K versus only 1.54 W/m/K in the axial direction. The UTRC study also examined the effect of hydrogen cycling on the mechanical strength of the compacts as well as their rate to uptake and release hydrogen. The study used a biaxial flexure testing method often used to measure the strength of materials. An average strength of 10 MPa (1.4 kpsi) was measured for the NaAlH_4 compacts which was reported to be higher than what is typically seen in binder-reinforced green ceramic powder compacts. The biaxial strength of the compact was found to be unaltered for 3 cycles but steadily decreased on continued cycling to about 2 MPa after only 15 cycles. A plot of NaAlH_4 compact volume, diameter and thickness versus cycling is shown in Figure 7.

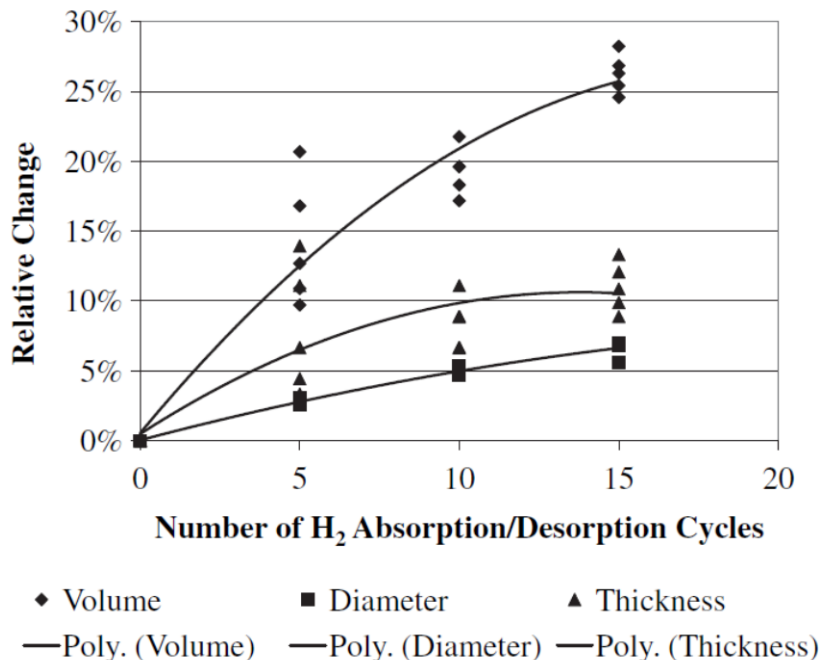


Figure 7: Relative change in NaAlH_4 pellets as a function of hydrogen absorption and desorption cycles.

Substantial changes to the compact only after 15 cycles led to the use of reinforcements to reduce the expansion, increase strength and increase thermal conductivity. Preliminary results using aluminum mesh was found to increase the strength of the compact but at the expense of added weight and material complexity (see Figure 8). The rate of hydrogen absorption and desorption was also measured and the increased initial density of the compact was found not to adversely affect the rate. More detail and information on the UTRC studies can be found in references [27, 28].

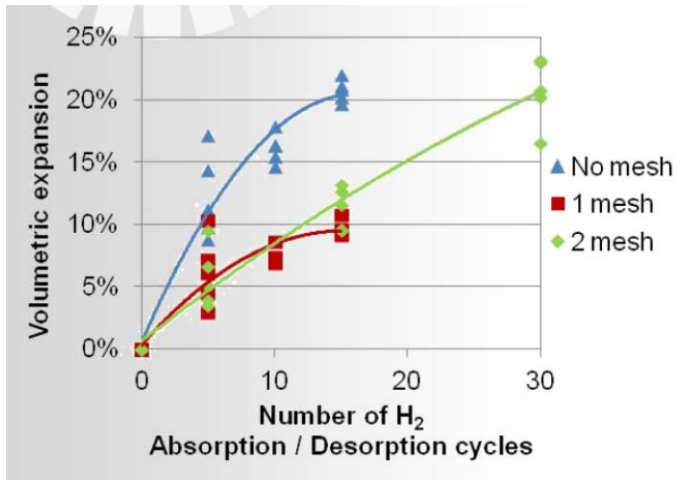


Figure 8: Comparison of NaAlH₄ compact Expansion versus absorption and desorption cycles for unreinforced and reinforced aluminum mesh material samples.

GM performed similar studies [29, 30] to engineer the properties of compacted NaAlH₄ pellets with similar results. GM used stoichiometric amounts of NaH and Al, 3 mol % TiCl₃ with 18 wt% excess aluminum and was able to press this material to somewhat higher pressures (69-345 MPa). The additional aluminum and the higher compaction pressure led to higher densities and thermal conductivity values than reported earlier by UTRC. Figure 9 compares the thermal conductivity and density of the GM materials along with an extrapolation of even higher values if higher compaction densities were able to be achieved. GM also evaluated the performance of its pellets for up to 50 hydrogen absorption and desorption cycles and other than needing approximately 10 cycles to fully activate the more densely compacted pellets they found that they were able to obtain the full hydrogen capacity. The study also reported that within 30 cycles there was a 50% loss in pellet density and by 50 cycles a loss of the pellets structural integrity made the pellets difficult to handle.

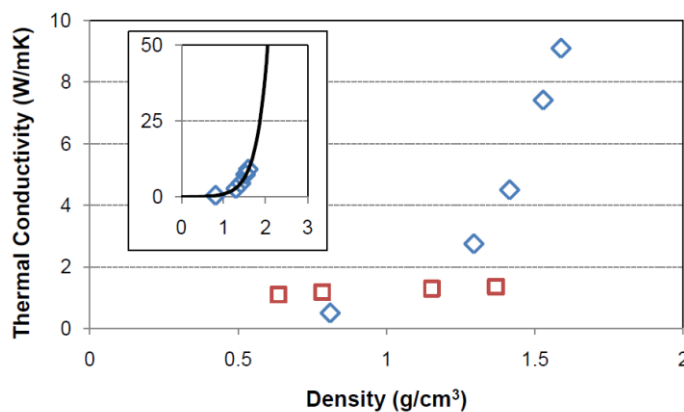


Figure 9: Thermal Conductivity of pelletized Ti-doped NaH + Al (diamonds) and Ti-doped NaAlH₄ (squares) compared with density. Inset shows exponential fit of NaH + Al data.

GM also tried adding ENG and ENG flake by both low and high temperature milling. The results in Figure 10 show that the highest thermal conductivity was in the pellet with the

excess aluminum but without the additional ENG. The lowest thermal conductivity was measured in pellets that were pressed at low pressures and made using high energy milling. Apparently, the high energy milling damaged the high thermal conductive carbon array making them less effective. These results are not so different from those obtained by UTRC using ENG powders. UTRC was only able to achieve thermal conductivities values greater than 9 in the radial direction with ENG worm materials. GM did find that the addition of graphite enhancers did aid in countering some of the loss of thermal conductivity with cycling, however, not to the extent to compensate for the additional loss in hydrogen capacity.

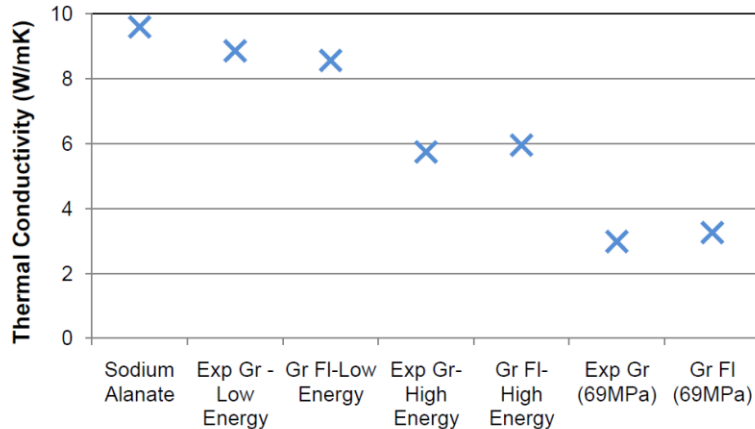


Figure 10: Thermal conductivity of Ti-doped NaAlH_4 with and without 5 mol % ENG (Exp Gr = expanded graphite, Gr Fl = graphite flake). Pellets pressed at 345 MPa unless otherwise noted.

A later phase of the GM study [30] examined mechanical confinement of the NaAlH_4 pellets with rigid aluminum tubing (see Figure 11). The confinement resulted in a reduction in the pellet expansion by 50% compared to the unconfined pellets over 30 cycles, 5 times greater thermal conductivity over 10 cycles and the pellets maintained their integrity over the entire 50 cycles. Some of the heat transfer improvement is attributed to reducing the contact resistance between the pellet and the container as well as the neighboring pellets. UTRC [28] also found a similar, about 50% reduction in volume expansion in experiments, with confined NaAlH_4 pellets on heat exchanger tubes after about 15 cycles and discussed the need for additional work on further reducing the contact resistance between the materials and the system. Some of the results of incorporating the engineered material properties into heat transfer and system models by UTRC and other HSECoE members will be discussed in more detail in the next section.

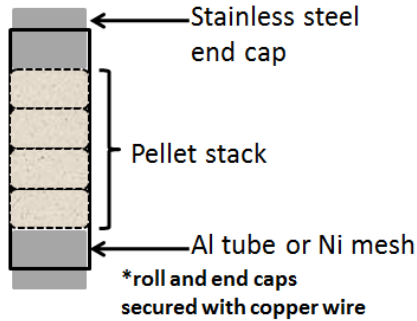


Figure 11: Illustration of confinement of NaAlH_4 pellets in aluminum tubing (12.7 mm OD and 9.32 mm OD).

3.2 MODELING AND ANALYSES

One of the main activities of the HSECoE was to develop engineering, design and system models which address onboard hydrogen storage systems, including refueling, hydrogen discharge profiles, thermal management and the storage-delivery interface. The behavior of the various storage media during charging and discharging of hydrogen is quite complex, involving chemical kinetics or thermodynamics coupled with mass, momentum and thermal transport processes. The modeling approach adopted for the HSECoE expanded upon the hierarchical sequence of models, the *Hierarchical Modeling System*, developed by SRNL [31]. The system consisted of screening models, detailed two- and three-dimensional models and system models. The screening models are used to quickly determine whether the storage media, storage system component designs, and the overall storage system configurations meet the performance criteria. If so, they are analyzed with more detailed two- and three-dimensional models that couple the transport equations with chemical kinetics. System models are then used to couple the storage tank to the storage system balance of plant, the fuel cell and other vehicle components to evaluate a specific storage system's performance with respect to DOE targets and standard vehicle drive cycles. Figure 12 shows the integration of the various models used to evaluate hydrogen storage systems by the HSECoE.

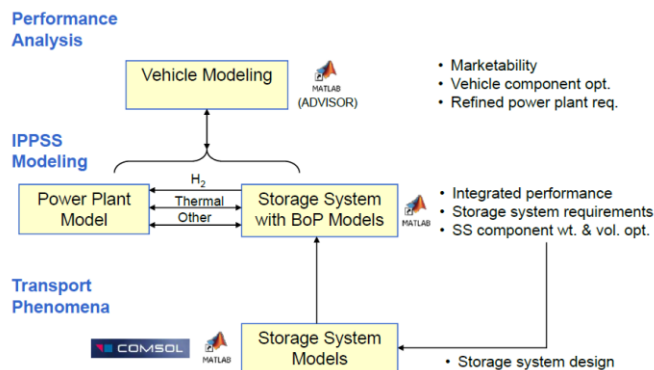


Figure 12: Schematic of integrated models employed by the HSECOE.

Starting from the bottom of Figure 12, using the transport properties associated with specific storage materials and vessel design, various screening and more detailed two- and three-dimensional models are used to develop an overall storage system design. The storage system

design is then input to the Integrated Power Plant Storage System (IPPSS) model which integrates the storage system with the fuel cell or other power plant model to evaluate its fuel and thermal interactions. Finally the Vehicle Model is used to integrate the combined storage system and power plant with vehicle performance to better assess DOE targets affecting vehicle operability and efficiency. The remainder of this section of the report will provide more detailed information on the metal hydride activities associated with developing and evaluating the various screening, system and detailed heat and mass transport models used by the HSECoE to select and compare metal hydride-based hydrogen storage systems for light duty vehicle applications.

3.2.1 Preliminary and Scoping Models

Given the complex processes that occur during hydrogen charging and discharging, it is essential to use detailed numerical models to design storage systems capable of meeting the DOE targets. The models must couple heat and mass transport with temperature, pressure, and composition-dependent chemical/sorption kinetics for the media. Detailed models, however, require a significant amount of time to develop and run. It is thus useful to have simplified models that can quickly estimate optimal loading and discharge kinetics, effective hydrogen capacities, system dimensions, and heat removal requirements. The simplified models also serve to quickly screen out system designs that cannot meet the performance criteria. To this end a tool was developed to screen candidate media and storage vessel designs. The screening tool identifies the range of parameters for the coupled media and storage vessel system that allow it to meet performance targets. The range of acceptable parameters forms a multi-dimensional volume, or envelope. Hence, the screening tool is referred to as the Acceptability Envelope Analysis [32].

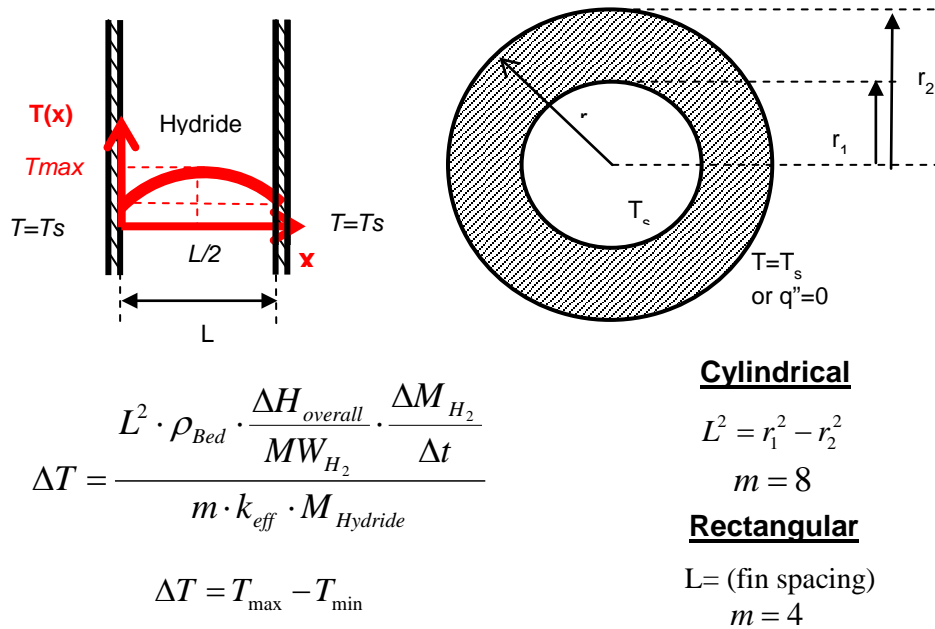
During charging, metal hydrides undergo exothermic chemical reactions that release a significant amount of heat. Conversely, during discharge the reactions are endothermic. At a given pressure, the temperature of the hydride determines whether it uptakes or releases hydrogen. Hence, heat transfer is the most important consideration in the design of storage vessels for use with metal hydrides. Typically, heat transfer within the storage vessel is accomplished either by packing the hydride between fins or around tubes that contain a flowing heat transfer fluid. In both cases, heat transfer within the hydride bed can be represented as a collection of periodic cells, in rectangular coordinate (RC) or cylindrical coordinate (CC) geometry. The packed hydride is referred to as a hydride bed, and it is through this packed bed that heat conduction to the heat transfer surfaces must take place. With increased compaction of the metal hydride, mass transfer limitations may also play a role in the performance of the storage system. However, for this analysis, heat transfer was assumed to be the sole dominant factor in meeting performance targets.

The thermal model, which is the basis of the acceptability envelope, employs the following assumptions:

1. The process is steady-state.
2. The heat transfer process is one dimensional.
3. The thermal conductivity is isotropic and constant within the bed.
4. Convective heat transfer due to hydrogen passing through the bed is negligible.

5. Mechanical work (i.e. compression or expansion) done to uptake (discharge) hydrogen (related to the pressure variation) is negligible.

Using the above assumptions, a one-dimensional energy balance was used to relate the characteristics of the metal hydride media and the system to the storage system performance targets. Figure 13 summarizes the reduced equation in both RC and CC geometries. More detailed information on the derivation of the Acceptability Envelope equations can be found in reference [32].



L	Distance between heat transfer surfaces (m)
ΔT	Temperature range required for acceptable chemical kinetics (to give specified charge/discharge rate) (K)
$\Delta H_{overall}$	Overall heat of reaction (kJ/mol H ₂)
ρ_{Bed}	Hydride bed density (kg/m ³)
k_{eff}	Effective bed thermal conductivity (W/m K)
$M_{Hydride}$	Mass of hydride required to load target amount of hydrogen (kg)
MW_{H_2}	Molecular Weight of Hydrogen (kg H ₂ /mol H ₂)
$\frac{\Delta M_{H_2}}{\Delta t}$	Rate of charging/discharging (kg H ₂ /s)

Figure 13: Acceptability Envelope Analysis equation.

The equation for ΔT shown in Figure 13 can be rearranged to the expression shown in Figure 14, where a linear relationship between charging/discharging rate and y , which is a function of media and system parameters, can be formed.

$$y = \left(\frac{1}{L^2} \right) \left(\frac{k M_{Hyd_eff} \Delta T}{-\Delta H_{overall} \rho_{Hydride}} \right) = \frac{1}{mM_{H2}} \frac{\Delta m_{H2}}{\Delta t}$$

Vessel parameter
Media parameters

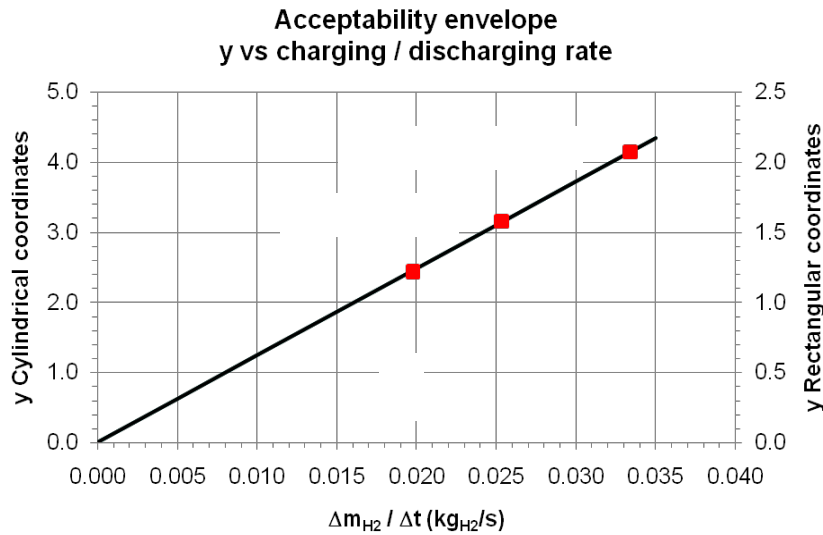


Figure 14: Linear relationship between vessel and media parameters and charging/discharging rate

This linear relationship shown in Figure 14 makes the acceptability envelope tool very flexible and useful. Knowing the values for the media parameters for a given material one can calculate the vessel parameter L for various charging and discharging rates, including those represented by the current DOE targets. Figure 15 illustrates an example of the use of the acceptability envelope equation by examining the differences in the required distance between two heat transfer surfaces (L) at various charging times for NaAlH₄ for a baseline case (BC) and a case where a graphite additive (GA) is used to increase the thermal conductivity of the material.

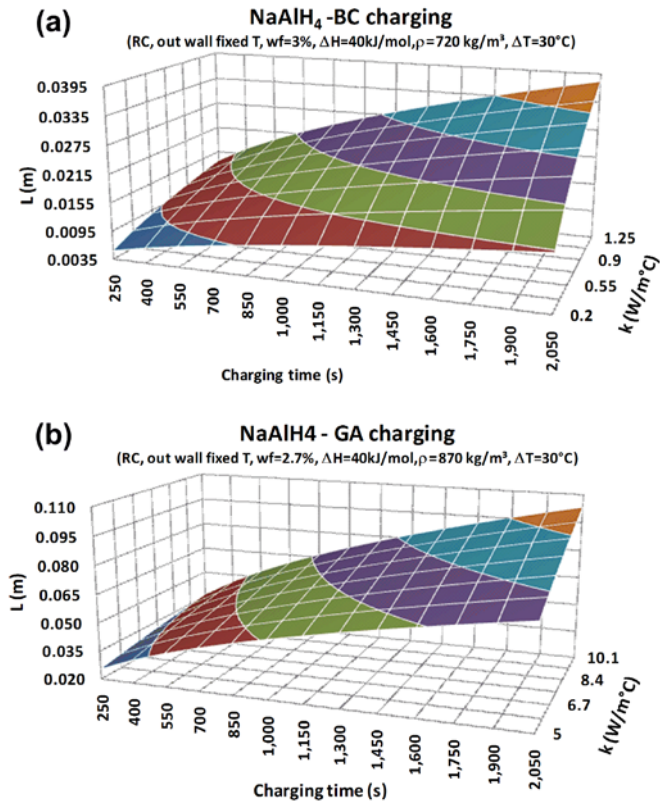


Figure 15: $NaAlH_4$ bed profiles vs charging times and thermal conductivity for rectangular coordinates with (Fig. 15b “GA charging”) and without (Fig. 15a “BC charging”) added graphite to the material.

From Figure 15 it can be seen that adding graphite to the $NaAlH_4$ material increases the thermal conductivity by more than an order of magnitude from approximately $0.8 W/m^{\circ}C$ to values on the order of $8 W/m^{\circ}C$. Similarly, the value of L becomes approximately 3 times larger when graphite is added to the unmodified $NaAlH_4$ material. Similar results were found when this analysis was applied to the other HSECoE candidate materials from Table 8. Based on these analyses and engineering judgment it was determined that the value of L needs to be on the order of $0.025 m$ to minimize the heat exchanger and system weight and for the system and still be able to meet reasonable charging times [32]. Figures 16a and b compares the results from the acceptability envelope analysis for various candidate materials with respect to L and wt% (hydrogen capacity). Figure 16a shows that the heat transfer rate for all of the candidate materials can be dramatically improved by the addition of graphite but only those materials with heats of reaction less than about $40 kJ/mol H_2$ exhibited L values on the order of $0.025 m$ needed to achieve reasonable charging rates. For this study a reasonable charging rate for the screening analysis was defined as 10.5 minutes. In Figure 16b, the gravimetric hydrogen density of the various materials are compared to each other with and without 10% graphite and compared against a 3.6 wt% material target (or an estimated 1.8 wt% system target). Both the charging rate and capacity targets selected for this study were based on 40% of the DOE 2010 targets.

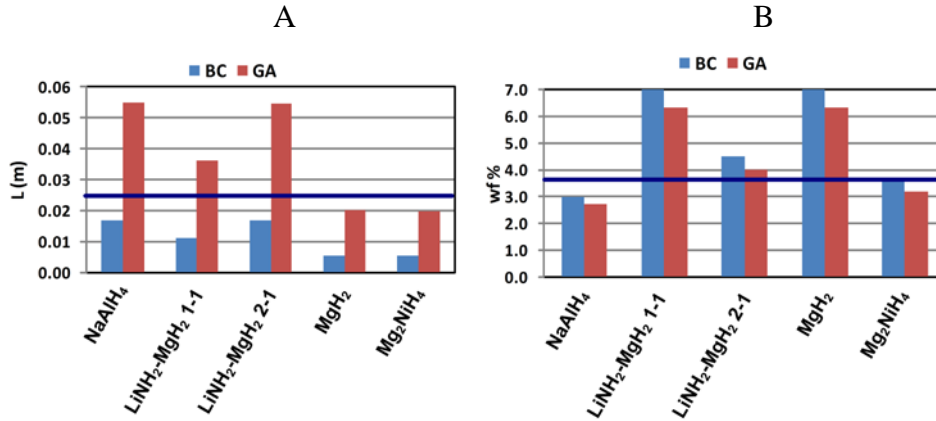


Figure 16: Results from applying Acceptability Envelope screening analyses to various candidate metal hydride materials with and without added graphite - a) characteristic spacing between heat transfer surfaces, L in rectangular coordinates - b) hydrogen gravimetric capacity (wt%) with 10% graphite (GA) and without (BC).

The 40% value of the DOE Target was selected for preliminary material screening to justify excluding some materials that were far away from meeting the targets but also not to exclude possible candidate materials that still had potential to meet many, if not all of the DOE targets. Results from Figures 16a and b shows that the most promising metal hydrides, with regards to achieving 40% of the 2010 DOE technical targets, were those based on Li and Mg. High capacity and high temperature materials, like MgH₂ and MgNiH₄, because of their high heats of reaction were judged to have difficulty meeting reasonable charging rates. TiCrMnH₂ (not shown) and NaAlH₄, while acting as good surrogate materials, would not be able to meet the minimum hydrogen capacity requirements. All of the materials benefitted by having higher thermal capacities using additives like ENG.

3.2.2 Detail Heat and Mass Transport Models

In the previous section, a screening model (Acceptability Envelope Analysis) was described and results from the model were used to identify the best candidate materials for more detailed study and analysis. To fully understand the complex processes occurring during charging and discharging processes in hydrogen storage systems more detailed models are essential. These models can help assess the viability of a particular system or provide options for improving its design. For a given media and system design, the models enable researchers to predict local hydrogen loading/discharge rates, media temperatures, and chemical composition throughout the bed. The detailed models can be used to identify design changes that yield the most significant improvement in system performance. Input to the detailed models will include the transport equations along with temperature, pressure, and composition-dependent hydrogen uptake/discharge kinetics relations. Output from the detailed models will include temperatures, pressures, concentrations of media species, hydrogen velocities, correlation-based parameters, and any quantity that can be derived from these parameters, including derivatives and integrals.

A study by Hardy [31], that was initiated just prior to the start of the HSECoE, included a good literature survey of past mathematical models that were developed for metal hydride

beds. Hardy also describes the development of general 2 or 3-dimension models that can be adapted to any geometry or storage media. The two-dimensional model serves to provide rapid evaluation of bed configurations and physical processes, while the three-dimensional model, which requires a much longer run time, is used to investigate detailed effects that do not readily lend themselves to two-dimensional representations. The model was initially applied to a hydrogen storage system similar to that tested by UTRC. The system modeled was a modified cylindrical shell and tube geometry with radial fins perpendicular to the axis, with NaAlH_4 as the hydrogen storage medium (see Figure 5 a). During Phase 1 of the HSECoE, the general model by Hardy [31] was used to assess various vessel design modifications and to explore new design concepts for proposed metal hydride systems. This work by the various HSECoE participants is described in more detail below.

A series of analyses of a Ti-doped NaAlH_4 storage system using the basic UTRC cylindrical shell and tube prototype design shown in Figure 5a was carried out by a team from UQTR and SRNL for the HSECoE [33]. Figure 17 shows the cross section and the geometric slice used for the 3-D modeling effort. In this study the modeling tool was used to evaluate the influence of varying the fins thickness and the number of coolant tubes on both the loading and discharge processes. The objective of the study was to optimize the loading and discharge times while still maintaining the lowest system volume and weight for the storage system.

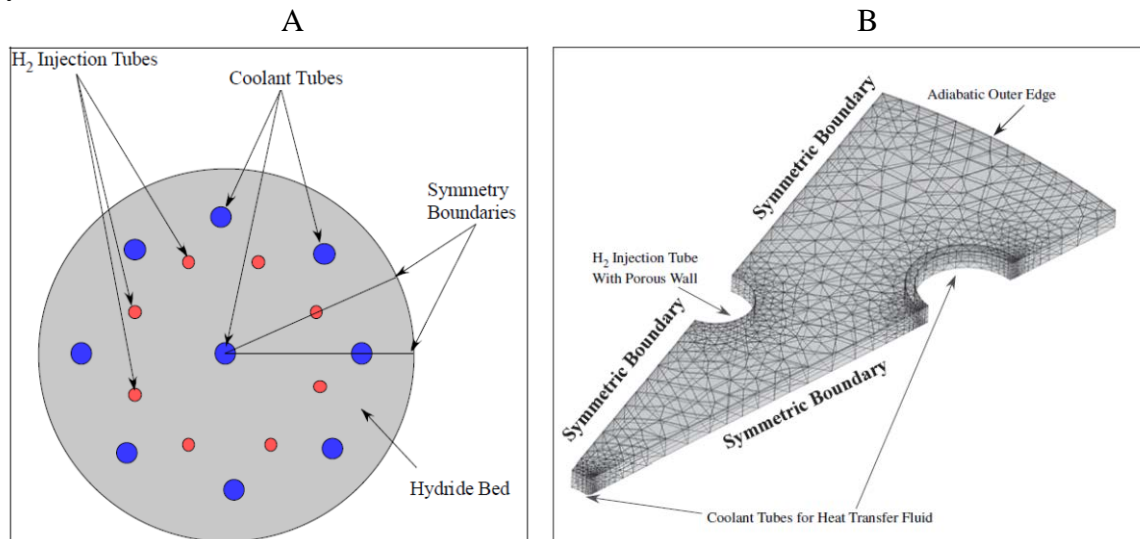


Figure 17: Cross section illustration and geometry slice of a NaAlH_4 vessel used for computation of 3-D model [33].

The results of the study concluded that the thickness of the fins had no significant effect on the overall loading times but did have an effect on the discharge rate. The improved discharge rate with increased fin thickness was attributed to having a more uniform temperature distribution in the hydride bed. As described earlier (see equations 2.1 and 2.2), the decomposition of NaAlH_4 involves a two-step process where there is an optimal temperature in the hydride bed to maximize the hydrogen decomposition needed from both reactions. Too rapid a decomposition of NaAlH_4 can cause bed cooling which can lower the kinetic rate needed for the decomposition of Na_3AlH_6 to NaH . While adding fin thickness was found to improve the discharge rate of the system in the study, it also found that this was at the expense of additional vessel weight and increased volume for the system. In another

part of the study the influence of adding more cooling tubes was also examined. For all of the cases examined finned tubes were found always to be superior to finless tubes. The study found that increasing the number of tubes to 82 for a finless system and 25 for a finned system did improve the amount of hydrogen released, but again at the expense of a decrease in volumetric and gravimetric capacities of the storage system. Each system design would have an optimum number of finned tubes to maximize the systems volumetric and gravimetric capacities. For loading it was determined that the rate was limited by kinetics of the materials alone and improvement to the kinetics of the material or another material would be required to achieve DOE charging times.

In a follow-on modeling study conducted by UQTR and SRNL, the thermal efficiency of a multi-tubular reactor with longitudinal fins as thermal enhancers was investigated [34]. Figure 18 shows multi-tube reactor configuration used for the analysis. The objective of the study was to evaluate the effect of the geometrical properties of the longitudinal fins such as their number, their thickness and their interconnectivity with the hydride tubes on the charging process and still taking into account the compromise between the optimization of the hydrogen loading rate with the mass and volume of the storage system.

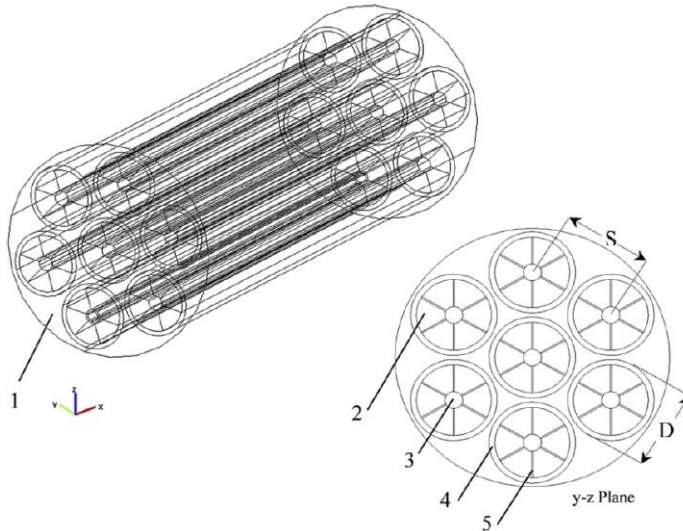


Figure 18: Multi-tubular reactor configuration: (1) coolant media, (2) hydride bed, (3) hydrogen filter, (4) reactor element, (5) longitudinal fin.

The result of this study, using Ti-doped NaAlH_4 , found similar results to the previous study [33] for the number of fins and their thickness. This study found that fin thickness had only a marginal effect on the hydrogen loading rate and that a change of the number of fins on the reactor element from 6 to 12 resulted in only a small improvement in thermal management but increased the overall mass of the storage system by about 6%. However, the study did find that the tip clearance (the clearance between their tips and the inner surface of the tubes) was a major parameter affecting the performance of the hydrogen storage system. During charging, heat is transferred from the fin surface through the fin tip to the bend radius of the cooling tube wall. Any increase in the tip clearance can result in an increase in the heat transfer resistance and hence a decrease in the amount of hydrogen that can be stored in a given time. During the study, it was found that the weight fraction of stored hydrogen could

be increased by 26% after 720 s of charging for the case with perfect contact versus a 0.1 cm tip clearance.

In the final analysis performed by UQTR and SRNL, a novel metallic honey-comb structure was considered as the heat exchanger in a metal hydride storage bed [35]. An example of the type of honey-comb material and a schematic of the material in a NaAlH₄ storage system is shown in Figure 19.

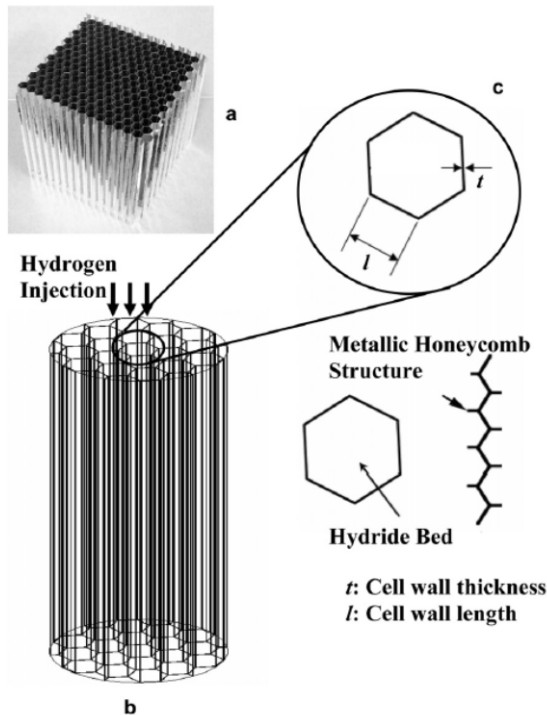


Figure 19: An example of a honeycomb core. Cell size: 0.952 cm (3/8 in) [37] (a), schematic of (b) the alanate hydride storage system, and (c) hexagonal honeycomb metallic structure.

In previous studies by both SRNL and UTRC [17, 19, 23], open-celled aluminum foam was used to enhance the heat transfer in metal hydride beds. Recent advances in low-cost processing have enabled the fabrication of honey-comb structures with different cell sizes. These cellular materials offer a lower cost alternative to foam materials but still providing light weight and excellent heat transfer properties. A two-dimensional heat transfer model of a metal hydride storage system employing an aluminum honey-comb heat transfer structure was evaluated. The effect of cell wall length on the hydrogen charging process was numerical evaluated and is summarized here.

An initial analysis was performed both with and without external cooling of the storage vessel. When the storage media was isolated from external cooling, changing the cell wall length from 2.54 to 0.952 cm had no significant effect on the loading rate and the hydrogen uptake was slow. If the honey-comb is connected to the external cooling surface a significant improvement is observed especially at the shorter cell lengths. However, the loading rate was found to still be less than expected and the addition of circular and hexagonal cooling tubes to the system was examined. It was found that using the smallest cell length (0.952

cm), where the coolant flows through the hexagonal tube versus a circular tube led to faster charging rates and the highest volumetric and gravimetric system capacities. Further improvements were obtained with thinner cell wall honey-comb structures and that good thermal contact between the hydride powder and the wall was necessary.

Additional detailed modeling activities were also carried out in the HSECoE by GM. These efforts which will be summarized briefly here were combined with system modeling activities, which will be discussed in more detail in the next section of this report. In one study [36], GM evaluated refueling dynamics and the temperature distribution inside the bed of a NaAlH_4 hydrogen storage system using a two-dimensional finite element model. A refueling target of 10.5 minutes was selected and an overall heat transfer coefficient was calculated from the 2-D model for later use in a lumped parameter system level model. A schematic of the storage bed configuration used by GM is shown in Figure 20. The thermal conductivity of the material used in the analysis was 8.5 W/m K and was assumed to contain ENG or other enhancement additives.

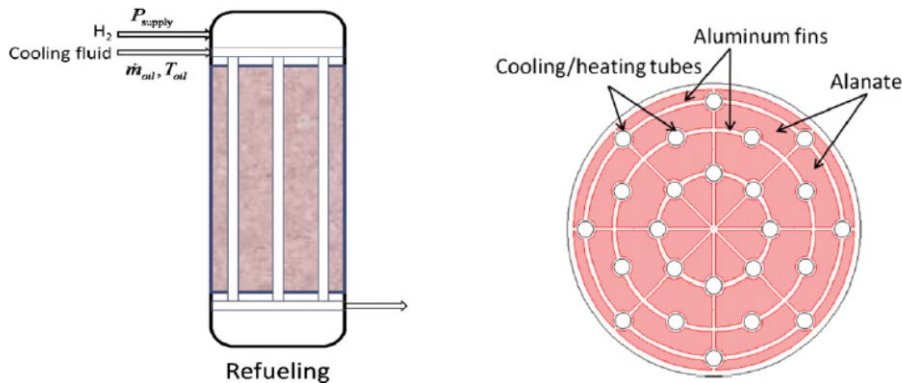


Figure 20: Schematic of NaAlH_4 hydrogen storage bed showing profile and cross-sectional views

During the GM study the sensitivity of the system is analyzed for the following parameters: 1) initial bed temperature, 2) bed pressure, 3) coolant flow temperature, 4) coolant flow rate, and 5) thermal conductivity. The study found that weight fraction of hydrogen absorbed increase with increasing temperature due to improved kinetics but that care must be taken to avoid the tetra-hydride (NaAlH_4) melt temperature of around 180°C . Increasing supply pressure from 100 to 300 bar also increased the amount of total hydrogen absorbed but it was found that at high initial bed temperatures, the use of higher supply pressure would cause the bed temperature to exceed the melt temperature of the tetra-hydride. A similar observation was observed by the UQTR and SRNL study [34]. Coolant flow from values of 10 to 50 l/min were analyzed and it was found that even though the heat transfer rate increased with coolant flow rate the amount of hydrogen absorbed was highest for a middle value of flow rate of 25 l/min. Again this was due to the relationship between optimum kinetics and bed temperature. At lower flow rates the bed becomes too warm and the absorption kinetics slow down. At higher flow rates the bed cools too low and the kinetics also slow down. A similar observation was made in the UQTR/SRNL study [34], where the effect of coolant velocity from 0.5 to 8 m/s was examined during bed charging. The results indicated that the hydrogen

bed weight fraction increased with increasing flow velocities from for 0.5 to 2 m/s but the amount of stored hydrogen began to decrease when flow velocities increased from 2 to 8 m/s. Lower bed temperatures and slower kinetics were also mentioned as the reason. Both the GM study [36] and the UQTR/SRNL study [34] also examined the effect of coolant temperature on the amount of hydrogen absorbed. Both studies found a middle value as the best coolant temperature that was able to maintain an optimum bed temperature to maximize the kinetics and hence the amount of hydrogen absorbed. The values for the best coolant temperatures for hydrogen uptake from the GM and the UQTR/SRNL were 107 °C and 115 °C, respectively, which shows excellent agreement despite somewhat different material formulations and system configurations.

The thermal conductivity of pure NaAlH₄ is in the range of 0.1 to 1.0 W/m K, depending on the packing density. As described earlier in this report the addition of aluminum or graphite to the NaAlH₄ material was found to increase the thermal conductivity by an order of magnitude [29]. The GM study [36] examining the effect of increased thermal conductivity on weight fraction of absorbed hydrogen found that at thermal conductivity values of 2 W/m K and lower the amount of hydrogen absorbed in a given time was poor. Increasing the thermal conductivity to 8.5 resulted in increased bed hydrogen weight fraction but at values higher than 12 W/m K the bed hydrogen weight fraction began to drop. Again this is believed to be caused by a lowering of the bed temperature below an optimum value. The effect of thermal conductivity during hydrogen charge and discharge was also examined by UQTR/SRNL [33] and compared to cases with and without longitudinal fins. It was found that the amount of hydrogen charged and discharged to a hydride bed increased with increasing thermal conductivity for the case without fins up to 5.2 W/m K, which was the maximum value reported, but that no appreciable improvement was found in the case with fins.

Another GM study [37] compared three different metal hydride heat exchanger designs using refueling simulations performed in COMSOLTM for various sets of geometric design parameters. In order to avoid setting up the geometries and other parameters repeatedly, a COMSOL-MATLABTM interface was used to automate the process. All of the designs used Ti-doped NaAlH₄ as the surrogate material and for each case refueling was set at 150 bar and for 10.5 minutes. Each design was modeled and optimized to achieve good heat transfer rates with minimum heat exchanger mass and volume. The heat exchanger designs considered were: 1) shell and tube with NaAlH₄ in shell, 2) helical coil and 3) shell and tube with NaAlH₄ in tubes.

The shell and tube design with NaAlH₄ in the shell selected for this study was the previous GM design shown in Figure 20. During the study the effects of varying bed diameter, fin thickness, placement of cooling tubes and cooling tube diameter were examined. The results showed that increasing the bed diameter led to higher than wanted bed temperatures. For the cooling tube diameters evaluated (0.015 and 0.020 m) the results showed only a slight effect on the beds gravimetric capacity. Very thin fin thicknesses (0.0015 m) were found to insufficiently cool the bed for the cooling rate selected while thicker fins (0.0025 m) added weight and to a lesser extent volume to the overall system. Figure 21 adapted from Table 1 in reference [37] shows case 3 as having the best gravimetric and volumetric densities and

still satisfying bed temperature constraints for the shell and tube design with the metal hydride in the shell.

Table 1 – Effect of different geometric parameters on the system level targets.

	Case 1	Case 2	Case 3	Case 4	Case 5	Case 6	Case 7	Case 8
Bed radius (m)	0.1847	0.1644	0.1847	0.205	0.225	0.2456	0.1842	0.1852
r1 (m)	0.1656	0.1472	0.1656	0.184	0.2024	0.2208	0.1656	0.1656
r2 (m)	0.1242	0.1104	0.1242	0.138	0.1518	0.1656	0.1242	0.1242
r3 (m)	0.0675	0.06	0.0675	0.075	0.0825	0.09	0.0675	0.0675
Fin thickness (m)	0.002	0.002	0.002	0.002	0.002	0.002	0.0015	0.0025
Tube thickness (m)	0.002	0.002	0.002	0.002	0.002	0.002	0.0015	0.0025
Tube diameter (inner) (m)	0.02	0.015	0.015	0.015	0.015	0.015	0.015	0.015
Length of the bed (m)	1	1	1	1	1	1	1	1
Weight fraction H ₂ absorbed	0.0316	0.0298	0.031	0.03	0.0281	0.0254	0.0308	0.031
Maximum temperature (K)	488	456	491	516	537	550	505	470
Mass of HEX (kg)	29.9	26.02	28.93	31.85	34.76	37.76	21.73	36.12
Mass of alanate (kg)	88.56	71.03	92.21	115.99	142.35	171.3	94.3	90.13
Total mass (kg)	118.45	97.05	121.14	147.84	177.11	208.96	116.03	126.25
Total volume (m ³)	0.107	0.085	0.107	0.132	0.159	0.189	0.107	0.108
H ₂ stored (kg)	2.798	2.117	2.859	3.480	4.000	4.351	2.904	2.794
Weight of H ₂ stored per unit weight of bed ^a (kg/kg)	0.0231	0.0213	0.0231	0.0230	0.0221	0.0204	0.0244	0.0217
Weight of H ₂ stored per unit volume of bed ^a (kg/L)	0.0261	0.0249	0.0267	0.0264	0.0252	0.0230	0.0272	0.0259

^a Includes only the alanate and the heat exchanger, the containment vessel is not included. Hydrogen in the gas phase is not included.

Figure 21: Table showing the effect of different geometric parameters on the system level targets for a shell and tube heat exchanger configuration with NaAlH₄ in the shell, adapted from [37].

An alternative shell and tube design using a helical coil as the coolant tube (see Figure 22) was also evaluated by GM [37]. During the study the gravitational and volumetric capacities were compared after 10.5 minute loadings for cases which varied the shell radius, helical radius and helical pitch. For the range of conditions studied only small changes in the weight fraction of hydrogen absorbed were observed with only less than a 5% decrease in hydrogen weight fraction absorbed by decreasing the vessel radius (from 0.045 to 0.40 m). Increasing the vessel diameter also showed a moderate decrease in hydrogen weight fraction. Overall the helical coil design was reported to have a reduced heat exchanger weight compared to the shell and tube design discussed previously and shown in Figure 20. The helical coil was reported to be 7% of the NaAlH₄ material loaded in the vessel compared to greater than 30% of the weight of the NaAlH₄ for the shell and tube configuration shown in Figure 20.

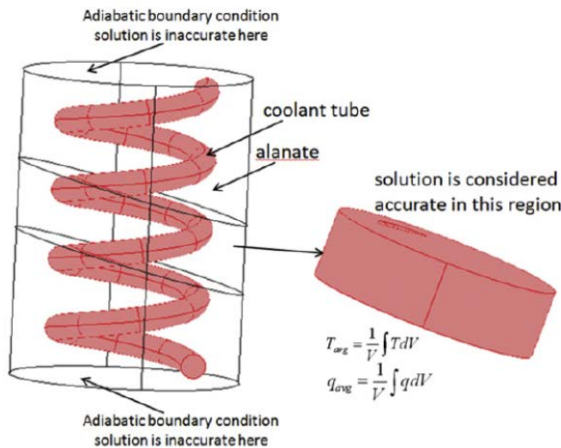


Figure 22: Helical coil heat exchanger design (adapted from [37])

The third design examined by GM [37] involved a shell and tube design with the NaAlH₄ residing in the tubes and the heat transfer fluid flowing through the shell. This design is similar to the experimental testing configuration reported on earlier performed by GM/SNL [22] and GKSS [24] and shown in Figures 5b and 5c, respectively. A schematic of this type of system modeled by GM [37] is shown in Figure 23.

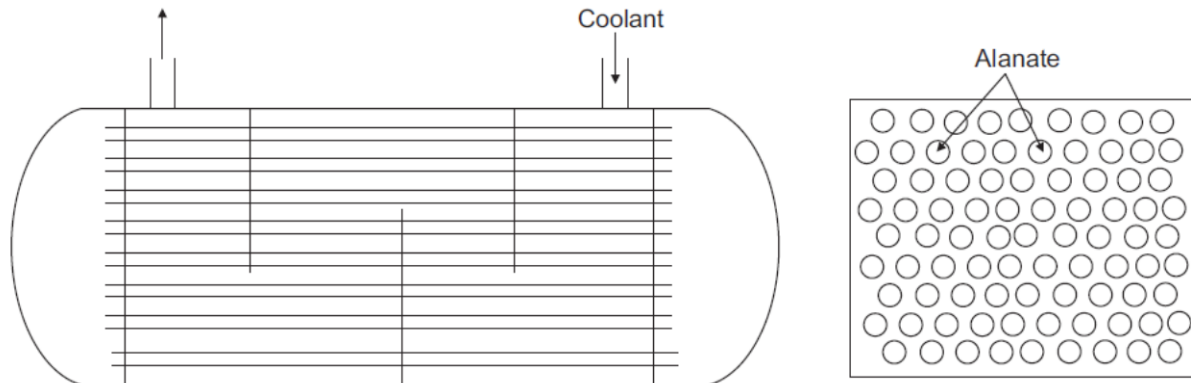


Figure 23: GM shell and tube heat exchanger schematic with NaAlH₄ in tubes.

The GM study for the system shown in Figure 23 only optimized the system for tube diameter. The tube thickness was fixed by the required strength of materials as the diameter varied and the spacing was fixed at 10% of the tube diameter. From the analysis, which varied the inner tube diameter from 0.035 to 0.070 m, a tube inner diameter of 0.050 m appeared to be optimal with respect to the weight fraction of hydrogen absorbed at the maximum temperature in the tubes. This configuration typically leads to high heat transfer rates, especially for small diameter tubes, but a major problem with this configuration when scaled to a system level is the weight of the heat transfer fluid residing in the shell. A system analysis was carried by GM for a 5.4 kg of usable hydrogen system with the configuration shown in Figure 23. The design consisted of 81, one-meter long tubes arranged in a 9 x 9 staggered grid arrangement with 3 mm spacing between the tubes. The heating oil mass required to heat the entire shell side was calculated to be 286 kg, which is more than 30% of the total system mass. A driving scenario was proposed to reduce the oil weight by 1/9th by dividing the storage system into 9 modules and using the oil to heat each module one at a time until each module was empty. This arrangement, however, adds additional complexity in terms of additional piping and valves to the system.

The above analysis pointed toward the helical coil design as having the highest gravimetric and volumetric densities over the other two designs. However, the example of the weight of the oil in the shell points to the need to evaluate some of the better design concepts with overall system analyses that include the weight and volume contributions from the other balance of plant (BOP) components. In the next section the HSECoE metal hydride system modeling effort will be discussed and how using what information from the more detailed heat transfer models can be applied to lumped parameter system models to not only predict weight and volume system information but also performance data against various driving cycles and other vehicle operations.

3.2.3 System Models

In the previous section of this report a number of detailed numerical models were described for different media-based storage systems. However these models are restricted to a specific storage media and vessel geometries, which include placement and function of heat transfer elements. While useful for evaluation of particular storage system designs, the analyses in the literature are not suitable for general systematic assessment of storage vessel/media configurations against a set of performance targets. The detailed models also require time to develop and run. As part of the HSECoE modeling effort, it was found useful to have simplified models that can quickly estimate optimal loading and discharge kinetics, effective hydrogen capacities, system dimensions and heat removal requirements. Parameters obtained from these models can then be input to the detailed models to obtain an accurate assessment of system performance that includes more complete integration of the physical processes. This next section of this report will describe the methodology developed for conducting such system models across the HSECoE and present some of the performance results from studies focused on metal hydride systems [38].

To meet the objectives of the HSECoE there was a need to quickly and efficiently evaluate various material-based storage systems and to compare their performance against DOE light duty vehicle targets. To accomplish this task a modeling approach was created that enabled the exchange of one hydrogen storage system for another while keeping the vehicle and fuel cell systems constant [38]. Figure 24 shows a block diagram of the modeling “framework” that was used for system evaluation and comparison by the HSECoE. The framework was used to implement the integrated power plant and storage system model (IPPSSM) approach described previously in this report and depicted in Figure 12.

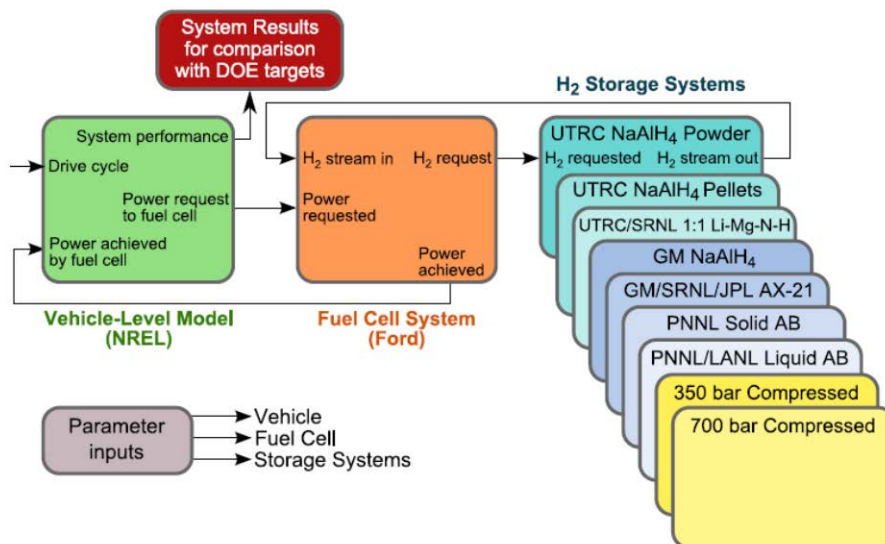


Figure 24: HSECoE framework system model showing main blocks, inputs, outputs and a sample of storage systems that were implemented [38].

The framework shown in Figure 24 was implemented using a commercial software platform, Simulink^R. The vehicle-level model was developed by NREL based on their HSSIM (Hydrogen Storage SIMulator) which was originally developed to simulate hydrogen fuel cell vehicle running on compressed gas tanks. A standard mid-sized vehicle class was

selected that included a 100kW electric motor and a 20kW/1kWh battery to capture regenerative braking and provide minor propulsion assistance. The vehicle glider weight (excluding the hydrogen storage system) was 1610 kg. More specific details on the vehicle characteristics can be found in [38]. The fuel cell system was developed by Ford and is based on an 80kW net stack operating at 80 °C. The fuel cell efficiency was consistent with the DOE fuel cell system targets for 50% efficiency at rated power and 60% at quarter power. The fuel cell model included only the essential elements to interface with the vehicle and the hydrogen storage blocks. These included a polarization curve to translate vehicle power to hydrogen required, parasitic power from the compressor and stack temperature to provide waste heat.

Examples of some of the different storage systems evaluated by the HSECoE in the framework model are shown in Figure 24. These included various metal hydride, chemical hydride and adsorbent storage systems in addition to compressed gas systems, which were included to benchmark the other systems. In this report only the evaluation of the metal hydride storage systems led by UTRC and GM will be discussed. Most of the metal hydride storage systems involved NaAlH₄ because of its existing material property data and previous modeling studies. The use of a common storage media also allowed for a good comparison of different engineering concepts and configurations on the systems performance.

In addition to the storage, fuel cell, and vehicle systems, the HSECoE team also developed a standard matrix of test cases to exercise the different hydrogen storage systems against the DOE performance targets. The test cases made use of 5 EPA fuel economy drive cycles shown in Figure 25. Cases 1 through 4 are looped until the storage system can no longer provide the required hydrogen flow rate. Case 1 is used to determine if the storage system can provide its required 5.6 kg of usable hydrogen to the vehicle. It uses a 55%/45% weighting factor between UDSS (city) versus HWFET (highway) driving. Case 2 uses the US06 (aggressive) drive cycle to confirm the storage system can deliver the DOE peak flow of 1.6g-H₂/s to the fuel cell. Case 3 (cold case) is used to evaluate the storage systems performance for -20 °C cold startup scenarios. Case 4 (hot case) runs the system at 35°C with SC03, the EPA air conditioning test conditions. Case 5 tests for dormancy of the storage system for cryogenic systems and was not used for the metal hydride systems in the framework.

Table 2 – Test cases for exercising the storage system. All of these, with the exception of case 5, have been implemented in the framework. Case 5 is tested offline for the relevant systems, such as those that require cryogenic operating conditions.

Case	Test Schedule	Cycles	Description	Test Temp (°F)	Distance per cycle (miles)	Duration per cycle (minutes)	Top Speed (mph)	Average Speed (mph)	Max. Accel. (mph/sec)	Stops	Idle	Average H ₂ flow (g/s)	Peak H ₂ flow (g/s)	Expected Usage
1	Ambient drive cycle - Repeat the EPA FE cycles from full to empty and adjust for 5 cycle post-2008	UDDS	Low speeds in stop-and-go urban traffic	75 (24 °C)	7.5	22.8	56.7	19.6	3.3	17	19%	0.09	0.69	1. Establish baseline fuel economy (adjust for the 5 cycle based on the average from the cycles) 2. Establish vehicle attributes 3. Utilize for storage sizing
		HWFET	Free-flow traffic at highway speeds	75 (24 °C)	10.26	12.75	60	48.3	3.2	0	0%	0.15	0.56	
2	Aggressive drive cycle - Repeat from full to empty	US06	Higher speeds; harder acceleration & braking	75 (24 °C)	8	9.9	80	48.4	8.46	4	7%	0.20	1.60	Confirm fast transient response capability – adjust if system does not perform function
3	Cold drive cycle - Repeat from full to empty	FTP-75 (cold)	FTP-75 at colder ambient temperature	-4 (-20 °C)	11.04	31.2	56	21.1	3.3	23	18%	0.07	0.66	1. Cold start criteria 2. Confirm cold ambient capability – adjust if system does not perform function
4	Hot drive cycle - Repeat from full to empty	SC03	AC use under hot ambient conditions	95 (35 °C)	3.6	9.9	54.8	21.2	5.1	5	19%	0.09	0.97	Confirm hot ambient capability - adjust if system does not perform function
5	Dormancy test	n/a	Static test to evaluate the stability of the storage system	95 (35 °C)	0	31 days	0	0	0	100%	100%			Confirm loss of useable H ₂ target.

Figure 25: Test cases for exercising the storage systems using various EPA fuel efficiency drive cycles (taken from Table 2 in [38])

Both GM [36, 37, 39 and 40] and UTRC [38] led system modeling activities for several of the hydrogen storage systems shown in Figure 24. These lumped parameter models incorporated input from detailed transport models to test the storage system's ability to meet fuel cell demand for different drive cycles and operating conditions. These simulations provided a rapid way to evaluate and compare different storage systems for onboard vehicle application against DOE targets. Several of GM's system simulations used a shell and tube, vessel configuration similar to what is shown in Figure 20. This vessel design was used to evaluate the performance of both NaAlH₄ and a high-pressure, intermetallic, metal hydride material (Ti_{1.1}CrMn) [40]. A schematic flow chart of the high-pressure Ti_{1.1}CrMn system in a vehicle is shown in Figure 26. Ti_{1.1}CrMn only has a hydrogen absorption capacity of 1.9 wt% but has the advantage of having a high volumetric energy density, good cold start capability and very fast kinetics. These advantages allow for a simple overall storage system where the waste heat from the fuel cell can be used to liberate the needed hydrogen for most conditions.

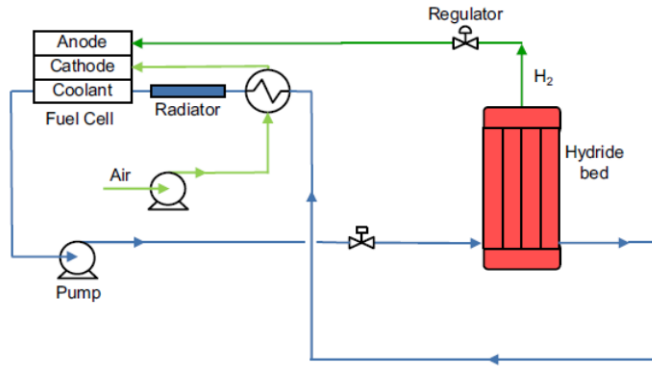


Figure 26: System flow chart of high-pressure metal hydride system

By comparison Figure 27 shows a flow chart for a NaAlH_4 -based system. Despite the higher hydrogen capacity (approx. 3.5 wt% reversible at selected conditions) the slower desorption kinetics in the NaAlH_4 material results in the need to add a catalytic burner, which burns some of the hydrogen, to liberate the hydrogen supplied to the fuel cell to meet its demand requirements. Also not shown in Figure 27 is the possible addition of a hydrogen gas buffer tank to accommodate cold start and some more rapid transient operations. The need for the buffer tank will depend on the amount of void or gas space incorporated into the NaAlH_4 vessel(s).

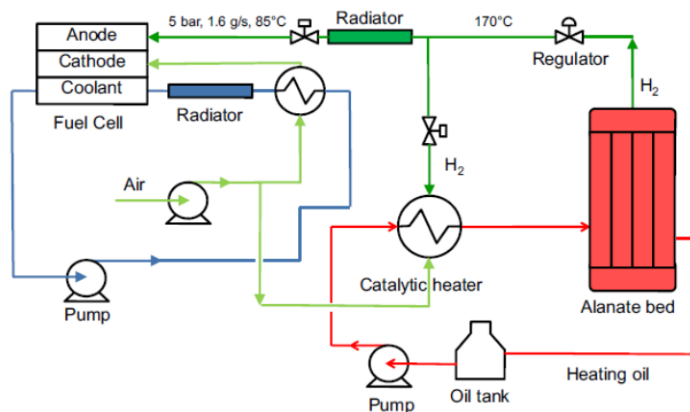


Figure 27: System flow chart for a NaAlH_4 storage system

The results from both refueling and drive cycle simulations were analyzed for the high-pressure $\text{Ti}_{1.1}\text{CrMn}$ system. The results for a full-scale automotive application indicate that a coolant flow rate of 360 l/min at 0 °C is required to charge the system in 5 minutes. Faster refueling rates on the order of 3.5 minutes were found to be possible but they would require doubling the coolant fluid flow rate or decreasing the fluid coolant temperature to -20 °C. Both a standard U.S. drive cycle (FTP75) and a more aggressive drive cycle (US06) were evaluated and both were found to be achievable with a radiator fluid flow rate of 12 l/min at 65 °C. The hydrogen gravimetric capacity of the storage system (only including the weight of the hydride, the aluminum fins and the coolant tubes) was found to be 1.45 wt%. The volumetric capacity of the system was around 0.05 kg H_2 /l.

A similar simulation study was conducted by GM [36] using the same vessel design shown in Figure 20 but using NaAlH₄ as the storage medium. Because of the slower absorption kinetics and higher heats of reaction it was found to be difficult to achieve a refueling time of less than 5 minutes for this material system. The cooling target was set at 10.5 minutes, which was 40% of the DOE 2010 target of 4.2 minutes. As shown in Figure 27, a hydrogen combustor and an oil heating loop is required for a NaAlH₄ system to provide the additional heat needed to liberate the hydrogen to meet the fuel cell and vehicle demand. For the simulation a 12kW catalytic burner was used with an assumed 90% burner efficiency. A buffer tank with 100 g of hydrogen at 150 bar and 27 °C was also included. Similar to the high-pressure metal hydride case several vehicle drive cycles were used to test the hydrogen storage system performance. For the standard drive cycle (FTP75) it was found that the NaAlH₄ bed could meet the drive cycle by providing 2.75 kg of net hydrogen to the fuel cell and another 885 g (or 24% of the available H₂) to the oil burner. A similar NaAlH₄ system developed by GM [39] was also evaluated in the HSECoE framework model. The system was comprised of two metal hydride beds with 2.75 kg of usable hydrogen to provide a total of 5.5 kg of hydrogen. The tanks were lined carbon composite tanks (Type III) operated up to 150 bar and 180 °C. Result obtained from testing with the standard drive cycle resulted in about a 16 h driving time utilizing all of the available hydrogen. Tests using the aggressive drive cycle resulted in 6 hours less of driving time and the inability of the system to provide all of the available hydrogen leaving over 25% of the hydrogen still in the bed. The estimated gravimetric and volumetric hydrogen capacities calculated for the overall system was estimated at 1.2 wt% and 0.0148 kg H₂/l, respectively. Table 9 compares some of the key material properties and system parameters for the TiCrMn and the NaAlH₄ systems.

Table 9: Comparison of Material Properties and System Parameters for TiCrMn and NaAlH₄ Systems (system values based on results obtained from framework model)

	TiCrMn	NaAlH ₄	DOE 2015
Material Properties			System Targets
Crystal density (kg/m ³)	6200	1400	
Bulk density (kg/ m ³)	4000 ¹	1000	
Reaction enthalpy (kJ/mole H ₂)	22	37 ² /47 ³	
Specific heat (J/kg K)	500	1230	
H ₂ gravimetric capacity (wt%)	1.9	3.7	
System Parameters			
System maximum temperature (°C)	65 ⁴	180	
System maximum pressure (bar)	500	150	
Effective thermal conductivity (W/m K)	9.5 ⁵	8.5 ⁵	
H ₂ gravimetric capacity (wt%)	1.2	1.2	5.5
H ₂ volumetric capacity (kg H ₂ /l)	0.03	0.0115	0.04
Charging time - 5.5 kg usable H ₂ (min)	<5	10.5	3.3
Onboard efficiency (%)	99	78	90

Notes:

1. assuming 0.35 void fraction
2. reaction enthalpy for tetrahydride

3. reaction enthalpy for hexahydride
4. based on maximum radiator coolant temperature
5. assuming the addition of graphite or other thermal conductivity enhancement

From the results in Table 9, it can be seen that despite only having about half of the material gravimetric capacity, the TiCrMn system generally outperforms the higher capacity NaAlH₄ material on a system level. The reasons for the poorer performance associated with the NaAlH₄ system is due to the material's higher reaction enthalpy and slow kinetics. This required burning some of the available hydrogen and adding a catalytic burner and other associated components to the system. Despite the somewhat better performance by the TiCrMn system neither system was found to meet all of the DOE targets, especially system gravimetric capacity. However, for NaAlH₄ and other high capacity complex hydride materials several solutions still exist to improve their system performance. Some of these include: 1) compacting the media to improve the volumetric density to reduce overall system size and weight; 2) reducing the operating pressure and temperature to take advantage of lighter weight vessels and components and 3) improving the material's kinetic properties and improving the efficiency of heat exchangers and catalytic burners to reduce the size of the BOP components. Unfortunately, with low gravimetric capacity materials like TiCrMn not many opportunities for engineering improvements exist. Future improvements are generally limited mostly to discovery and development of new higher capacity materials.

Additional system simulations were carried out by UTRC [38] with un-compacted and compacted NaAlH₄ and with a higher capacity Li-Mg-N-H complex hydride, often referred to as a 1:1 Li:Mg formulation. The 1:1 Li:Mg material has a reported [38] theoretical hydrogen capacity of 8.1 wt%. The vessel design was similar to the design shown in Figure 5a, which was a shell and tube heat exchange with aluminum radial disk-type fins with media located between the disks and coolant tubes running through the center of the disks. The target pressure was set at 100 bar at a maximum temperature of 170° C. A decision was made not to use a buffer tank but to utilize the void space in the pressure vessel as the buffer. The tank selected was a Type IV tank to further reduce weight over a Type III metal lined tank. All four of the drive cycles shown in Figure 25 were included as part of the testing. During the simulations it was discovered that insufficient void space existed during startup and additional tank volume had to be added. For the 1:1 Li:Mg study, the lack of available material data led to the need to make some additional assumptions. Some of the assumptions involved were to increase the kinetic rate to meet a 7 wt% hydrogen fill in 10.5 minutes and to assign the thermal properties of the tank to match that of the NaAlH₄ tank. More detail on the assumption used can be found in [38]. Under these assumptions, approximately 92 kg of Li:Mg material either in powder or pellet form would be needed to provide 5.6 kg of hydrogen to the fuel cell. It was also found for the cold case (case 3) an additional 90 l of tank space is required for both the powder and pellet systems to run from the cold (-20 °C) start. Table 10 compares the system capacities for the various systems tested in the study.

Table 10: Comparison of hydrogen gravimetric and volumetric system capacities for various materials and system configurations

	NaAlH ₄ powder	NaAlH ₄ pellets	1:1 Li:Mg powder	1:1 Li:Mg pellets
wt% H ₂	1.37	1.42	2.33	2.75
system wt (kg)	409	395	240	218
kg H ₂ /l	0.012	0.015	0.016	0.018
system vol (l)	480	377	348	311

The results shown in Table 10 for NaAlH₄ are similar to those found for the GM system. Some improvement to the gravimetric capacity is gained by eliminating the buffer tank and choosing a lighter Type IV tank. Media compaction was also shown to improve the volumetric capacity but not as much as expected due to a reduction in pore or void volume in the tank that has to be added back to meet startup conditions. The preliminary capacity results for the 1:1 Li:Mg (using all of the assumptions made) follow a similar trend to the NaAlH₄ results. Doubling the hydrogen capacity of the material resulted in somewhat less than a doubling of the system capacity. This is most likely due to the little or no change to the BOP components. For the volumetric capacity, only a 20-30% improvement was observed by using a 2X higher capacity storage material. This is most likely due to the fact that as the material becomes lighter and lighter to increase its gravimetric hydrogen capacity it also becomes less dense which adversely affects its volumetric hydrogen density.

Additional information on how the system models and other scoping analyses were used to select candidate material to develop and evaluate new design concepts (Phase 2) will be described in more detail in Section IV. Section IV will also describe the results of the “ideal” metal hydride analysis, which applied reverse engineering to determine the minimum essential metal hydride properties needed to meet the DOE 2015 targets.

3.2.4 Performance and Energy Analyses

In the previous section, it was shown how the integrated system model was used to evaluate the performance of various metal hydride hydrogen storage systems. The test matrix (shown in Figure 25) was structured to evaluate the performance of the storage systems against the technical targets under standard and realistic transient driving condition. The matrix was also designed to exercise a given system from full to empty to provide an understanding of its performance over the entire range of fill conditions. Therefore, the test cases were designed to repeat a drive cycle or set of drive cycles until the storage system being evaluated was empty. Standard drive cycles are typically not long enough to achieve this and would not even deplete a buffer tank in some systems. The important point here is that when evaluating the complex dynamics of hydrogen storage systems, this approach of repeating drive cycles to create test cases is critical to gaining the feedback necessary to refine and improve the systems. As briefly described earlier and shown in Figure 25, the test matrix includes five test cases. The first case combines repeats of the urban dynamometer driving schedule (UDDS) and the highway fuel economy test (HWFET) until the storage systems is depleted. This is used to determine the vehicle-level fuel economy and from that figure the vehicle range. The fuel economy is calculated using the current Environmental Protection Agency (EPA) five-cycle procedure of adjusting and weighting the UDDS and HWFET to provide one fuel economy figure that represents real-world use—it is not the raw figures that come directly from running the cycles. Similarly, the range is then calculated from the adjusted and

weighted UDDS and HWFET figure and not simply the miles achieved until the hydrogen storage system is empty. The test matrix was found to be a key in providing a means to evaluate the fuel economy, range, and other vehicle level performance feature of the storage systems on a common and comparable basis [41]. Table 11 shows the simulated fuel economy, range estimates and onboard efficiency, from case 1 of the modeling framework, for the NaAlH₄ and TiCrMn systems as well as the results for the 350 and 700 bar compressed gas systems for comparison. As can be seen, both of the metal hydride systems performed worse on a vehicle level compared to the physical storage systems due to their poor gravimetric capacity and low onboard efficiency for the case of the NaAlH₄ system.

In addition to providing high-level feedback on the performance and design of a given material system, tradeoff studies quantifying the relative range impacts resulting from changes to the storage system capacity and reductions to the vehicle glider mass were also performed. Figure 28 shows an example of results from the application of this type of study to the NaAlH₄ system. Two methods to increase the vehicle range were examined. In the first case the amount of hydrogen stored was increased from 5 to 6.4 kg, which unfortunately increases the overall vehicle mass and adversely affects the fuel economy and the acceleration rate of the vehicle. In the second scenario the glider (vehicle without engine, fuel cell, power electronics and storage system) mass was decreased by 50% showing an alternative method of reducing vehicle weight to achieve and improving vehicle range and performance.

Vehicle Results	Units	NaAlH ₄	NaAlH ₄	NaAlH ₄
Usable H ₂	kg	5	6.4	5.6
Glider Mass	Kg	900	900	450
Vehicle Mass	kg	1791	1924	1398
UDDS Fuel Economy	mi/kg-H ₂	46.6	44.9	52.6
HWFET Fuel Economy	mi/kg-H ₂	51.5	49.8	57.0
Combined Fuel Economy	mi/kg-H ₂	48.7	47.0	54.5
Range	miles	244	301	305
0 – 60 mph time	sec	10.8	11.3	9.3

Figure 28: Example of tradeoff study on hydrogen stored versus glider mass on vehicle range for a NaAlH₄ system

Other energy analyses on the various storage system designs were also performed to provide high-level estimates on the overall energy inputs required by a given system, including well-to-power-plant (WTPP) efficiency (%), cost of hydrogen at the station (\$/kg) and greenhouse gas (GHG) emissions (carbon dioxide equivalent) on a gram per mile basis. Examples of some of these analyses obtained from running the H2A Hydrogen Delivery Scenario Model (HDSAM) are shown below in Table 12. Use of HDSAM requires a specific hydrogen delivery scenario as well as specific information for each storage system. Tables 13 and 14 show the specific delivery and storage system information used for these analyses. Tables 11 and 12 show modeling framework and HDSAM results indicating that the metal hydride

systems investigated in general do not outperform compressed gas systems. The higher enthalpy of reaction for the NaAlH_4 results in lower efficiencies and additional system weight by requiring a catalytic burner and an associated oil loop. The high pressure TiCrMn system fares better in onboard efficiency but suffers from low gravimetric capacity. The TiCrMn system was not exercised through the HDSAM model, but due to the reasons discussed above, it is anticipated that this systems would perform better than the NaAlH_4 system on a WTW basis, but would still be below the physical storage systems in terms of well-to-power plant efficiency.

Table 11: Vehicle Performance results for NaAlH_4 and TiCrMn compared to Compressed Gas.

Hydrogen Storage System	Adjusted Fuel Economy (mpgge)	Range (mi) 5.6kg H ₂	Onboard Efficiency (%) UDSS/HFET	Gravimetric Density (wt. %)	Volumetric Density (g/l)
NaAlH_4	36.4	204	77	1.2	11.39
TiCrMn	45.9	257	100	1.1	26.53
350 bar Compressed Gas	49.9	280	100	4.8	17.03
700 bar Compressed Gas	49.9	279	100	4.7	25.01

Table 12: Vehicle WTW results for NaAlH_4 compared to Compressed Gas

Hydrogen Storage System	WTW H ₂ Cost (\$/kg)	WTW Energy Efficiency (%)	WTW GHG Emissions (g/mile)
NaAlH_4	\$7.32	44.1	198
350 bar Compressed Gas	\$4.26	56.7	197
700 bar Compressed Gas	\$4.71	54.2	208

Table 13: HSECoE Base Assumptions for HDSAM

Production: SMR (Steam Methane Reforming)
 Market: Sacramento, 15% Mkt. Penetration
 Plant (and Regeneration) 62 miles (100 km) from city gate
 Electricity: US Grid
 Large scale storage – Geologic, LH₂, Liquid
 Transport: Plant to City Gate Terminal
 GH₂ – pipeline
 LH₂, Liquid Carrier – truck
 Distribution: City Gate Terminal to Refueling Stations – Truck
 Refueling Station Size – 1000 kg/day max. (may be limited by one delivery per day or 9% coverage)

Table 14: Storage System Information Required for HDSAM Analysis

System weight, wt%, density, and volume
 Total and usable H₂ (5.6 kg)
 Venting rate and dormancy time
 System T & P at full and ¼ tank
 Energy used to release H₂
 System cost
 Cooling load at refueling station
 Fill time
 Fuel Economy (from HSSIM)

Because of the decision not to continue the metal hydride activities in the HSECoE beyond Phase 1, only a limited number of performance and energy analyses were carried out. The limited results obtained point to the common shortcoming of most metal hydride systems. The intermetallic systems (such as TiCrMn) generally perform well but are hampered by their very low gravimetric hydrogen capacity. On the other hand newly discovered complex metal hydrides (such as NaAlH₄, Mg-Li) often have to deal with slower kinetics, higher heat of reaction and lower volumetric capacities, which add complications to the storage system increasing their overall weight, volume and cost. More information on the characteristics needed for of an “ideal” metal hydride material to meet the DOE targets are presented in Section IV.

3.3 SYSTEM ELEMENTS, BOP COMPONENTS AND COST ESTIMATION**3.3.1 Enabling Technologies**

HSECoE efforts under Enabling Technologies aimed to identify, evaluate, and implement technologies in the areas of hydrogen purity/separation, fuel system sensors, containment/pressure vessels, insulation requirements and materials compatibility. During Phase 1 the major emphasis for metal hydride systems fell under containment/pressure vessels. Most of the metal hydrides considered by the HSECoE had no obvious hydrogen purity issues other than potential particulate contamination, which can normally be addressed

with suitable submicron filters. The only exception was for the Li-Mg materials, which have been reported to release ammonia under certain operating conditions. However, not enough data on the Li-Mg systems was available to provide a detailed analysis of a purification system. A preliminary system analysis for a Li-Mg system was carried out [38] and reported on briefly in Section III where the system's overall weight and volume took into account an estimate for an ammonia purification system.

Early during Phase 1, LANL initiated a project to see if a simple acoustical method could be used to assess the state of hydrogen charge in a metal hydride container. Unlike compressed gas containers, where the amount of hydrogen in a container can be derived from changing pressure, metal hydride systems typically exhibit a relatively flat pressure-composition relationship for a large portion of their charging range. This relationship, which is often referred to as the material's "plateau" pressure, makes it difficult to assess the amount of hydrogen in a material at any one time. The approach used by LANL [42] was to interrogate the solid hydride system with sound waves at different hydrogen charge states to see if the change in stiffness of the hydride material during charging could be correlated to a change in sound propagation and attenuation speeds. This initial work wanted to determine if inexpensive commercially available piezoelectric transducers could be used to measure the amount of hydrogen in a metal hydride system. Figure 29 below shows a schematic of a typical acoustical experimental setup and two of the small commercial metal hydride containers used for some of the testing. Preliminary results presented in Figure 30 show a clear difference in the amplitude of the acoustical signal over a frequency range from 0 to 300 kHz for the metal hydride containers that were either fully charged or discharged. Experiments in empty metal hydride containers filled only with argon or hydrogen gas and with different transducer placements showed that sound waves were coupling with the metal hydride and stainless steel container vessels and not due to secondary effects. Experiments repeated after a two week period showed good replication of results. Figure 31 shows the results from follow on testing at LANL in which different states-of-charge for a metal hydride bed were tracked using the acoustical sensor. Despite successful preliminary results, which include a submitted patent application, this work was cancelled due to the decision not to continue metal hydride activities into Phase 2 and due to other higher priorities in the other material storage systems in Phase 2.

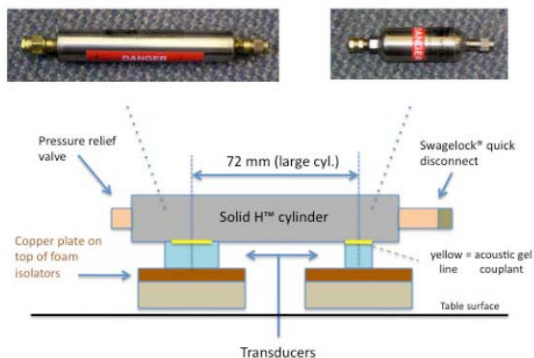


Figure 29: Schematic of the acoustical experimental setup for hydrogen fuel gauge testing

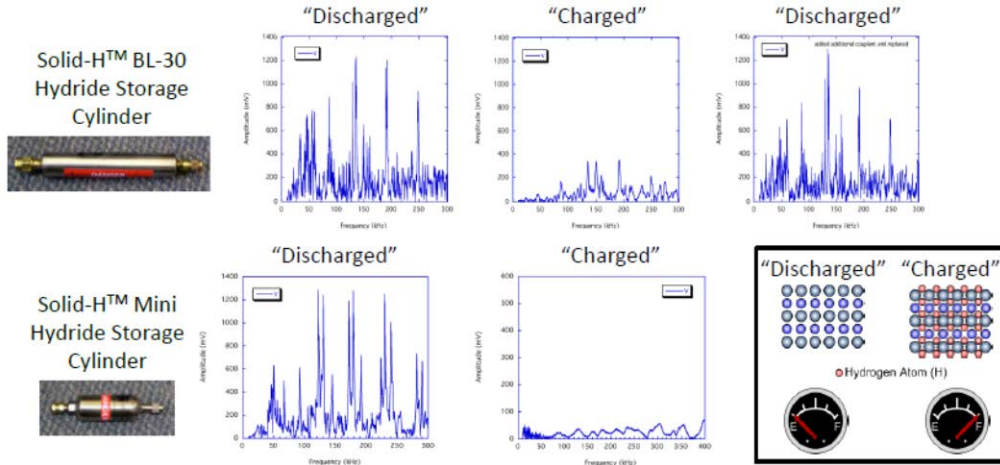


Figure 30: Preliminary results showing charged and discharged state of metal hydride containers

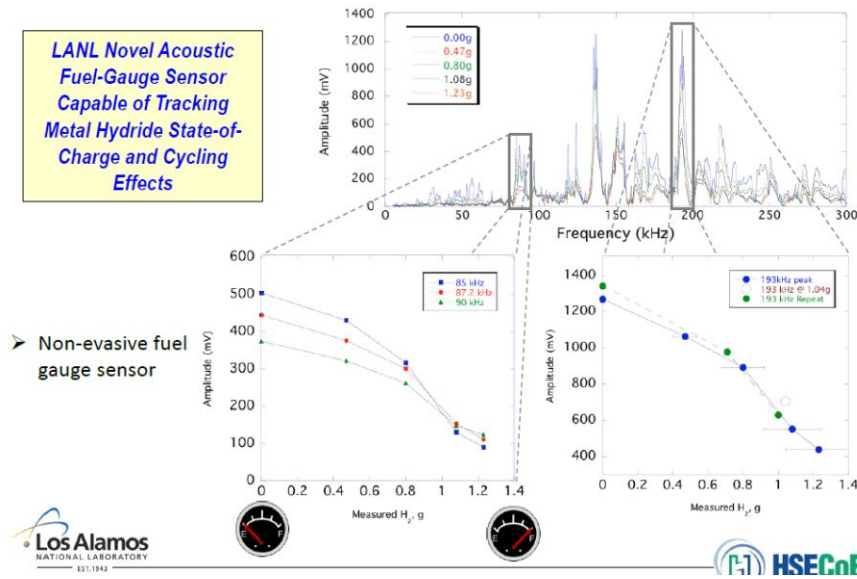


Figure 31: Proof of concept for acoustical hydrogen fuel gauge for a metal hydride system

Very few enabling technology issues involving insulation were identified for metal hydride systems. This is mostly because of the near ambient operating temperatures for most of the metal hydride systems. Standard insulation solutions appeared to be effective. As mentioned earlier in this section most of the efforts for metal hydrides involving enabling technology dealt with vessel containment/pressure vessels issues which will be discussed in more detail in the following section of this report.

3.3.2 Balance of Plant Tanks and Components

Working with the other HSECoE partners, PNNL led the effort under Phase 1 to develop a baseline mass, volume, and cost estimates for the metal hydride systems under consideration. During Phase 1, activities planned for Phase 2 were identified to minimize the BOP components and reduce the mass, volume and cost of the overall system. Based on input received from the MH System Architect and system modelers (such as system schematics

with predicted temperatures, pressures, and flow rates), the PNNL team then sized the appropriate components (valves, heat exchangers, etc.) and identified specific components from vendors. Using this information, a BOP Catalogue was developed which lists the device, volume, mass, cost, operating parameters, model numbers, and links to vendors. Dimensions and materials of construction were used to estimate the mass or volume for components which did not have the information available.

Based on guidance from the U.S. DRIVE Hydrogen Storage Tech Team, the storage systems were designed to be standalone and did not assume that any components from the fuel cell (i.e. radiator) or other vehicle systems could be shared. This limitation made the mass and volume projections larger than if the fuel cell, storage systems, HVAC, etc. were integrated. Figure 32 is a schematic of the metal hydride system that was used as the baseline system. The system is based on the NaAlH₄ system is similar to the NaAlH₄ system shown previously in Figure 27 but it includes more system and BOP component details.

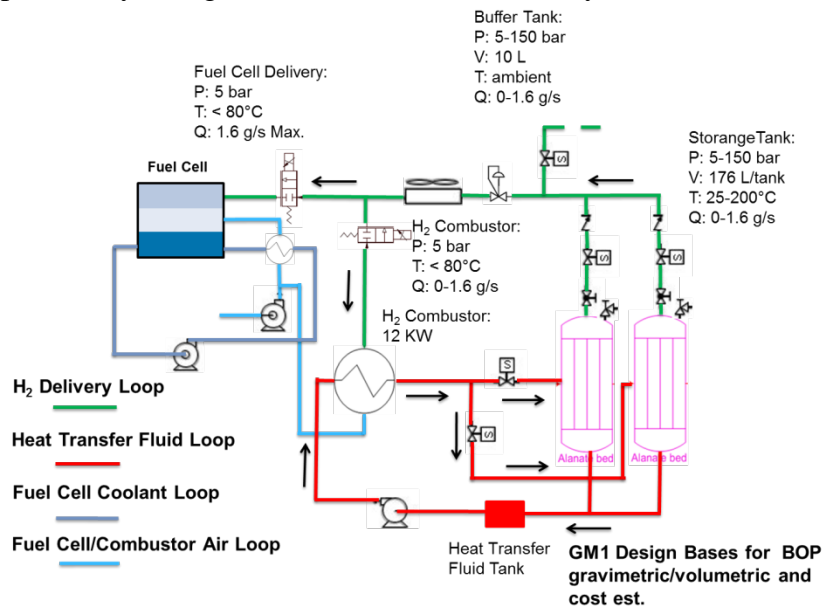


Figure 32: Baseline metal hydride system schematic

Figure 33 shows the mass and volume projections based on this bottoms-up approach along with the 2010 and 2015 targets for comparison. The mass of the system is dominated by the weight of the storage material but a considerable amount of mass is taken up by the storage vessel containers and internal heat exchangers (36% total). The oil pump and loop also represents 8% of the total system mass. For the volume projection, most of the volume (86%) is taken up by the storage vessels but other significant contributors include the oil pump/loop (5%) and the hydrogen buffer tank (3%).

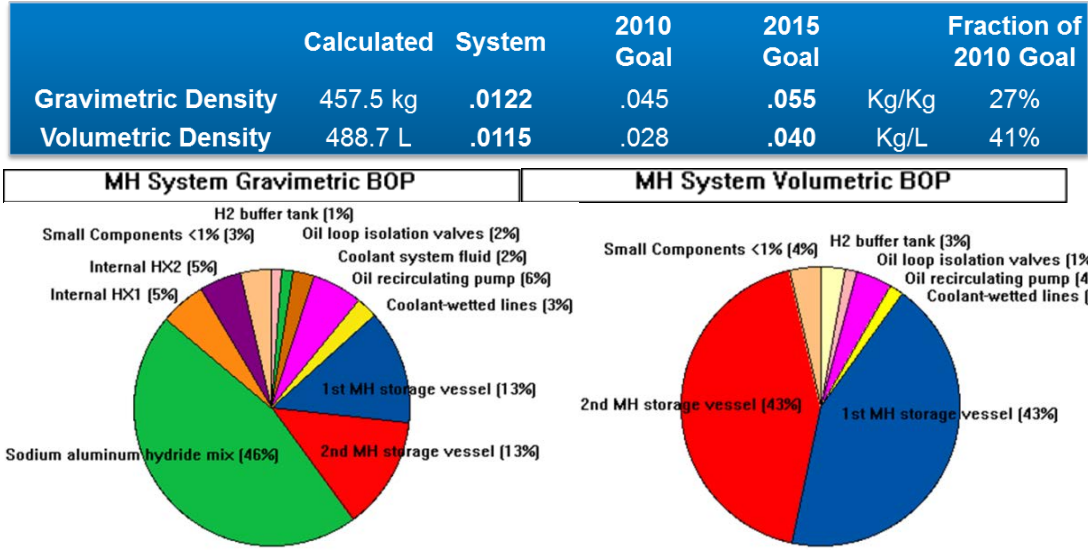


Figure 33: Baseline metal hydride system and BOP mass and volume projections

Some of the plans for Phase 2 were to improve on the mass and volume projections for future metal hydride systems. For the system mass a combination of improved tanks, BOP and heat exchanger designs were recommended. The baseline metal hydride system employed two Type III tanks, which included metallic liners. A combination of compacting the material to use a single tank, switching to a lighter weight, polymer lined, Type IV tank and reducing major BOP components like the weight of the oil pump and internal heat exchanger was expected to lead to a 50% reduction in the tank and BOP weight resulting in a 25% overall system gravimetric improvement. These same changes were also expected to realize a 25% volumetric system improvement. Further system mass and volume improvement can be realized by using higher capacity hydrogen storage materials with lower heats of reactions. Figure 34 shows the results of a system scenario analysis which doubled the materials gravimetric capacity, halved the material enthalpy and reduced the system to a single lighter weight tank. The scenario resulted in a metal hydride with a 54% and 50% reduction in gravimetric and volumetric density, respectively.

	Calculated	System	2010 Goal	2015 Goal		Fraction of 2010 Goal
Gravimetric Density	247.6 kg	.0226	.045	.055	Kg/Kg	50%
Volumetric Density	243.1 L	.0230	.028	.040	Kg/L	82%

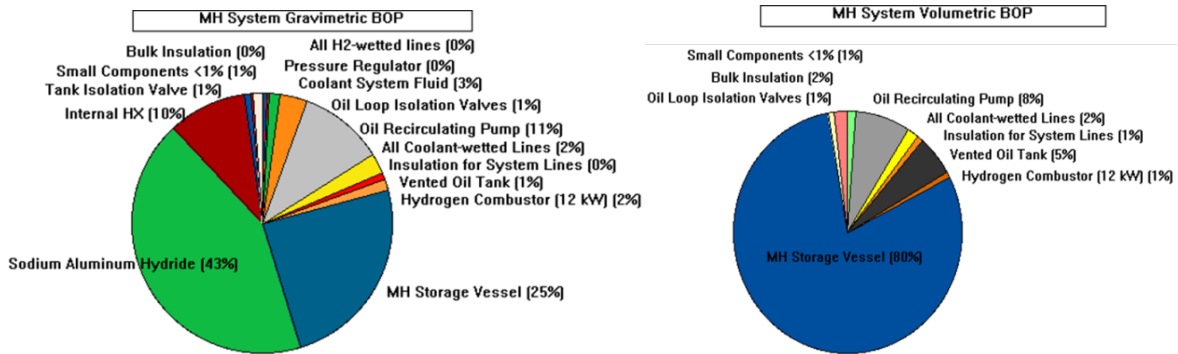


Figure 34: Reduced mass and volume scenario analysis for a metal hydride system

The design of suitable and reliable lightweight containers for future hydrogen storage systems was identified as a key objective of the HSECoE. To support this activity a series of carbon fiber and metal and polymer lined tank designs were analyzed using an ANSYS finite element model. The HSECoE needed to determine a realistic range of weights and volumes for the tanks. The initial model was developed using tables comparing different liner materials and pressure combinations that would give the system architects an initial estimate of tank weight and volume. The model was later refined by working with HSECoE partner, Lincoln Composites (currently Hexagon Lincoln) to provide a more detailed analysis to minimize the tank weight and volume. A simple computational tool for estimating the mass and material composition of cylindrical Type I, Type II, Type III and Type IV vehicular hydrogen storage tanks was developed and is available to the public on the HSECoE website (<http://hsecoe.org/models.php>). The tool is useful for cross-comparison of various pressure vessel types, to estimate gravimetric, volumetric, and cost performance of hypothetical tanks in the conceptual phases of design. The “Tankinator” tool provides an estimate of basic tank geometry and composition from a limited number of geometric and temperature inputs. This estimate covers the tank shell material only; all other component masses needed to be added to determine full system mass. The model uses finite element analysis to confirm that the wall thicknesses predicted by the estimation tool result in an acceptable stress state. More information on the “Tankinator” tool can be found at reference [43].

One of the BOP components evaluated during the Phase 1 activities for the HSECoE was the hydrogen combustor. An earlier study [44] on a NaAlH₄ system design estimated the hydrogen combustor at 9.3 liters and 22.3 kg. Oregon State University (OSU), one of the HSECoE partners, with world-class expertise in microchannel systems design was asked to look into this area to see if an alternative could be developed. Hydrogen storage involves coupled heat and mass transfer processes that are significantly impacted by the size, weight, cost, and performance of system components. Micro-technology devices that contain channels of 10-500 microns in characteristic length offer substantial heat and mass transfer enhancements by greatly increasing the surface to volume ratio and by reducing the distance that heat or molecules must traverse. These enhancements often result in a reduction in the size of energy and chemical systems by a factor of 5-10 over conventional designs, while attaining substantially higher heat and mass transfer efficiency [45]. In cooperation with the

OSU Microproducts Breakthrough Institute (MBI) and groups at PNNL, SRNL, and LANL, an alternative microchannel-based combustor was developed.

Combining the combustion and heat exchanger systems and the use of microchannels for enhanced heat and mass transfer was found to drastically reduce the size and weight required for this function, while simultaneously increasing efficiency. The OSU led team, using microchannel architecture, developed a test-cell microchannel combustor that had a projected system design of only 1 liter and 3.8 kg for the 12kW baseline metal hydride storage system. This is a 9X improvement in volume and 6X improvement in weight over a conventional design [44]. A substantial reduction in the combustor cost is also expected. A substantial safety benefit of a microscale combustor is that flames cannot be sustained in the sub-millimeter microchannels. Figure 35a shows a sketch of the integrated microchannel combustor/heat exchanger that would be used to safely and efficiently produce heated oil, which is used to discharge hydrogen from the storage bed. Figure 35b is a photograph of a unit cell used to experimentally validate the performance and size estimates of the integrated microchannel combustor. Testing of the single unit cell resulted in a measured efficiency of 92% (thermal energy transferred to the oil/chemical energy in the feed stream).

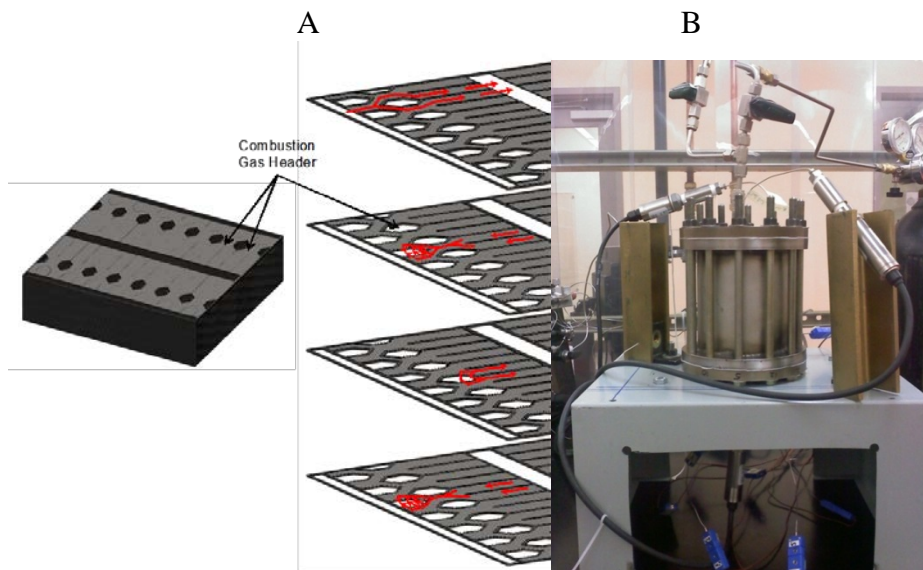


Figure 35: a) integrated microchannel combustor sketch and b) unit test cell.

3.3.3 Material and System Cost Estimation

In addition to evaluating performance and system capacities, another major objective of the HSECoE was to provide system cost estimates. This work was led by PNNL, which used both bottoms-up and top-down approaches to estimating the costs. Vendors identified in the BOP catalogue were contacted to provide estimates at production levels of 10,000, 30,000, 80,000, 130,000 and 500,000 units per year. Most manufacturers, especially valve manufacturers could not provide large quantity estimates because they didn't have the annual production capacity. Estimates that were provided became the basis for discounts and progress ratios to determine costs at the differing levels of production. Discounts were

applied to the vendor estimates if the cost estimate was from a distributor and not the manufacturer. Progress ratios were applied to account for scaling, learning, and OEM requirements [46]. These progress ratios were analogous to those used by the DOE in their fuel cell and tank cost estimates [44]. OSU provided the cost estimate for the combustor. Dynatek provided the tank price estimates. In addition, chemical manufacturers were approached for estimated prices of NaAlH_4 , TiCl_3 and expanded natural graphite. For the metal hydride (NaAlH_4), titanium dopant plus a carbon additive to increase thermal conductivity was used as the baseline material with a cost range of \$126 to \$9/kg. A summary of the estimated system costs for the baseline, NaAlH_4 system is shown in Table 15. For all the systems, the highest cost component was the storage vessel, with the hydrogen storage media a close second, and the BOP next. The cost estimate in Table 15 used the two-tank, baseline metal hydride system design and shows a baseline cost of \$42.9/kWh for high volume 500,000 per year production. A similar cost estimate was carried out using a single tank system design (also using a material with a 2X capacity improvement) resulted in cost of \$26.8/kWh for the same high volume 500,000 per year production case. For comparison the current DOE 2020 and Ultimate hydrogen storage system cost target are \$10/kWh and \$8/kWh, respectively.

Table 15: Metal hydride system cost across all production levels for baseline NaAlH_4 system case

	Production Amount				
	<u>10,000</u>	<u>30,000</u>	<u>80,000</u>	<u>130,000</u>	<u>500,000</u>
Total Costs	20,201	18,267	16,679	14,804	8,008
\$/kWh					42.9
Item	<u>10,000</u>	<u>30,000</u>	<u>80,000</u>	<u>130,000</u>	<u>500,000</u>
Tanks	5,187	4,652	4,250	4,073	3,756
Media	9,016	8,843	8,588	7,373	2,105
Media Cost/kg	39	38	37	32	9
Balance of Plant	4,347	3,307	2,570	2,290	1,817
Assembly	1,652	1,465	1,271	1,068	329

A previous cost analysis of a NaAlH_4 system by TIAX [44] estimated the system cost from \$11-\$14/kWh. Comparing the HSECoE results to the TIAX study found that the media costs were higher but on the same order as the previous studies. TIAX estimated sodium alanate costs at approximately \$5/kg although TIAX stated that manufacturer's indicated the cost of the processed mixture would be in the \$10/kg region. The HSECoE estimated the costs at \$9/kg at 500,000 units. The HSECoE media weighed approximately 40 percent more than the TIAX estimate. Also, one significant difference between the TIAX estimate and the HSECoE estimate was the requirement for two tanks instead of just one. The HSECoE price for one tank was estimated at approximately \$1,500 whereas; TIAX estimated their tank cost at

\$580. Media cost varied considerably on the source of Ti dopant used. If less expensive Type IV tanks were available and a single bed could be used a substantially lower system cost would be possible. Plans and activities to help lower these costs were planned for Phase 2.

BOP costs were much higher than TIAX, on the order of 3-5 times. BOP costs are shown in Table 16. The catalytic combustor as estimated by OSU was approximately 6 times more expensive than the TIAX combustor. The blower and flow controller added significantly to the dehydrating cost at \$113 and \$127 each, respectively. The blower estimate came directly from the manufacturer. The BOP associated with the heat exchangers in the two tanks also added significant cost at nearly \$650. The in-tank heat exchangers were estimated from an OSU heat exchanger model by analogy based on material costs and indirect costs. The heat exchanger to reduce the temperature of hydrogen flowing to the fuel cell was estimated directly from the OSU model. The oil pump and the isolation valves were the most expensive items adding \$270 and \$108 to system costs, respectively. The progress ratio for the pumps was pretty significant at 0.70 while the isolation valves progress ratio was 0.90.

Table 16: Cost estimates for metal hydride system balance of plant components

<u>Item</u>	<u>Quantity</u>	<u>Wt</u>	<u>10,000</u>	<u>30,000</u>	<u>80,000</u>	<u>130,000</u>	<u>500,000</u>	<u>Each</u>
BOP								
Internal to Tank heating fluid								
Oil Tank	1		94	78	66	61	49	49
Oil pump	1		808	459	277	216	108	108
Coolant Valve	2		157	133	114	106	86	43
Oil (Paratherm MR)	14 liters		63	58	54	52	47	3
Tubes	5	Meters	91	88	86	85	83	17
Isolation Valves	2		489	414	357	331	270	135
Hydrogen BOP								
blower for combustor	1		293	224	177	157	113	113
Catalytic Heater (12 kW)	1	0.95	740	504	358	302	188	188
Flow controller	2		291	291	291	255	255	127
H2 Lines	12	Meters	37	37	36	36	35	3
Pressure Transducer	1		50	43	37	34	28	28
Pressure Regulator	1		125	120	114	112	106	106
Valves								
Check valve	2		138	104	80	71	50	25
Pressure Relief Valve	5		388	263	186	157	97	19
Manual Valve	4		80	80	80	80	80	20
Pressure Gauge	1		21	20	20	19	19	19
Cooling H2 to ambient								
Heat exchanger to cool H2 to ambient	1		437	352	200	180	171	171
Buffer tank	1		44	41	38	36	33	33
Total BOP			4,347	3,307	2,570	2,290	1,817	

Figure 36 provides a breakdown by major system components. The media and the tanks comprise approximately 73 percent of total system costs. Valves add another 12 percent while other BOP provides 10 percent and assembly another 4 percent.

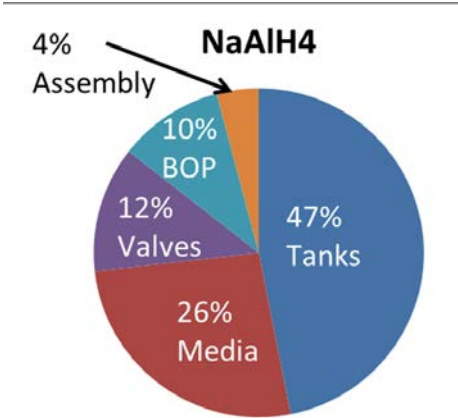


Figure 36: Cost breakdown major system components

Figure 37 compares the metal hydride system to other HSECoE Phase I system cost estimates. The metal hydride system costs (~\$42/kWh), because of its two tanks and large quantity of media, were almost twice as expensive as the solid AB system (~\$24/kWh) and almost 3 times more expensive than the higher pressure (200 bar) MOF-5 system (\$15/kWh). Valve costs were similar to the MOF-5 system.

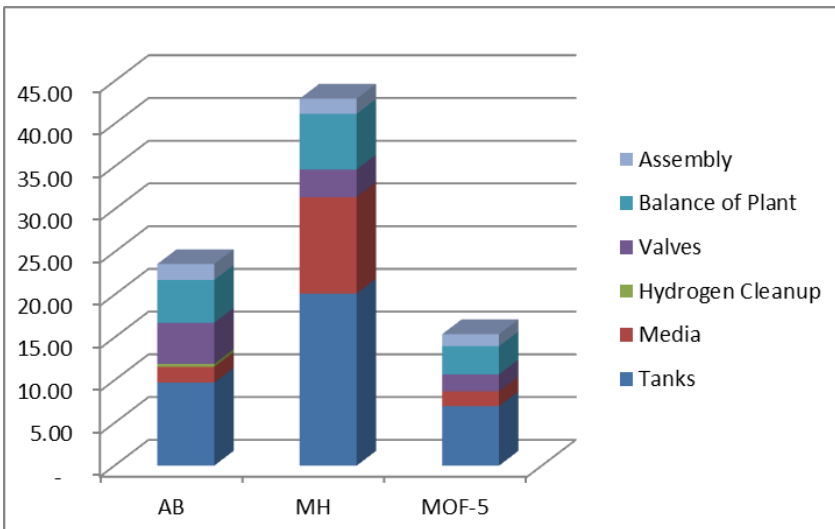


Figure 37: Comparison of Phase I system cost estimate

4.0 DISCUSSION AND SUMMARY

4.1 PHASE 1 TO PHASE 2 TRANSITION ANALYSIS

As described earlier in Section I of this report, the HSECoE program was divided into three Phases. Each Phase had an associated Go/No-Go decision point by DOE to assess the progress and the feasibility of achieving future technical objectives prior to moving on to the next phase. The objective of Phase 1 was to utilize an understanding of storage system requirements for light-duty vehicles and to begin the design of innovative system concepts and components. The Go/No-Go decision points for the HSECoE were organized by material systems. For the metal hydride material system the specific objective for Phase 1 were to: 1) obtain and collect engineering property data for existing metal hydride materials, 2) develop screening and more detailed transport models to assess the performance and cost of various metal hydride systems against DOE hydrogen storage targets, 3) create a baseline system using DOE 2010 targets to track future system improvements and progress, 4) down select the best metal hydride material systems for further engineering development and component testing going into Phase 2.

It has hopefully been shown, as described in this report, how the HSECoE attempted to achieve our Phase 1 objectives. Previously in Section 3.1 of this report, the collection and organization of engineering property databases for available metal hydride materials was described. Preliminary material property screening requirements were established and implemented. Also described were the engineering efforts used to enhance the capacity and heat transfer properties of various materials. Section 3.2 described the metal hydride HSECoE modeling activities. This included the development of the Acceptability Envelope Analysis and other screening tools to the development of more detailed 2D and 3D transport models and finally the creation and adaptation of the integrated framework system models to assess the systems performance against DOE targets. Section 3.3 describes some of the engineering and preliminary analyses of novel system and BOP components from an acoustical hydrogen fuel gauge to a microchannel combustor. Section 3.3 also calculated and categorized system and BOP component costs, weights and dimensions to arrive at a baseline metal hydride system to be used as a benchmark for future system development. Some of the tools created to look at various “what-if” scenarios to help define and prioritize the engineering tasks needed in Phase 2 have also been described.

Table 17 below lists the results of the analysis of the baseline NaAlH₄ metal hydride system (see Figures 30 and 31) compared to the DOE 2010 and 2015 storage targets. The table lists the baseline current values along with the 2010, 2015 and ultimate targets that were available at the time. Another way of examining these results is by plotting the results in a “spider” chart. Figure 36 shows such a “spider” chart with the percent of predicted attainment for the baseline system for each of the 2010 target values. A completely shaded circle would mean that the system was predicted to meet all of the 2010 targets. From Figure 38 it can be seen that the baseline system as configured can meet many of the targets associated with operation conditions such as maximum and minimum delivery temperatures and pressures as well as expected safety requirements. The targets that present the greatest challenges for the baseline metal hydride systems are gravimetric and volumetric density and fill time. These three areas

will be discussed in more detail below along with future material and system recommendations. Note that system cost was not included in the 2010 chart but will also be discussed briefly below.

Table 17: DOE 2010 and 2015 System Targets Compared to SAH Base Case Model Results

Prioritized Technical Targets: On-Board Hydrogen Storage Systems				
Prioritized Target	Units	2010	2015	Ultimate
* Permeation & Leakage	scc/hr			
* Toxicity				
* Safety				
1 Gravimetric Density	kg H ₂ /kg System	0.045	0.055	0.075
2 Min. Delivery Temp.	°C	-40	-40	-40
3 Max. Delivery Temp.	°C	85	85	85
4 (PEMFC) Min. Delivery Pressure	bar	5	5	3
5 Max. Delivery Pressure Min. Operating	bar	12	12	12
6 Temperature Min. Operating	°C	-30	-40	-40
7 Temperature Max. Operating	°C	50	60	60
8 Min. Full Flow Rate	[g H ₂ /s]/kW	0.02	0.02	0.02
9 System Cost	\$/kWh net	4	2	TBD
10 On-Board Efficiency	%	0.9	90	90
11 Volumetric Density	kg H ₂ /liter	0.028	0.040	0.070
12 Cycle Life	N	1000	1500	1500
13 Fuel Cost	\$/gge	3 to 7	2 to 6	2 to 3
14 Loss of Useable H ₂	[g H ₂ /hr]/kg H ₂	0.1	0.05	0.05
15 WPP Efficiency	%	60	60	60
16 Fuel Purity	%	99.97	99.97	99.97
17 Transient Response Start Time to Full Flow	sec.	0.75	0.75	0.75
18 (-20C) Start Time to Full Flow	sec.	15	15	15
19 Fill Time Start Time to Full Flow (20C)	min.	4.2	3.3	2.5
20 (20C) Start Time to Full Flow	sec.	5	5	5

Current Values	Assumptions/Model Ref	Ref Date
satisfactory	based on type 3 tank information	03/07/11
satisfactory	based material properties	03/07/11
satisfactory	based on system confinement	03/07/11
0.012	based GM1 optimized for fill time	03/07/11
-40	based on high 140C op. temp	03/07/11
85	based on system heat exchanger	03/07/11
5	system control system	03/07/11
12	system pressure regulator	03/07/11
-30	system buffer tank	03/07/11
50	based on system op at 140C	03/07/11
0.02	system buffer tank & cat. Heater	03/07/11
49	dual type 3 tanks + hig mat costs	03/07/11
0.78	mostly based on heat of reaction	03/07/11
0.12	dual tanks optimized for fill time	03/07/11
1000	based on vessel design comps	03/07/11
7.3	H ₂ AHDSAM, SMR, Sacramento	03/07/11
0.1	based on Type 3/4 tank data	03/07/11
44.1	H ₂ AHDSAM, SMR, Sacramento	03/07/11
99.97	based on SAH data, filters etc.	03/07/11
0.75	system buffer tank	03/07/11
15	drive cycle 4 & buffer tank	03/07/11
10.5	GM1 optimized for fill rate	03/07/11
5	drive cycle 3 & buffer tank	03/07/11

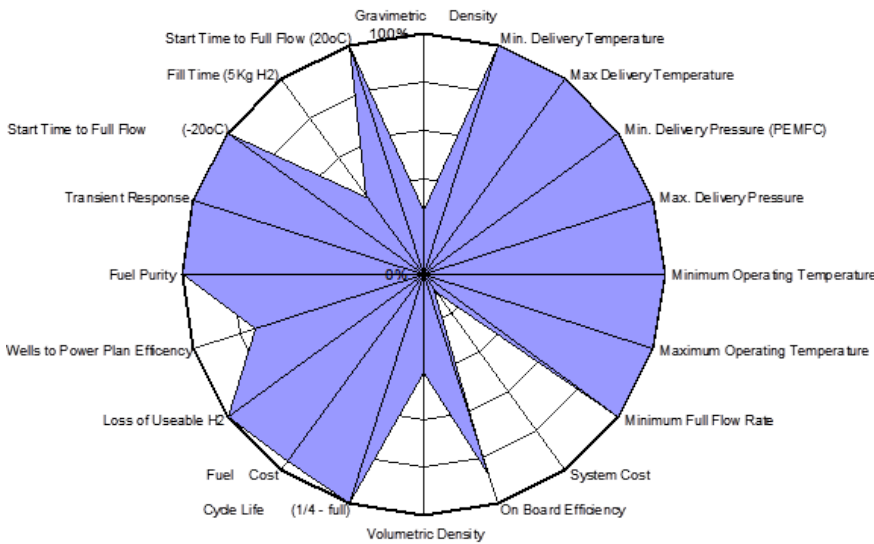


Figure 38: Baseline metal hydride design results shown as the percent attained compared with the Individual DOE 2010 System Targets

Gravimetric Density

Achieving high hydrogen system gravimetric densities has always been a challenge for metal hydride systems. The recent advent of complex metal hydride materials like NaAlH₄ and Li-Mg-amide have opened the door to obtaining substantially higher hydrogen gravimetric densities but often at the expense of slow kinetics, high heats of reaction, reduced cycle life and low volumetric density. NaAlH₄ has a theoretical hydrogen capacity of 5.6 wt% but due to its slow kinetics and high heat of reaction, the overall system gravimetric density for most NaAlH₄ systems are less than 2 wt% H₂. The baseline case, discussed above, exhibited a system gravimetric density of only 1.2 wt% H₂. Much of this was due to designing the system to minimize the charging time to 10.5 minutes. By relaxing the charging requirements for the system to an hour or more, the gravimetric density of the system increased, but it was still less than 2 wt% H₂.

Approximately 50% of the system weight comes from the weight of the material itself. However, the weight of the storage vessels, heat exchangers and the remainder of the BOP contribute substantially to the overall system weight. The recommended path forward to improve the gravimetric density of the baseline metal hydride systems is to 1) focus on higher gravimetric density materials like the 1:1 Li-Mg-amide material (theoretical material gravimetric hydrogen density of > 8wt%) 2) reduce the system to a single vessel, which eliminates vessel weight as well as the weight of the associated BOP components and 3) minimize the size and weight of the internal heat exchangers and the oil pump. Preliminary system calculations show that an overall reduction of the system weight of 50% is possible by incorporating the above three steps.

Volumetric Density

Achieving reasonable volumetric densities for most metal hydride systems has not been a major challenge due to the very high hydrogen volumetric capacities of many of the traditional, intermetallic, metal hydride materials. The introduction of complex metal hydrides, unfortunately, because of their very low bulk density, has made achieving high volumetric hydrogen more difficult. As an example, the predicted value for the baseline system is found to be just 0.12 kg H₂/liter. Approximately, 85% of the system volume is occupied by the metal hydride materials and their containment vessels. Preliminary testing has shown that many of the complex metal hydride materials like NaAlH₄ can be compacted. This compaction can reduce the overall system volume substantially and also allow the use of single vessel designs which can further reduce the system volume associated with the BOP components. It was determined from this study that using a combination of a single tank design, material compaction and BOP size reductions (especially in the oil and buffer tank) could reduce the overall system volume by over 33% yielding a total system volume of about 330 liters (or 0.16 kg H₂/l).

Fill Time

The rate of hydrogen absorption in most intermetallic metal hydrides is very rapid and typically only limited by the rate at which heat can be removed from the system. Preliminary studies on the TiCrMn-hydride systems have shown charging rates for a 5.6 kg usable hydrogen system to be less than or equal to 5 minutes. However, complex metal hydride

systems with NaAlH_4 and Li-Mg-amide materials do not charge readily mostly due to their slower kinetic absorption rates. The baseline NaAlH_4 case examined in this study achieved a charging time of 10.5 minutes for a system containing 5.6 kg of usable hydrogen. This required substantial gravimetric and volumetric penalties to the system by limiting the amount of hydrogen that could be absorbed in the available time as well as the increased weight and volume associated with additional heat exchanger and thermal conductivity enhancement materials. To achieve faster fill times and still maintain reasonable gravimetric system densities in metal hydride systems, materials with substantially faster hydrogen uptake kinetics will be needed. A preliminary analysis on a Li-Mg-amide system has shown that a 50X improvements in the current absorption kinetics may be required. Additional improvements in heat transfer designs may also help with charging times once materials with reasonable kinetic charging rates have been identified.

System Cost

While the initial DOE Storage System Cost Targets were listed at \$4 and \$2 per kWhr for the 2010 and 2015 targets, respectively, DOE recently revised these values to \$10 and \$8 per kWh for their 2020 and Ultimate target values. The preliminary cost analysis performed on the baseline system yielded a high cost estimate of \$43/kWhr. More than 75% of the cost is associated with the hydride vessel and the BOP. The largest cost, 43%, is associated with the Type III vessels themselves. Methods to substantially lower the system cost for future metal hydride systems involve reducing the system to a single vessel design, evaluating the use of lighter and less expensive vessels and reducing the size and the costs of the oil circulating pump and hydrogen combustor. Adoption of these methods is expected to reduce the overall system cost for metal hydride systems by more than 50%. (Note that the thermal stability and chemical compatibility of the polymer Type IV vessel liner would still need to be investigated for the specific metal hydride material and operating conditions.)

Several DOE Storage System Targets, mainly gravimetric/volumetric hydrogen capacity and fill times, continue to be a challenge for metal hydride systems. Engineering studies and analyses performed by the HSECoE have projected that substantial improvements in these and other targets can be made to the Metal Hydride baseline system by lowering the weight, volume and consequently the cost of the vessel and other BOP system components. However, developing a metal hydride system that can meet all of the DOE targets will require the development of a new material with improved hydrogen performance characteristics over the current materials available today. To this end DOE asked the HSECoE to use our system modeling and engineering tools developed as part of the HSECoE to estimate the “ideal” material requirements needed for a metal hydride material that when incorporated into a storage system would meet the DOE 2020 system targets. The HSECoE’s efforts to address this revised Metal Hydride System deliverable is described in more detail below. The decision by DOE to have the metal hydride portion of the HSECoE proceed into Phase 2 was based on the review of these predicted values and the other information presented in this report.

4.2 “IDEAL” METAL HYDRIDE STUDY

As mentioned above, to be in a better position to evaluate whether the metal hydride work in the HSECoE should proceed to Phase 2, the DOE asked if a HSECoE could use some of its

screening and modeling tools developed during Phase 1 to determine the minimum material-level requirements for metal hydrides to satisfy the 2020 system-level targets. The approach used was to choose a value of the enthalpy and capacity of material and then using a minimum BOP system, determine the weight and volume of the system that could be refueled in 1.5 kg H₂/min (2020 refueling rate from Table 2) and also be able to deliver 5.6 kg of hydrogen to the fuel cell under standard driving conditions. The study made use of the Acceptability Envelope Analysis (described in more detail in Section IIIB of this report) to determine the tube spacing and hence the weight and volume of the internal heat exchanger and tank volume. This was done by fixing the refueling rate at 1.5 kg H₂/min, the DOE target value. Equilibrium temperature and pressure correlations were estimated as a function of material enthalpy from the DOE Hydrogen Storage Material Database [6]. The DOE Hydrogen Storage Material Database was also used to correlate material crystal density with volumetric and gravimetric hydrogen material capacity. A Type IV pressure vessel was assumed rated for a 100 bar refueling pressure. A “tankinator-like” tool similar to what was described in Section IIIC was used to calculate the required vessel wall thickness and therefore the weight of the hydride container. Now that the pressure vessel design and the internal and total weight and volume can be assumed, the framework simulator was used to determine whether any additional hydrogen needed to be combusted to meet the 5.6 kg of delivered hydrogen and other drive cycle requirements. Another assumption made was that 10% by weight of a heat transfer enhancer like ENG was added to the hydride material to result in a thermal conductivity value of 9 W/m K. The material kinetics was assumed to follow a single-step kinetic expression with parameters adjusted to meet 85% of the theoretical maximum hydrogen material capacity in the 3.3 minute, DOE target fill time. Depending on the need to burn additional hydrogen to meet the drive cycle requirements, either of two basic minimal system designs (similar to those shown in Figures 26 and 27) were assumed: one that did not require a combustor or oil loop and one that did.

The results from the study showed that for enthalpy values greater than about 30 kJ/mol, higher storage system operating temperatures are needed. These higher temperatures (> 60°C) are higher than what the fuel cell can reliably supply as waste heat. This results in the need to combust some of the hydrogen to meet all the drive cycle requirements. The higher temperature also leads to a higher equilibrium pressure and a thicker and heavier tank which further adds to the weight and volume needed to accommodate the additional combustor and oil loop. The final results of the study are represented in Figures 39 and 40 which show the weight and volume distribution for the two system design cases. Figure 39 shows the distributions for a material with an enthalpy of 27 kJ/mol that can run entirely on fuel cell waste heat. The minimum required gravimetric capacity for this material is predicted to be 11 wt% H₂. Figure 40 shows similar distributions for a 40 kJ/mol material that requires an additional hydrogen combustor and an oil loop. To balance these additional imposed weight and volume requirements the predicted minimum gravimetric material capacity now needs to be 17 wt% H₂. More detailed and information on the “ideal” study can be found in Pasini et al [3] and in DOE HSECoE Annual Merit Review and DOE HSECoE Annual Reports [47, 48].

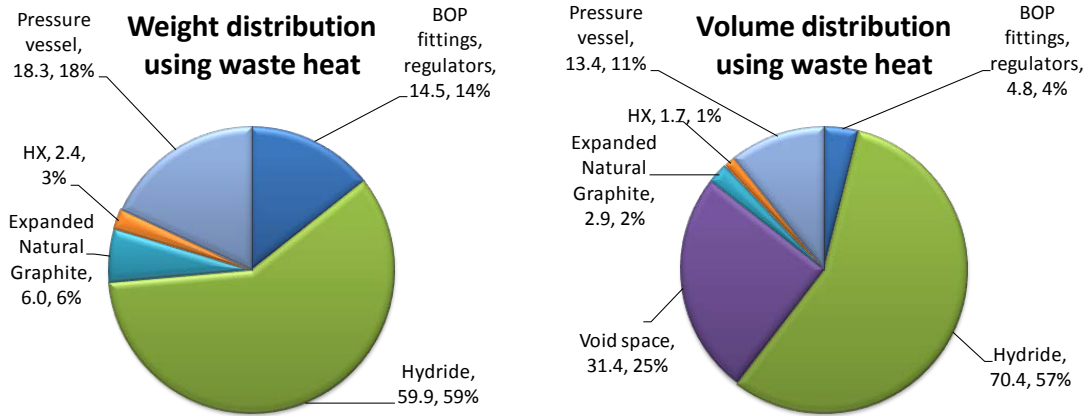


Figure 39: Weight (kg) and volume (l) distribution for a 11 wt% H₂ material and a $\Delta H = -27$ kJ/mol

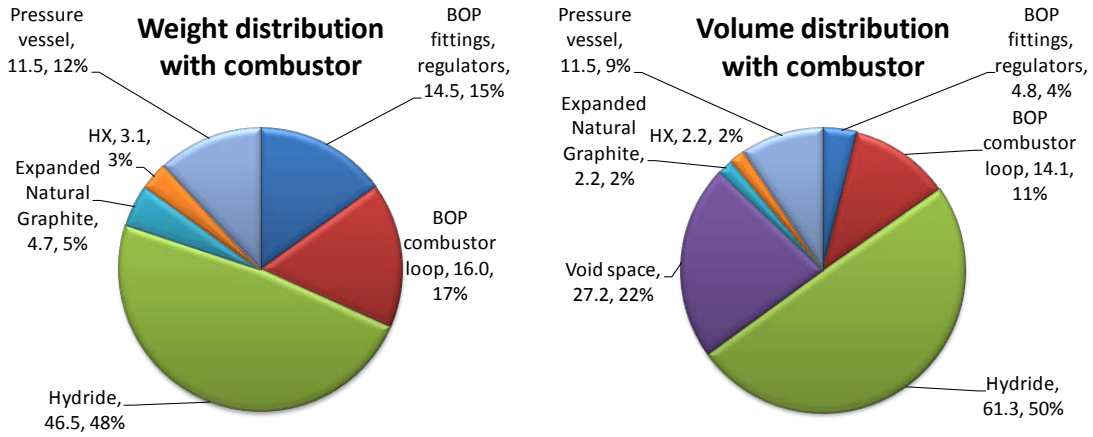


Figure 40: Weight (kg) and volume (l) distribution for a 17 wt% H₂ material and a $\Delta H = -40$ kJ/mol

5.0 CONCLUSION AND PATH FORWARD

On August 31, 2011, upon DOE review of the information provided by the HSECoE on the completion of Phase 1 activities, which included comparisons of all targets, required for light-duty vehicles, work on Reversible Metal Hydrides within the HSECoE was recommended not to continue into Phase 2. It was determined that the analyses recently performed and presented to the DOE by the HSECoE for highly optimized vessel configurations that could adequately manage thermal and mass flow rates needed for reversible onboard hydrogen storage to meet the DOE performance targets imposed requirements substantially exceeding the properties and behavior of any single, currently existing candidate hydride. In particular, the necessary combination of gravimetric and volumetric capacities, reaction kinetics, thermodynamic properties and reversibility have not been found simultaneously in any metal hydride investigated to date. Furthermore, the HSECoE had not identified any engineering solutions that will allow any currently known metal hydride, when incorporated into a complete system, to simultaneously meet all DOE performance targets. Therefore the decision has been made to not continue work on metal hydride systems during Phase II/III of the HSECoE.

The decision by DOE was specific to work ongoing in the HSECoE, not metal hydride R&D in general. DOE clearly stated that its decision would not impact future potential work related to R&D activities on reversible metal hydride systems for other stationary and portable hydrogen applications as well as to continue material discovery efforts on metal hydrides and other novel hydrogen storage materials for potential future use for onboard hydrogen storage applications. Much of what was learned in the 2.5 years working on reversible metal hydride system in the HSECoE can be applied to the design of other metal hydride applications and also down the road for light-duty vehicles should new higher capacity materials be discovered.

Major accomplishments for the HSECoE in the metal hydride area included:

- Development of the Acceptability Envelope Analysis and other screening tools to more efficiently and better utilize detailed modeling efforts as well as to help direct material research and development.
- Adoption of a hierarchical modeling construct that made use of screening, 2D and 3D transport models and system models to rapidly and cost effectively evaluate materials and systems against critical targets and requirements.
- Disseminating various metal hydride models and design tools to the public on the HSECoE website: Acceptability Envelope Analysis, Finite Element Transport Model and the “Tankinator”, pressure vessel sizing tool.
- Adding to the understanding of hydrogen storage material compaction and methods to improve the thermal conductivity of powder materials.
- Inventing a novel highly efficient hydrogen and gas combustor/heat exchanger.
- Development of a potential acoustical gas gauge technique for metal hydride storage containers.
- Creation of an engineering property material database for high potential metal hydride candidate materials.

- Publishing over 16 articles in peer reviewed journals and at least one invention disclosure in the area of metal hydride material and system engineering (see Appendix A-3).

|

6.0 REFERENCES

- [1] Financial Assistance Funding Opportunity Announcement, U.S. Department of Energy Office of Energy Efficiency and Renewable Energy Hydrogen, Fuel Cells and Infrastructure Technologies Program Golden Field Office, Hydrogen Storage Engineering Center of Excellence Funding Opportunity Number: DE-PS36-08GO98006, CFDA Number: 81.087 Renewable Energy Research and Development, 2/27/2008.
- [2] US DOE Targets for Onboard Hydrogen Storage Systems for Light-Duty Vehicles; http://www1.eere.energy.gov/hydrogenandfuelcells/storage/pdfs/targets_onboard_hydro_storage.pdf.
- [3] J.M. Pasini, C. Corgnale, B.A. van Hassel, T. Motyka, S. Kumar, K. L. Simmons, Metal hydride material requirements for automotive hydrogen storage systems, *Intl. J. Hydrogen Energy* 2013; 38:9755-9765.
- [4] M. Hirscher (Editor), *Handbook of Hydrogen Storage, New Materials for Future Energy Storage*, (Wiley-VCH Verlag GmbH & Co., KGaA, Weinheim, Germany, 2010) ISBN: 978-3-527-32273-2.
- [5] Sandrock G. and Houston E., How metals store hydrogen, *Chemtech*, pp. 754-762, December, 1981.
- [6] United States Department of Energy, Hydrogen storage materials database, URL: <http://hydrogenmaterialssearch.govtools.us/>; 2011.
- [7] Felderhoff M, Bogdanović B., High Temperature Metal Hydrides as Heat Storage Materials for Solar and Related Applications, *Int. J. Mol. Sci.* 2009; 10:325-344.
- [8] Harries D, Paskevicius M, Sheppard D, Price T, Buckley C. Concentrating solar thermal heat storage using metal hydrides. *Proceedings of the IEEE* 2012; 100:539-549.
- [9] Bogdanovic, B.; Schwickardi, M. Ti-doped alkali metal aluminum hydrides as potential novel reversible hydrogen storage materials. *J. Alloys Compd.* 1997, 253-254, 1-9.
- [10] Klebanoff, L.; Keller, J. 5-Year Review of Metal Hydride Center of Excellence. *Int. J. Hydrogen Energy* 38 (2013) 4533-4576.
In *Proceedings of the 2010 U.S. DOE Hydrogen Program Annual Merit Review*, Washington, DC, USA, 7-11 June 2010; Available online: http://www.hydrogen.energy.gov/pdfs/review10/st029_klebanoff_2010_o_web.pdf.
- [11] Guther V, and Otto A., Recent developments in hydrogen storage applications based on metal hydrides, *Journal of Alloys and Compounds* 293-295 (1999) 889-892.

- [12] Sakintunaa, B., Lamari-Darkrim F., Hirscher M., Metal hydride materials for solid hydrogen storage: A review, *International Journal of Hydrogen Energy* 32 (2007) 1121 – 1140.
- [13] Wang QD, Chen CP, Lei YQ, The recent research, development and industrial applications of metal hydrides in the People's Republic of China, *Journal of Alloys and Compounds* 253–254 (1997) 629–634.
- [14] Verbetsky VN, Malyshenko SP, Mitrokhin VV, Solovei, YU, Shmal KO, Metal hydride properties and practical applications: Review of the works in CIS-Countries, *Int. J. Hydrogen Energy*, Vol 23, No. 12, 1165-1177, 1998.
- [15] Sandrock G, Bowman Jr RC. Gas-based hydride applications: recent progress and future needs. *J Alloy Compd* 2003; 356e357:794e9, [http://dx.doi.org/10.1016/S0925-8388\(03\)00090-2](http://dx.doi.org/10.1016/S0925-8388(03)00090-2).
- [16] B. Bowman and L. Klebanoff, “Historical Perspectives on Hydrogen, Its Storage, and Its Applications,” Chapter 3 in *Hydrogen Storage Technology Materials and Applications*, edited by L. Klebanoff (CRC Press, Boca Raton, FL, USA, 2013) pp. 65-90.
- [17] Jacobs WD, Heung LK, Motyka T, Summers WA. Operation of a hydrogen-powered hybrid electric bus, in: *Proceedings of the Future Transportation Technology Conference & Exposition*, Costa Mesa, CA, USA, August 1998, SAE Tech Paper 981923 1998, <http://dx.doi.org/10.4271/981923>.
- [18] Fuchs M, Barbir F, Nadal M. Performance of third generation fuel cell powered utility vehicle #2 with metal hydride fuel storage. In: *Proceedings of the 2001 European Polymer Electrolyte Fuel Cell Forum*, Lucerne, Switzerland, July 26, 2001.
- [19] Heung LK, Motyka T, Summers WA. Hydrogen storage development for utility vehicles, Tech. Rep.; US Department of Energy report for contract no. DE-AC09-96SR18500; 2001.
- [20] Sandrock G., State-of-the-Art Review of Hydrogen Storage in Reversible Metal Hydrides for Military Fuel Cell Applications, contract number N00014-97-M-0001, 1997.
- [21] Komiya K, Mori D, Miura S, Haraikawa N, Yoshida K, Watanabe S, et al. High-pressure hydrogen-absorbing alloy tank for fuel cell vehicles. SAE Tech Paper 2010-01-0851 2010, <http://dx.doi.org/10.4271/2010-01-0851>.
- [22] Johnson TA, Jorgensen SW, Dedrick DE., Performance of a full-scale hydrogen-storage tank based on complex hydrides. *Faraday Discuss* 2011;151:327e52. <http://dx.doi.org/10.1039/C0FD00017E>.

- [23] Mosher DA, Tang X, Brown RJ, Arsenault S, Saitta S, Laube BL, et al. High density hydrogen storage system demonstration using NaAlH₄ based complex compound hydrides. 2007. Final report for DOE contract DE-FC36-02AL67610.
- [24] Bellosta von Colbe JM, Metz O, Lozano GA, Pranzas PK, Schmitz HW, Beckmann F, Schreyer A, Klassen T, Dornheim M, Behavior of scaled-up sodium alanate hydrogen storage tanks during sorption, *Int J Hydrogen Energy* 2012; 37: 2807- 11.
- [25] Luo, W., Gross KJ, *Journal of Alloys and Compounds* 385 (2004) 224–231
- [26] Sandrock et al. *Journal of Alloys and Compounds* 339 (2002) 299 –308
- [27] van Hassel BA, Mosher D, Pasini JM, Gorbounov M, Holowczak, J, Tang X, Brown R, Laube B, Pryor L, Engineering improvement of NaAlH₄ system, *Int J Hydrogen Energy* 2012; 37: 2756- 2766.
- [28] van Hassel BA, ,Gorbounov M, Holowczak, J, Tang X, Brown R, Advancement of system designs and key engineering technologies for materials-based hydrogen storage, *Journal of Alloys and Compounds*, 580, 2013, S337- S342.
- [29] Sulic M, Cai M, Kumar S, Cycling and engineering properties of highly compacted sodium alanate pellets, *Int J Hydrogen Energy* 2012; 37: 15187- 15195.
- [30] Sulic M, Cai M, Kumar S, Controlled degradation of highly compacted sodium alanate pellets, *Int J Hydrogen Energy* 2013; 38: 3019- 3023.
- [31] B.J. Hardy, D.L. Anton, Hierarchical methodology for modeling hydrogen storage systems. Part I: Scoping models, *Intl. J. Hydrog. Energy* 34 (2009) 2269– 2277, and Hierarchical methodology for modeling hydrogen storage systems. Part II: Detailed models, *Intl. J. Hydrog. Energy* 34 (2009) 2992–3004.
- [32] Corgnale C, Hardy BJ, Tamburello DA, Garrison SL, Anton DL, Acceptability envelope for metal hydride-based hydrogen storage systems. *Int J Hydrogen Energy* 2012;37:2812e24 <http://dx.doi.org/10.1016/j.ijhydene.2011.07.037>.
- [33] Bhourri M, Goyette J, Hardy B, Anton D, Sensitivity study of alanate hydride storage system, *Int J Hydrogen Energy* 2011; 36: 621- 633.
- [34] Bhourri M, Goyette J, Hardy B, Anton D, Numerical modeling and performance evaluation of multi-tubular sodium alanate hydride finned reactor, *Int J Hydrogen Energy* 2012; 37: 1551-1567.
- [35] Bhourri M, Goyette J, Hardy B, Anton D, Honeycomb metallic structure for improving heat exchange in hydrogen storage system, *Int J Hydrogen Energy* 2011; 36: 6723-6738.

- [36] Raju M. and Kumar S. (2011) System Simulation Modeling and Heat Transfer in Sodium Alanate based Hydrogen Storage Systems, *Int J Hydrogen Energy* 2011; 36: 1578-1591.
- [37] Raju M. and Kumar S. (2010) Optimization of heat exchanger designs in metal hydride based hydrogen storage systems, *Int J Hydrogen Energy* 2012; 37: 2767-2778.
- [38] Pasini, JM, van Hassel BA, Mosher DA, Veenstra MJ, System modeling methodology and analyses for materials-based hydrogen storage, *Intl. J. Hydrog. Energy*, 37 (2012) 2874-2884.
- [39] Kumar S, Raju M, Kumar VS. System simulation models for on-board hydrogen storage systems. *Int J Hydrogen Energy* 2012;37:2862-73, <http://dx.doi.org/10.1016/j.ijhydene.2011.04.182>.
- [40] Raju M, Ortmann JP, Kumar S, System Simulation Models for High-Pressure Metal Hydride Hydrogen Storage Systems. *Int. J. Hydrogen Energy* 2010; 35: 8742- 8754.
- [41] M. Thornton, A. Brooker, J. Cosgrove, M. Veenstra, J.M. Pasini, Development of a vehicle-level simulation model for evaluating the trade-off between various advanced on-board hydrogen storage technologies for fuel cell vehicles, SAE Technical Paper 2012-01-1227 (2012) doi:10.4271/2012-01-1227.
- [42] Brosha E. L., P. K. Sekhar, R. Mukundan, T. Williamson, F. H. Garzon, L. Y. Woo, R. R. Glass, Development of Sensors and Sensing Technology for Hydrogen Fuel Cell Vehicle Applications, ECS Transactions: Fuel Cell Seminar and Exposition 2009, LLNL-JRNL-422205, January 7, 2010.
- [43] U.S. DOE EERE Fuel Cell Technologies Program Hydrogen Storage Engineering Center of Excellence, <http://hsecoc.srs.gov/models.html>.
- [44] U.S. Department of Energy Hydrogen Storage Cost Analysis, Final Public Report, TIAX Reference No. D0268, March 11, 2013, www.osti.gov/scitech/servlets/purl/1082754.
- [45] DOE Hydrogen and Fuel Cell 2011 Annual Progress Reports, IV.D.10, Microscale Enhancement of Heat and Mass Transfer for Hydrogen Energy Storage, www.hydrogen.energy.gov/pdfs/progress11/iv_d_10_drost_2011.pdf.
- [46] DOE Hydrogen and Fuel Cell 2011 Annual Progress Reports, IV.D.6 Systems Engineering of Chemical Hydride, Pressure Vessel, and Balance of Plant for On-Board Hydrogen Storage, www.hydrogen.energy.gov/pdfs/progress11/iv_d_6_holladay_2011.pdf.
- [47] DOE Hydrogen and Fuel Cell Library, Annual Merit Reviews for the HSECoE (2009-2012) http://www.hydrogen.energy.gov/annual_review.html.

[48] DOE Hydrogen and Fuel Cell Library, Annual Progress Reports for the HSECoE (2009-2012) http://www.hydrogen.energy.gov/annual_progress.html.

APPENDICES

APPENDIX A-1

Guideline for selection of HSECoE hydrogen storage materials

This document provides a guideline for how to justify the *selection* of HSECoE materials. In order for a material to be considered for application within the HSECoE, it must first pass *minimum screening criteria*, which will give the Center a rough assessment of its capabilities. The quantified minimum screening criteria for each materials group, i.e. Metal Hydrides, Chemical Hydrides and Adsorbent Materials, are listed below (see *Table A-1*). A material that passes the screening criteria is thereafter referred to as a *selected material*. Materials not found to improve system performance relative to selected materials, and that cannot meet the DOE system targets are not for further consideration and are thereafter referred to as *non-selected (or rejected)*.

Materials are grouped into *selected* (Tier 1 and 2) and *non-selected* materials according to Table 1. For *Tier 1* “Developed Materials” a data base was assembled and appropriate parametric models developed and verified where system data were available. *Tier 2* “Developing Materials” were selected as promising candidate materials for system consideration.

For each *selected and rejected* material the justification was documented. The 1-page documentation for each material contained the values for the *minimum screening criteria* and a *short summary* on when and why the decision was made.

The *reject decision* can be made:

- After filling out the ‘screening criteria form’ for a candidate material
- For a Tier 2 material; after evaluating collected/measured data for system considerations it may be revealed that it will not improve performance compared to Tier 1 materials
- For a Tier 1 material; during system modeling, it may be revealed that the material will not improve performance and will not meet DOE system targets

The *select decision* can be made:

- After filling out the ‘screening criteria form’ for a candidate material. Thus move material to Tier 2
- For a Tier 2 material; after evaluating collected/measured data for system considerations it may be revealed that it will improve performance compared to Tier 1 materials. Thus move material to Tier 1
- For a Tier 1 material; after performing system modeling, it may be revealed that the material will improve performance, and meet DOE system targets. Thus it will remain in Tier 1

Table A-I HSECoE Materials Categories

	<i>Tier 1</i> Developed Materials	<i>Tier 2</i> Developing Materials	Down-selected Materials
Adsorbents	AX-21 MOF 5	Pt/AC-IRMOF 8	MOF 177
Chemical Hydrides	NH ₃ BH ₃ (g) AlH ₃	NH ₃ BH ₃ (l) LiAlH ₄	
Metal Hydrides	NaAlH ₄ 2LiNH ₂ +MgH ₂	Mg(NH ₂) ₂ +MgH ₂ +2LiH TiCr(Mn)H ₂	MgH ₂ Mg ₂ NiH ₄

Minimum Screening Criteria for Metal Hydrides

Capacity: > 9wt% materials capacity to be able to meet the DOE 2015 system target

Absorption: RT to 250°C at 1-700 bar H₂ pressure, rate >20g/s (storing 5 kg usable H₂)

Desorption: 80°C to 250°C at 1-3 bar H₂-pressure, rate >20g/s (storing 5 kg usable H₂)

Enthalpy: <50kJ/mol

Crystal density: > 1g/cm³

Availability: (quantitative cost & time i.e. <\$10,000/kg in 30 day delivery)

Minimum Screening Criteria for Chemical Hydrides

Capacity: > 9wt% materials capacity to meet the DOE 2015 system target

Desorption: RT to 150°C, rate >30g/s

Enthalpy of formation: <20kJ/mol

Crystal density: > 1g/cm³

Availability: (quantitative cost & time i.e. <\$10,000/kg in 30 day delivery)

Minimum Screening Criteria for Adsorbent Materials

Capacity: Max Gibbs excess capacities >5wt% and 30g/L with storage T's from 77K to RT, and <50 bar at 77K

Desorption: measured between ~80K to RT, must meet DOE 2010/2015 target of 0.02g/s/kW

Hydrogen uptake: measured between ~80K to RT, <30bar, must be 30g H₂/s

Specific Surface Area: Prefer ~3000 m²/g, pore sizes ~0.7 to ~1.5 nm, pore volume ~1.2 cm³/g

Bulk density: >0.7 g/cm³

Availability: (quantitative cost & time i.e. <\$10,000/kg in 30 day delivery)

APPENDIX A-2 Sodium Aluminum Hydride Material Property Database (example)

Category	Property	reported value	reference
	Composition	Titanium doped Sodium aluminum hydride	
	Catalyst	Titanium chloride, TiCl ₃	
	Ratios	NaAlH ₄ : 86.3% NaAlH ₄ , 4.7% Na ₃ AlH ₆ , 7.5% free Al and 10.1% insoluble Al (with all analyses given in wt%).	Mosher et al. UTRC Final Report (2007)
Synthesis	Method	NaAlH ₄ combined with 2 mol% TiCl ₃ catalyst were ball milled for 24 hours using high energy SPEX ball milling under nitrogen	Mosher et al. UTRC Final Report (2007)
		1.12:1:0.04 NaH:Al:TiCl ₃ molar ration were milled under argon in a high-energy Spex mill for 30 minutes	W. Luo, K.J. Gross / Journal of Alloys and Compounds 385 (2004) 224–231
Decomposition Pathways	Intermediates	$(1-x)\text{NaAlH}_4 + x\text{TiCl}_3 \rightarrow (1-4x)\text{NaAlH}_4 + 3x\text{NaCl} + x\text{Ti} + 3x\text{Al} + 6x\text{H}_2 \quad (2)$ <div style="border: 1px solid black; padding: 2px; width: fit-content; margin: 5px auto;"> $3\text{NaAlH}_4 + \text{TiCl}_3 \rightarrow 3\text{NaCl} + \text{Ti}^0 + 3\text{Al}^0 + 6\text{H}_2$ $\text{Ti}^0 + 3\text{Al}^0 \rightarrow \text{TiAl}_3$ </div>	G. Sandrock et al. / Journal of Alloys and Compounds 339 (2002) 299–308 G. Krishna et al. / Journal of Physical Chem C 113 (2009) 15051-15057
	Hydrogen Impurities	None	
	Kinetic Model		$\left(\frac{dC_j}{dt}\right)_r = D_j \exp\left(-\frac{E_j}{RT}\right) \left(\frac{P_{e,i} - P}{P_{e,i}}\right) * (C_k)^{\gamma_i}$
Intrinsic properties	Decomposition rate of NaAlH₄	$-d(Hwt\%) / dt = K_{\text{out}} \exp\left(-\frac{E_{\text{out}}}{RT}\right) \ln\left(\frac{P_{\text{eq}}}{P_{\text{app}}}\right) x (Hwt\% - 1.67) (1.67 < Hwt\% < 3.9)$	W. Luo, K.J. Gross / Journal of Alloys and Compounds 385 (2004) 224–231
	Na₃AlH₆ formation:	$-d(Hwt\%) / dt = K_{\text{out}} \exp\left(-\frac{E_{\text{out}}}{RT}\right) \ln\left(\frac{P_{\text{app}}}{P_{\text{eq}}}\right) x (1.67 - Hwt\%) (Hwt\% < 1.67)$	W. Luo, K.J. Gross / Journal of Alloys and Compounds 385 (2004) 224–231
	Rate constant from Arrhenius equation	0.9 mol% TiCl ₃ , k = 2.06 x 10 ⁹ wt% H ₂ /h	G. Sandrock et al. / Journal of Alloys and Compounds 339 (2002) 299–308
		2 mol% TiCl ₃ , k = 7.19 x 10 ¹⁰ wt% H ₂ /h	G. Sandrock et al. / Journal of Alloys and Compounds 339 (2002) 299–308
		4 mol% TiCl ₃ , k = 1.81 x 10 ¹¹ wt% H ₂ /h	G. Sandrock et al. / Journal of Alloys and Compounds 339 (2002) 299–308
		4 mol% TiCl ₃ , k = 1.63 x 10 ¹¹ wt% H ₂ /h	G. Sandrock et al. / Journal of Alloys and Compounds 339 (2002) 299–308
	von Hoft Plot		
	Storage capacity	4.4 wt% during 1st desorption	Mosher et al. UTRC Final Report (2007)
	Isotherms	see included graphs	Mosher et al. UTRC Final Report (2007)
	Cyclic Degradation	10% decrease in capacity after 20 cycles, and the capacity loss rate appears to have decreased after 15 cycles	Mosher et al. UTRC Final Report (2007)
Density (crystalline)		NaAlH ₄ theoretical density: 1.3 g/cm ³	D.A. Mosher et al. / Journal of Alloys and Compounds 446–447 (2007) 707–712
		NaAlH ₄ (Tetragonal): 1.287 g/cm ³	Determined using lattice constants listed in Mosher et al. UTRC Final Report (2007)
		NaAlH ₄ (Tetragonal): 278.67 Å ³ , α-Na ₃ AlH ₆ (Monoclinic): 208.275 Å ³ , β-Na ₃ AlH ₆ (orthorhombic) 236.81 Å ³ , NaH (cubic) :112.67 Å ³	Determined using lattice constants listed in Mosher et al. UTRC Final Report (2007)
Lattice volume	Lattice parameters	NaAlH ₄ : Tetragonal a=b=5.00054, c=11.123, α=β=γ=90°	Mosher et al. UTRC Final Report (2007)
		α-Na ₃ AlH ₆ : Monoclinic a = 5.33, b = 5.53, c = 7.71, α=β=γ=90°	Mosher et al. UTRC Final Report (2007)
		β-Na ₃ AlH ₆ : orthorhombic a = 5.45, b = 5.53, c = 7.73, α=β=γ=90°	Mosher et al. UTRC Final Report (2007)
		NaH: cubic a = b = c = 4.83, α=β=γ=90°	Mosher et al. UTRC Final Report (2007)
Lattice Expansion			
Enthalpy		NaAlH ₄ decomposition: 79.5 kJ/mol	G. Sandrock et al. / Journal of Alloys and Compounds 339 (2002) 299–308
Enthalpy of formation		(-)229±9 kJ/mol Na ₃ AlH ₆ (-)75±2 kJ/mol TiAl (-)142±2 kJ/mol TiAl ₃ (-)411.12±0.34 kJ/mol NaCl	T. Dobbins et al./ Nanotechnology 20 (2009)
Enthalpy of reaction		ΔH ⁰ (part a) = -29 kJ/mol H ₂ ΔH ⁰ (part b) = -179 kJ/mol H ₂	G. Krishna et al. / Journal of Physical Chem C 113 (2009) 15051-15057
Gibbs Free energy of reaction		ΔG ⁰ (part a) = -62 kJ/mol H ₂ ΔG ⁰ (part b) = -175 kJ/mol H ₂	G. Krishna et al. / Journal of Physical Chem C 113 (2009) 15051-15057
Equilibrium pressure			

Category	Property	reported value	reference	additional notes
	Activation Energy	0.9 mol% TiCl ₃ , Ea NaAlH ₄ = 118.1 kJ/mol H ₂	G. Sandrock et al. / Journal of Alloys and Compounds 339 (2002) 299–308	
		2 mol% TiCl ₃ , Ea NaAlH ₄ = 72.8 kJ/mol H ₂	G. Sandrock et al. / Journal of Alloys and Compounds 339 (2002) 299–308	
		4 mol% TiCl ₃ , Ea NaAlH ₄ = 80.0 kJ/mol H ₂	G. Sandrock et al. / Journal of Alloys and Compounds 339 (2002) 299–308	
		6 mol% TiCl ₃ , Ea NaAlH ₄ = 78.5 kJ/mol H ₂	G. Sandrock et al. / Journal of Alloys and Compounds 339 (2002) 299–308	
	Entropy			
Specific Heat	1418 J/kg/K	Ahluwalia, R.K. (2007) Inter J of Hydro Energy 32		
Thermal Conductivity	0.5 (W/m°C)	D.A. Mosher et al. / Journal of Alloys and Compounds 446–447 (2007) 707–712		
Bulk properties	Density	NaAlH ₄ Original density with different milling processing: 0.46, 0.32, 0.50 g/mL	D.A. Mosher et al. / Journal of Alloys and Compounds 446–447 (2007) 707–712	
		NaAlH ₄ during vibratory settling: 0.74, 0.47, 0.63 g/mL	D.A. Mosher et al. / Journal of Alloys and Compounds 446–447 (2007) 707–712	
		NaAlH ₄ during enhanced densification: 0.75, 0.63, 0.84 g/mL	D.A. Mosher et al. / Journal of Alloys and Compounds 446–447 (2007) 707–712	
System Engineering	Bed Design Reactor Design			
	Materials Interactions Known Poisons Caveats			13333.33 mol/m ³ = concentration of NaAlH ₄ at bed density 1.94 cm = diameter of coolant tubes, 1.27 cm = diameter of H ₂ injection tubes tube material, 6061-T6 Al fin material, 6061-T6 Al porous insert, 6061-T6 Al
Integration	Environmental reactivity			
	minimum ignition energy	NaAlH ₄ : <7mJ, NaH: <7 mJ	D.A. Mosher et al. / Journal of Alloys and Compounds 446–447 (2007) 707–712	
	Safety Considerations pyrophoricity	Work with under inert gases and away from moisture		140 g/m ³ = min. exp. Con for NaAlH ₄ 90 g/m ³ = min. exp. Con for NaH
	Materials Reactivity			
	burn rate at 20°C spontaneous ignition 20°C	NaAlH ₄ with 2 mol% TiCl ₃ : 51 mm/s, Na ₃ AlH ₆ : 222 mm/s, NaH: 27 mm/s NaAlH ₄ : not pyrophoric, Na ₃ AlH ₆ : not pyrophoric, NaH: not pyrophoric	D.A. Mosher et al. / Journal of Alloys and Compounds 446–447 (2007) 707–712 D.A. Mosher et al. / Journal of Alloys and Compounds 446–447 (2007) 707–712	All these results were with 2 mol% TiCl ₃
burn rate at 80°C spontaneous ignition 80°C	NaAlH ₄ : 127 mm/s, Na ₃ AlH ₆ : spontaneous ignition, NaH: 40 mm/s NaAlH ₄ : not pyrophoric, Na ₃ AlH ₆ : pyrophoric, NaH: not pyrophoric	D.A. Mosher et al. / Journal of Alloys and Compounds 446–447 (2007) 707–712 D.A. Mosher et al. / Journal of Alloys and Compounds 446–447 (2007) 707–712		
IP Status	Composition/Catalyst	IP Status		
		US Patent 6793909 - Direct synthesis of catalyzed hydride compounds: 1.03 moles NaH + 1.0 mol Al +0.01 moles TiCl ₃	US Patent 7011768 - Methods for hydrogen storage using doped alinate compositions, Craig Jensen and Scott Redmond. The compositions comprise sodium alinate and [nS-CSH5]2TiH2 wherein the molar ratios of NaH:Al:Ti in the composition are respectively 0.7 to 1.0 to 0.1	
Synthesis Technique		fabrication of the alkali metal-aluminum hydride comprises mixing powders of an alkali metal (Li, Na, and K) with aluminum powder and a transition metal catalyst compound (typically a titanium catalyst compound such as TiCl ₃ , TiF ₃ , or mixtures of these materials) in the desired proportion and ball milling the constituents in an inert atmosphere of argon, for a period of up to about 2 hours, and then hydrogenating the milled mixture at high pressure while heating the mixture externally to an initial temperature of about 125° C.	In a cassette embodiment or any other embodiment, the doped sodium alinate compositions may be used to generate hydrogen for any type of known hydrogen utilizing system. In certain embodiments, such a hydrogen utilizing system may comprise a fuel cell.	
		the sample reaches about 90% of its initial first cycle capacity within about 20 hours, after which the rate of hydrogen absorption improves to about 5 hours in the subsequent half-cycles. A desorption rate (to about 90% of capacity) occurs within about 2 hours.		
Availability & Cost	Materials/Precursors	Availability		
	Materials Cost Point of Contact	Commercial grade NaAlH ₄ was purchased from the AlBemarle Corporation		

Summary of formation and decomposition activation energy of NaAlH ₄ and Na ₃ AlH ₆					
	K_o (abs)	E_{aa} (abs) (kJ/mol)	K_o (des)	E_{ad} (des) (kJ/mol)	E_{ad} (des) [3] (kJ/mol)
NaAlH ₄	6.25×10^8	61.6	1.9×10^{11}	85.6	80.0
Na ₃ AlH ₆	1.02×10^8	56.2	2.9×10^{10}	88.3	97.5

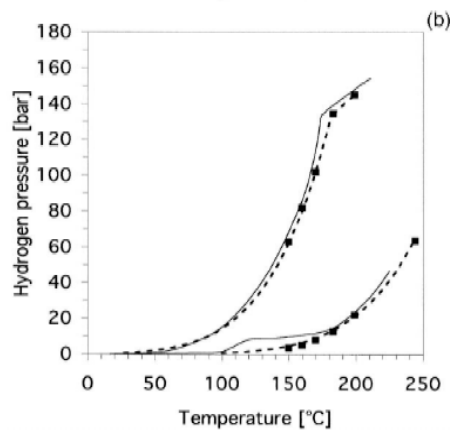
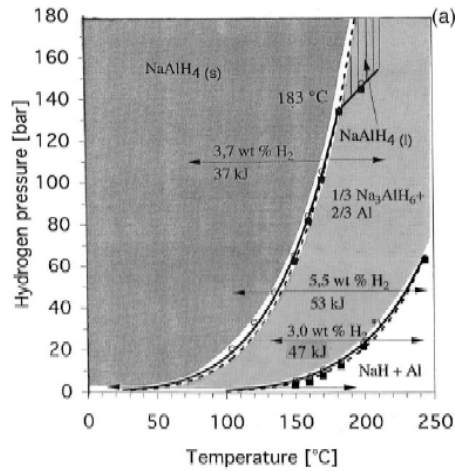
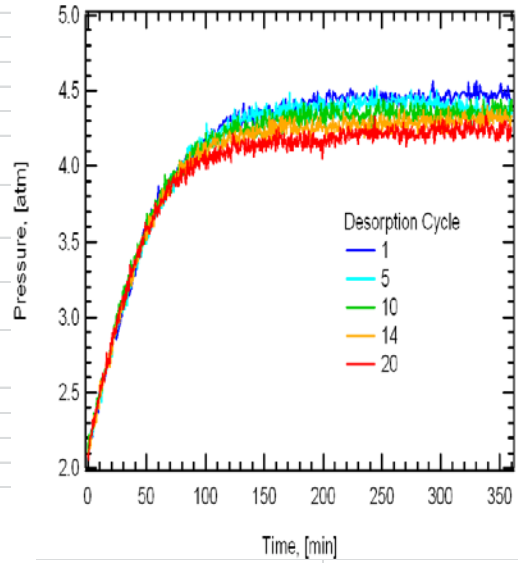


Fig. 9. (a) Pressure-temperature relations for the Ti-doped NaAlH₄ system; (—■—) desorption pressure; (—○—) absorption pressure; (*) hydrogen storage capacity of Na₃AlH₆ in absence of Al. (b) Comparison of hydrogen dissociation pressures for the Ti-doped NaAlH₄ system from PCI (a, ---) and direct measurements (—).

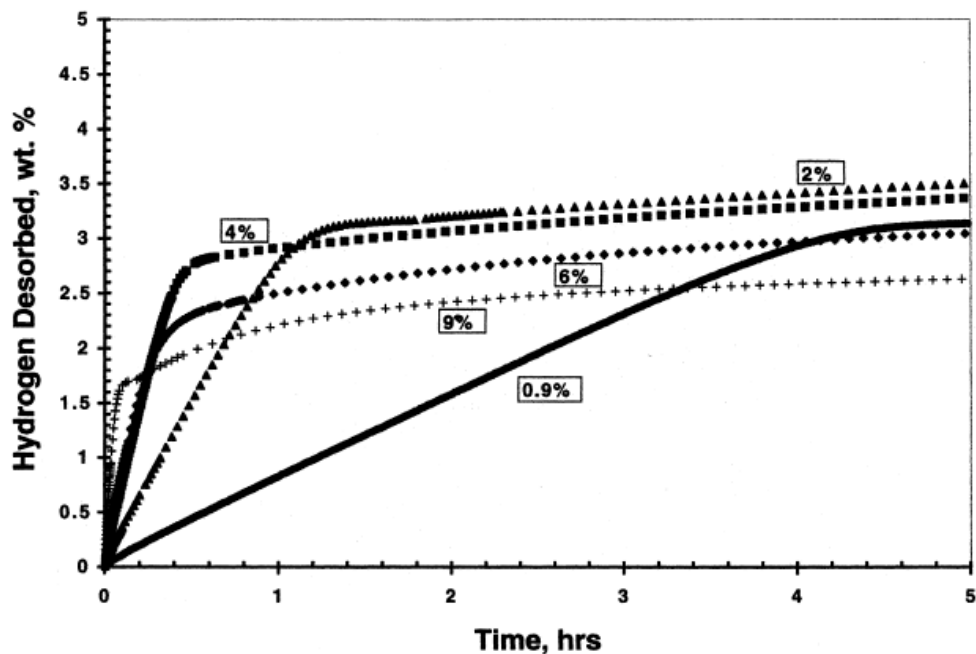


Fig. 2. H₂ desorption curves starting from NaAlH₄ as a function of added TiCl₃ catalyst precursor (expressed in mol.%). T_i = 125 °C.

G. Sandrock et al. / Journal of Alloys and Compounds 339 (2002) 299–308

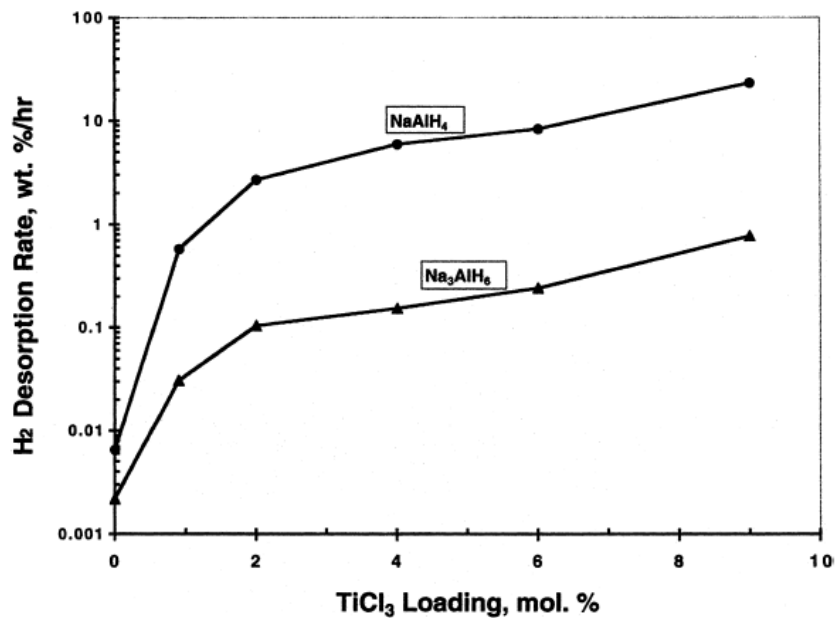


Fig. 8. Desorption rates for NaAlH₄ and Na₃AlH₆ as a function of added TiCl₃, as calculated for 125 °C from the Arrhenius equation (Eq. (3)) using the experimental parameters listed in Table 1.

G. Sandrock et al. / Journal of Alloys and Compounds 339 (2002) 299–308

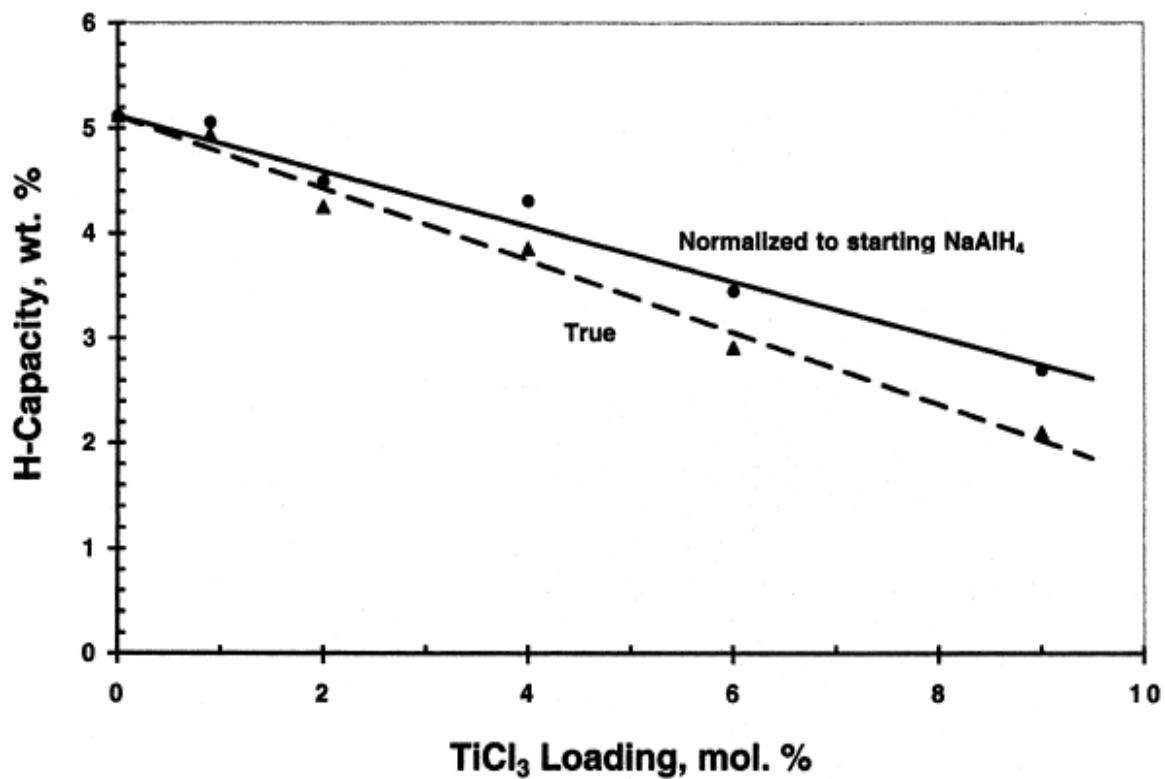
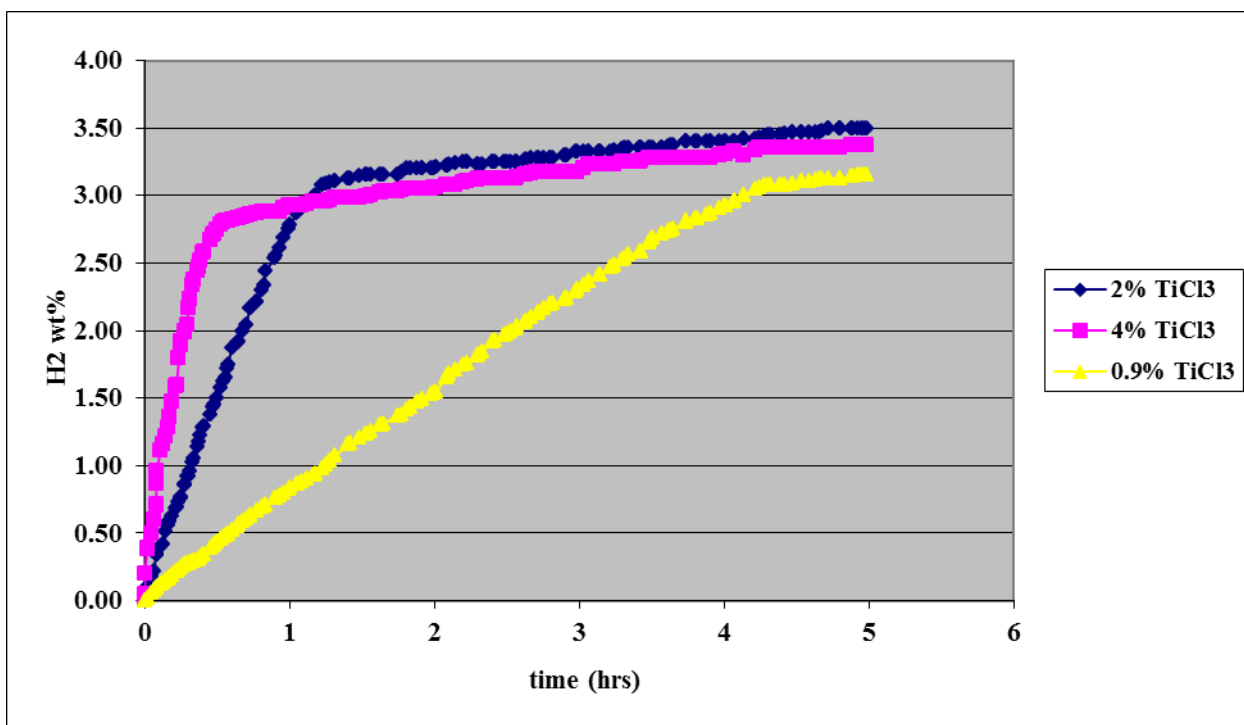


Fig. 3. Effect of TiCl₃ addition level on H-capacity of ball-milled NaAlH₄ + TiCl₃.

G. Sandrock et al. / Journal of Alloys and Compounds 339 (2002) 299–308

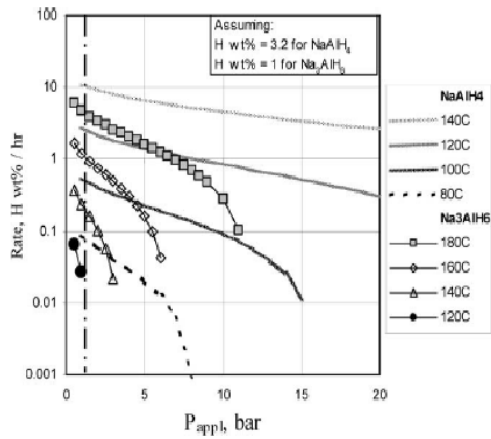


Fig. 7. Calculated decomposition rates of NaAlH₄ and Na₃AlH₆ over a typical range of applied pressures and temperatures for H wt.% = 3.2 (NaAlH₄) and H wt.% = 1 (Na₃AlH₆).
W. Luo, K.J. Gross / Journal of Alloys and Compounds 385 (2004) 224–231

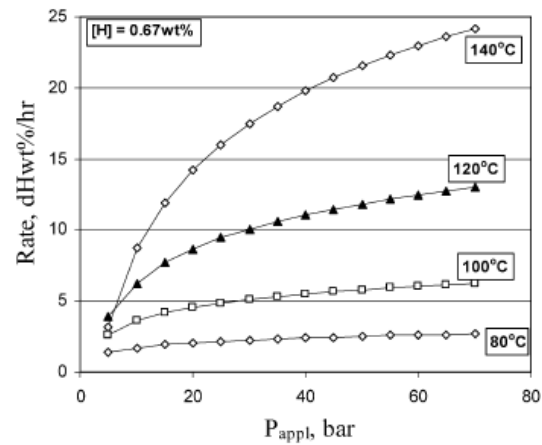


Fig. 6. Calculated formation rates for Na₃AlH₆ at selected temperatures and applied pressures.

W. Luo, K.J. Gross / Journal of Alloys and Compounds 385 (2004) 224–231

temperature. To evaluate the influence of temperature on the hydrogen desorption rates, Eqs. (5) and (7) can be rewritten using the values of activation energy and pre-exponential factor listed in Table 1, and assuming values of H wt.% = 1% for Na₃AlH₆ and H wt.% = 3.2% for NaAlH₄, which are close to the median hydrogen content in each plateau region.

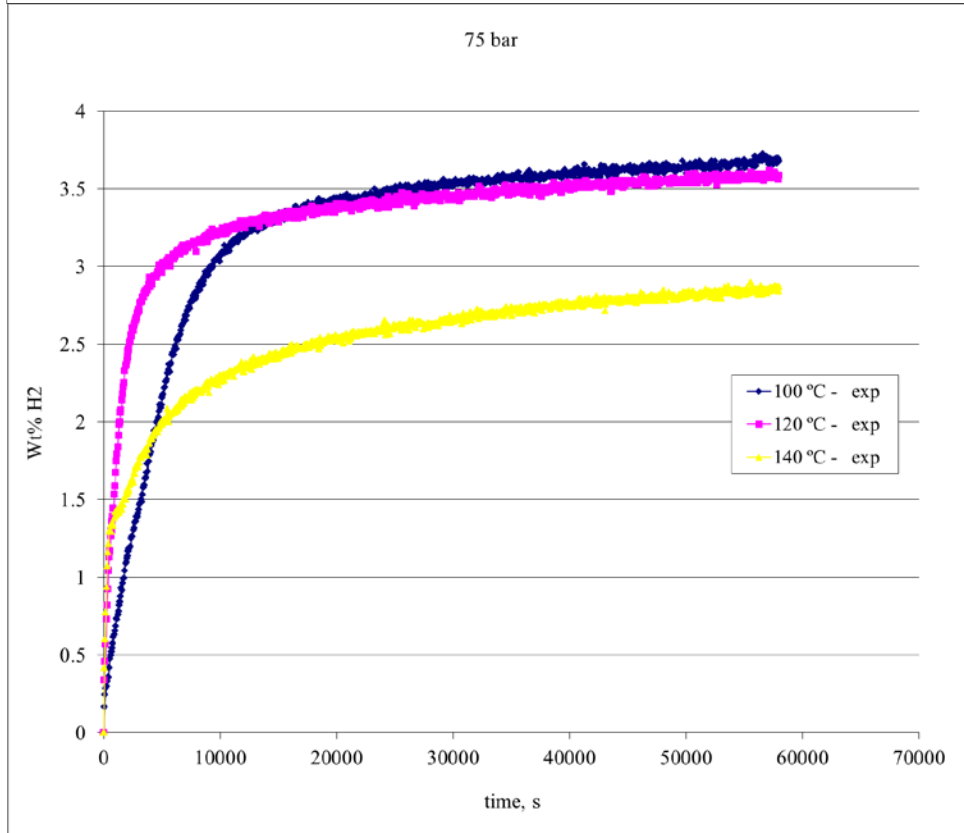
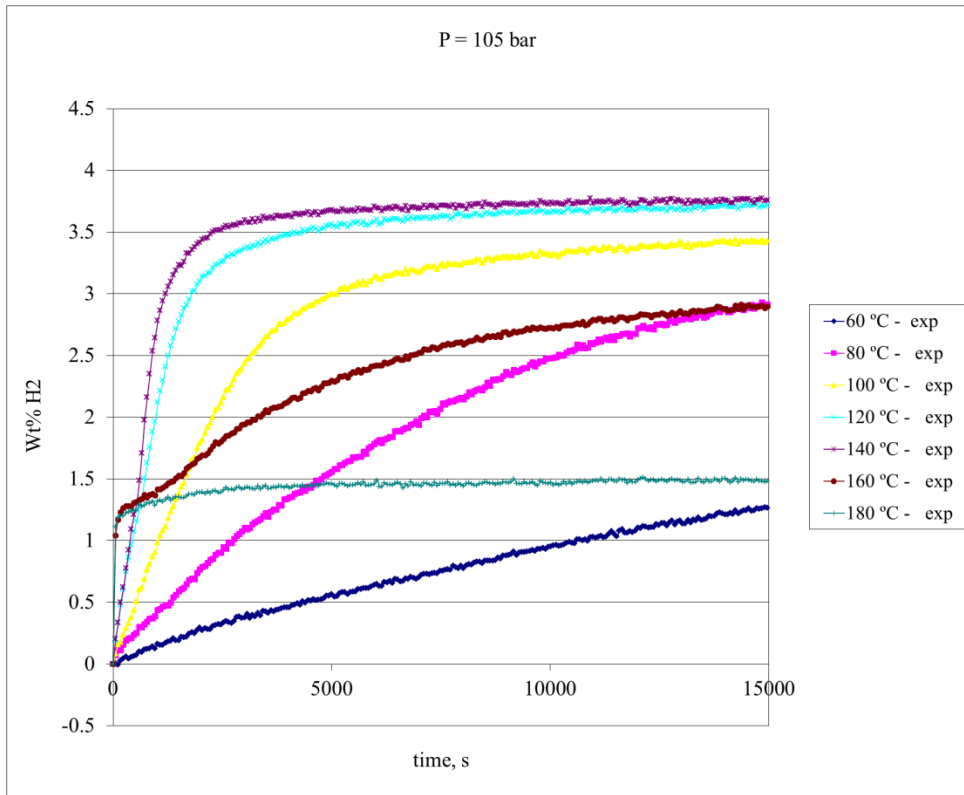
For NaAlH₄:

$$-d(\text{H wt.}\%)/dt = 1.9 \times 10^{11} e^{(-10.29/T)} \ln \left(\frac{P_{\text{eq1}}}{P_{\text{appl}}} \right) \quad (9)$$

For Na₃AlH₆:

$$-d(\text{H wt.}\%)/dt = 2.9 \times 10^{10} e^{(-10.62/T)} \ln \left(\frac{P_{\text{eq2}}}{P_{\text{appl}}} \right) \quad (10)$$

We used P_{eq} values calculated from the van't Hoff plot [14,15] for Eqs. (9) and (10) to calculate decomposition rates for Na₃AlH₆ and NaAlH₄. The results are plotted in Fig. 7.



APPENDIX A-3

HSECoE Metal Hydride Publications						
Institutions	Authors	Title	Journal	Volume	Pages	Year
GM	Raju M., Ortmann JP, Kumar S.	System Simulation Models for High-Pressure Metal Hydride Hydrogen Storage Systems	Int. J. Hydrogen Energy	35	8742-54	2010
GM	Raju M. and Kumar S.	System Simulation Modeling and Heat Transfer in Sodium Alanate based Hydrogen Storage Systems	Int. J. Hydrogen Energy	36	1578-1591	2011
GM	Raju M. and Kumar S.	Optimization of Heat Exchanger Designs in Metal Hydride based Hydrogen Storage Systems	Int. J. Hydrogen Energy	37	2767-2778	2012
GM	Kumar S., Raju M. and V. Senthil Kumar	System Simulation Models for On-Board Hydrogen Storage Systems	Int. J. Hydrogen Energy	37	2862-2873	2012
GM	Sulic M. Cai M., and Kumar S.	Cycling and Engineering Properties of Highly Compacted Sodium Alanate Pellets	Int. J. Hydrogen Energy	37	15187-15195	2012
GM	Sulic M., Cai M., and Kumar S.	Controlled Degradation of Highly Compacted Sodium Alanate Pellets,	Int. J. Hydrogen Energy	38	3019-3023	2013
NREL, Ford, UTRC	Matthew Thornton, Aaron Brooker, Jonathon Cosgrove, Michael Veenstra, Jose Miguel Pasini	Development of a Vehicle Level Simulation Model for Evaluating the Trade-off between Various Advanced On-board Hydrogen Storage Technologies for Fuel Cell Vehicles	SAE Technical Paper	1	1227	2012
SRNL	C. Corgnale, B. Hardy, D. Tamburello, S. Garrison and D. Anton	Evaluation of Acceptability Envelope for Materials-Based H2 Storage Systems	Int. J. Hydrogen Energy	37	2812-2824	2012
SRNL, DOE	R. Bowman, N. Stetson and D. Anton	Engineering Assessments of Condensed-Phase Hydrogen Storage Systems (Chapter 11)	Hydrogen Storage Technology: Materials and Applications (CRC Press, Taylor & Francis, Boca Raton, FL)	Ch 11	385-404	2013
SRNL, UQTR	M. Bhouri, J. Goyette, B. J. Hardy, D. L. Anton.	Sensitivity study of alanate hydride storage system	Int. J. Hydrogen Energy	36	621-633	2011
SRNL, UQTR	Maha Bhouri, Jacques Goyette, Bruce J. Hardy, Donald L. Anton	Honeycomb metallic structure for improving heat exchange in hydrogen storage system	Int. J. Hydrogen Energy	36	6723-6738	2011
SRNL, UQTR	M. Bhouri, J. Goyette, B. Hardy and D. Anton	Numerical modeling and performance evaluation of multi-tubular sodium alanate hydride finned reactor	Int. J. Hydrogen Energy	37	1551-1567	2012
SRNL, UQTR	B. Hardy, C. Corgnale, R. Chahine, M-A Richard, S. Garrison, D. Tamburello, D. Cossement and D. Anton	Modeling of adsorbent based hydrogen storage systems	Int. J. Hydrogen Energy	37	5691-5705	2012
SRNL, UTRC	S. Garrison, M. Gorbounov, D. Tamburello, B. Hardy, C. Corgnale, D. Mosher and D. Anton	Optimization of internal heat exchangers for hydrogen storage tanks using metal hydrides.	Int. J. Hydrogen Energy	38	2850-2862	2013
UTRC	B.A. van Hassel, D. Mosher, J.M. Pasini, M. Gorbounov, J. Holowczak, X. Tang, R. Brown, B. Laube and L. Pryor	Engineering Improvement of NaAlH ₄ System	Int. J. Hydrogen Energy	37	2756-2766	2012
UTRC	José Miguel Pasini, Bart A. van Hassel and Daniel A. Mosher	System modeling methodology and analyses for materials-based hydrogen storage	Int. J. Hydrogen Energy	37	2874-2884	2012
UTRC	B.A. van Hassel, M. Gorbounov, J. Holowczak, I. Feddchenia, X. Tang, R. Brown	Advancement of system designs and key engineering technologies for materials-based hydrogen storage	Journal of Alloys and Compounds	580	S337-S342	2013
UTRC, SRNL, GM, PNNL	José Miguel Pasini, Claudio Corgnale, Bart A. van Hassel, Theodore Motyka, Sudarshan Kumar, and Kevin L. Simmons	Metal hydride material requirements for automotive hydrogen storage systems	Int. J. Hydrogen Energy	38	9755-9765	2013